Novel Interaction, Regulation of Phosphorylation and Mitotic Localization of Cell Division Cycle Associated Protein 7 (CDCA7)

Shaon Parial

A thesis submitted to the Faculty of Graduate Studies
in partial fulfillment of the requirements for the degree of

Master of Science

Graduate Program in Biology

York University

Toronto, Ontario, Canada

April 2018

Abstract

Cell Division Cycle Associated Protein 7 (CDCA7) is a novel protein with poorly defined physiological significance. The proximity labeling method known as Biotin Identification (BioID) was used to determine candidate interactors of CDCA7. Mass spectrometry identified the microtubule spindle assembly protein TPX2 as a novel candidate interactor of CDCA7. Immunoprecipitation experiments verified interaction between CDCA7 and TPX2. The region of interaction was isolated to residues 195-204 of CDCA7. Based on inhibitor experiments, Aurora A kinase activity coincides with the phosphorylation of CDCA7 at the threonine (T) 163 residue. During mitosis, CDCA7 colocalizes with TPX2, localizes at centrosomes and undergoes phosphorylation at T163. These findings and previous findings in literature place CDCA7, TPX2 and potentially Aurora A kinase together within the context of mitosis. The results here demonstrate the direct interaction between CDCA7 and TPX2, and highlight residue T163 of CDCA7 as a prospective phosphorylation target of Aurora A kinase.

Acknowledgements

I would like to take the opportunity to thank my supervisor, Dr. Michael Scheid for the chance to pursue this degree in the first place. Your mentorship and advice really helped me cement my fundamental molecular biology skills. Also, responding to emails at midnight, that helped tons too. I absolutely must extend my thanks to Tim Gabor, who I can confidently say has taught me pretty much everything I know. I picked up many things from you and you taught me to be very resourceful. I don't think I'll ever forget the "there's always a reason" approach to problem solving. You also taught me how me to pull pranks, but I don't think I'll be at your level anytime soon. I would also like to thank my committee advisor, Dr. McDermott. Your patience during presentations and the massive amounts of feedback I received has helped immensely in these past 2 years.

A huge thanks goes out to David, walling ideas off you made this so much easier. You also got me into some pretty cool shows and even spotted me that parking pass. Thank you, Sam Kim, for your tutelage, advice and help. You also gave me enough life advice to last two reincarnations, much appreciated.

I must thank my parents for driving me to YorkU when the subway would shut down or picking me up at 3 AM so I wouldn't have to sleep on chairs. Also, thanks for giving birth to me, real game changer. I'm grateful to my sister for calming me down and keeping me in check during periods where results just wouldn't happen. I really appreciated having my cousin drop in from time to time, conversation makes a 6-hour incubation period pass by quite a lot faster. I also want to thank the rest of my family for supporting me through the past two years.

My best buddies Saadman, Al and Anthony, thank you for actually taking an interest in the type of research I've done. Hanging out with you guys during some rough times really helped me unwind and destress. My hamsters Coffee and Sesame also helped me distress. I would like to thank the Lungi Squad (Badgyal, RBC CEO, Yacktool, Pooptick, Avi24KB and PunGod). In particular, I would like to thank @marteezyparelly for looking like Akshay Kumar, which somehow made all this possible.

Last but certainly not least, I would like to extend my thanks to Tara Dubrow, RP, LLB. You got me through this really difficult writing process and the fact that someone is reading this is right now is all because of you.

Table of Contents

List of Tables

List of Figures

Chapter I: Introduction and Research Objectives

Cancer

Cancer encompasses a variety of diseases involving loss of cell cycle control, aberrant cell proliferation and metastasis. Cancer is prevalent throughout the world, with the most common types manifesting in lung, breast and colorectal regions. The most deaths occur with lung, liver and stomach cancers. The World Health Organization reports 8.2 million cancer-related deaths and 14.1 million new diagnosed patients in 2012.[1] If the demographic trends for gender, income and age in 2012 are kept constant, there will be 21.6 million new diagnosed cases of cancer by 2030, a 53% increase from 2012.[2] In Canada, there is a 50% chance that citizens will develop cancer in their lifetime and in 2017, 206, 200 new cases of cancer are expected to occur. Cancer is the leading cause of pathophysiological mortality in Canada, accounting for 30% of all deaths.[3]

The Oncogene c-Myc

A well-documented protooncogene is cellular-Myc (c-Myc) which will be referred to as Myc hereafter. The myelocytomatosis (Myc) gene, which encodes the Myc protein, may be the most well studied gene/protein so far. Between the years 1964-2012, more than 22,000 primary and review articles on Myc have been released. Millions of dollars in research are dedicated to Myc, with a publication rate of 3 publications per day.[4] The Myc protein functions primarily as a transcription factor that contains an amino (N) terminal transactivation domain. Myc associates with the transcription factor Max through a basic

helix loop helix domain[5]. Myc binding sites are present on 3465 genes, which accounts for approximately 15% of the human genome[6].

In normal cells, the Myc gene is subjected to a rigid degree of regulation though factors that are both genetic and epigenetic. Myc aids and drives tumorigenesis by deregulating several processes which include but are not limited to cell adhesion and cytoskeletal regulation[5], Deoxyribonucleic acid (DNA) replication[7], DNA transcription[8], protein synthesis[9], angiogenesis[10], the immune response[11], cell metabolism and growth[12], and apoptosis[13]. Myc-induced cancers are said to be addicted to the Myc oncogene, with suppression of the oncogene reversing the tumorigenic phenotypes[14]. Myc deregulation is estimated to occur in more than 70% of cancers[15].

Novel target genes of Myc have been identified, however the functions of several novel genes are yet to be determined. In one study, the Myc allele was conditionally expressed in lymphoma cell lines and microarray analysis was performed to identify target genes of Myc. The messenger ribonucleic acid (mRNA) expression of target genes was determined through experiments where the Myc gene was stimulated, deactivated and then reactivated. The candidate genes were then subjected to chromatin immunoprecipitation (ChIP) in order to determine which gene promoters were enriched with Myc. These experiments found 89 genes that were direct Myc target genes and 27 of these genes were non-annotated sequences (unknown function).[16] Comparison of gene expression between Rat1a fibroblasts and Rat1a fibroblasts stably expressing the Myc oncogene identified 20 differentially expressed genes.[17] The most differentially expressed gene was named JPO1.[18]

CDCA7

Gene Expression Regulation via Myc or E2F and Transcription Factor Capability

The JPO1 gene maps to chromosome 2q31 and consists of 2.5 kilo-basepairs which translates a 47 kilo-Dalton (kDa) protein. The protein contains a leucine zipper domain and a carboxyl (C) terminal cysteine rich domain. Cell lines stably expressing the Myc gene fused to the estrogen receptor (ER) showed that JPO1 mRNA expression increases when MycER cells are exposed to 4-hydroxytamoxifen (estrogen variant). Inhibition of protein synthesis with cycloheximide still resulted in an increase in JPO1 mRNA expression. As a result, JPO1 is a direct target gene of Myc which does not require the synthesis of an intermediate protein. The expression of JPO1 mRNA was measurable in the small intestine, thymus and colon, and sparse mRNA expression was found in bone marrow, spleen and leukocytes.[18] The JPO1 gene consists of 9 exons and ChIP experiments with several fragments of the JPO1 gene identified enrichment of Myc at two canonical E-boxes (5'-CACGTG-3') within intron 1.[19]

The expression of the transcription factor E2F1 resulted in an increase in JPO1 mRNA expression. Various promoter constructs of the JPO1 promoter linked to a luciferase reporter gene were generated. Deletion of the E2F consensus binding site upstream of the JPO1 transcription start site (TSS) resulted in no luciferase activity.[20] E2F1, E2F2 or E2F3 expression alone can force quiescent cells into the S phase of the cell cycle, where as E2F4 and the DP-1 transcription factor are required to transition quiescent cells into S phase.[21] E2F1, E2F2, E2F3 and E2F4 upregulate JPO1 expression, as evidenced by luciferase reporter assays. ChIP Experiments using the region adjacent to the TSS of JPO1, showed that E2F1, E2F2 and E2F4 are enriched at the E2F consensus binding sites.[20]

A similar protein, named JPO2 shares 45% homology with JPO1. Both JPO1 and JPO2 share similar C-terminal cysteine rich domains (88% homology) which encodes a putative zinc finger domain.[22] JPO2 has been shown to bind the monoamine oxidase A promoter at Sp1 sites and causes transcriptional repression as well as reductions in protein activity. The level of repression correlated to the level of JPO2 protein expression.[23] A construct containing the Gal4 DNA binding domain and the C-terminal region of JPO1 (residues 247-371) was created. This construct successfully induced expression of a construct with 5 Gal4 DNA binding sites and a TATA box fused to a luciferase reporter gene. Therefore, the C-terminal domain of JPO1 contains transcriptional capabilities.[20]

Protein Interactions with Myc or 14-3-3 and Akt Phosphorylation

JPO2 directly interacts with Myc in 293TV cells with the leucine zipper domain, binds to Myc at chromatin and colocalizes with Myc in the nucleus.[22] The human genome nomenclature committee has adopted the name Cell Division Cycle Associated protein 7 (CDCA7) for JPO1, and found that CDCA7 expression peaks around the G1/S transition of the cell cycle.[24] JPO1 will be referred to as CDCA7 hereafter. Residues 146 to 170 of CDCA7 have been shown to interact with residues 274-440 of Myc. The region of CDCA7 that interacts with Myc contains a bipartite nuclear localization sequence (NLS) which spans residues 160-190.[25] The region also contains an Akt phosphorylation consensus site. The consensus site requires serine or threonine as the main residue with arginine at residues -5 and -3 as well as a large hydrophobic residue at +1.[26] Threonine 163 of CDCA7 matches this perfectly (RPRRRTF). Threonine 163 (RRRTFP) also matches the 14-3-3 mode I phosphorylation

binding site[25], which requires serine or threonine as the central residue, arginine at -3 and proline at +2.[27]

Overexpression of Myc in cells subjected to serum withdrawal leads to apoptosis.[28] Stable expression of CDCA7 in Rat1a fibroblasts that are already stably expressing Myc (Rat1a-Myc) leads to an increase in serum-withdrawal induced apoptosis. However, deletion of the NLS abolishes apoptosis even in the presence of Myc overexpression. The NLS deletion may be acting as a dominant negative mutant[29] that potentially binds to the same promoters as Myc but does not bind to Myc itself. If Rat1a-Myc cells stably express short hairpin RNA (shRNA) which targets and knocks down CDCA7 expression, the number of apoptotic cells decreases and the cells exhibit less apoptotic morphology, even with Myc overexpression[25]. Thus, Myc and CDCA7 may induce apoptosis together, and interaction of Myc and CDCA7 is a requirement for serum withdrawal induced apoptosis.

Two-dimensional tryptic digest of wildtype (WT) CDCA7 and the threonine 163 to alanine (T163A) CDCA7 mutant showed that T163 of CDCA7 is phosphorylated. WT CDCDA7 primarily localizes to the nucleus with some cytoplasmic staining, while T163A CDCA7 only localizes to the nucleus. WT CDCA7 was stimulated by fibroblast growth factor (FGF) and platelet-derived growth factor (PDGF), while T163A CDCA7 was not. Both FGF and PDGF led to increases in cytoplasmic localization and phosphorylation of T163 (pT163). The putative NLS of CDCA7 was subjected to various deletions and mutations that led to cytoplasmic localization. Thus, CDCA7 contains a bonafide bipartite NLS.[25]

The adapter protein 14-3-3 binds to phosphorylated residues and can mask the NLS of target proteins, which leads to the sequestration of these proteins in the cytoplasm.[27] WT CDCA7 binds to 14-3-3 and localizes to both the nucleus and cytoplasm. The T163A CDCA7 mutant does not bind 14-3-3 and only localizes to the nucleus. Replacement of 20 amino acids around T163 with the R18 peptide that constitutively binds 14-3-3 through its aspartic acid (D) and glutamic acid (E) residues[30], causes cytoplasmic localization. Mutation of the DE residues with lysine (K) abolishes 14-3-3 binding and results in nuclear localization. Thus, pT163 CDCA7 binds to 14-3-3 and is shuttled to the cytoplasm[25].

Several lines of evidence support the notion that Myc and 14-3-3 compete for binding to CDCA7. The constitutive 14-3-3 binder DE-CDCA7 binds less Myc than WT CDCA7. Purified CDCA7 that is stripped of endogenous interactors will have a population of pT163 CDCA7. Addition of Myc to CDCA7 increases the amount of Myc associated with pT163 CDCA7, however, addition of Myc and 14-3-3 reduces the amount of Myc bound to pT163 CDCA7. The amount of Myc bound to CDCA7 may depend on 14-3-3 and may be determined by the phosphorylation status of T163.[25]

CDCA7 may be phosphorylated by the Akt kinase. In cells, growth factors bind to tyrosine receptor kinases, which then dimerize and autophosphorylate the cytoplasmic domains. These phosphorylated residues recruit phosphoinositide-3-kinase (PI3K). PI3K then converts phosphatidylinositol-4,5-biphosphase (PIP2) to phosphatidylinositol-3,4,5-triphosphase (PIP3) at the cell membrane. PIP3 then recruits phosphoinositide -dependent kinase 1 (PDK1) which fully activates Akt. Akt then translocates to the nucleus and phosphorylates target proteins.[31] Inhibition with LY294002, a PI3K inhibitor[32] and Akt

inhibitor VIII decrease T163 phosphorylation. Gag-Akt, a membrane bound Akt, restores pT163 levels in WT CDCA7 but not the T163A mutant. Mouse embryonic fibroblasts (MEFs) with deletion of Akt 1 and Akt 2 have no phosphorylated T163 CDCA7. PDGF increases phosphorylation of T163 CDCA7 in MEFs only when Akt 1 and Akt 2 are present. Akt also phosphorylates WT CDCA7 at T163 but not the T163A mutant *in vitro*. Taken together, the evidence supports the idea that CDCA7 is phosphorylated by Akt at T163.[25]

In summary, CDCA7 and Myc interact with one another and may promote apoptosis through transcription of apoptotic genes in serum starved environments. CDCA7 is also phosphorylated by Akt at T163. Phosphorylation at T163 leads to binding of 14-3-3 at this site, which masks CDCA7's NLS and sequesters it to the cytoplasm. Both Myc and 14-3-3 compete for binding to pT163. Accordingly, Akt phosphorylation determines the subcellular localization of CDCA7 which in turn determines CDCA7's phenotypic outcome. Refer to Figure 1.1 for a schematic representation.

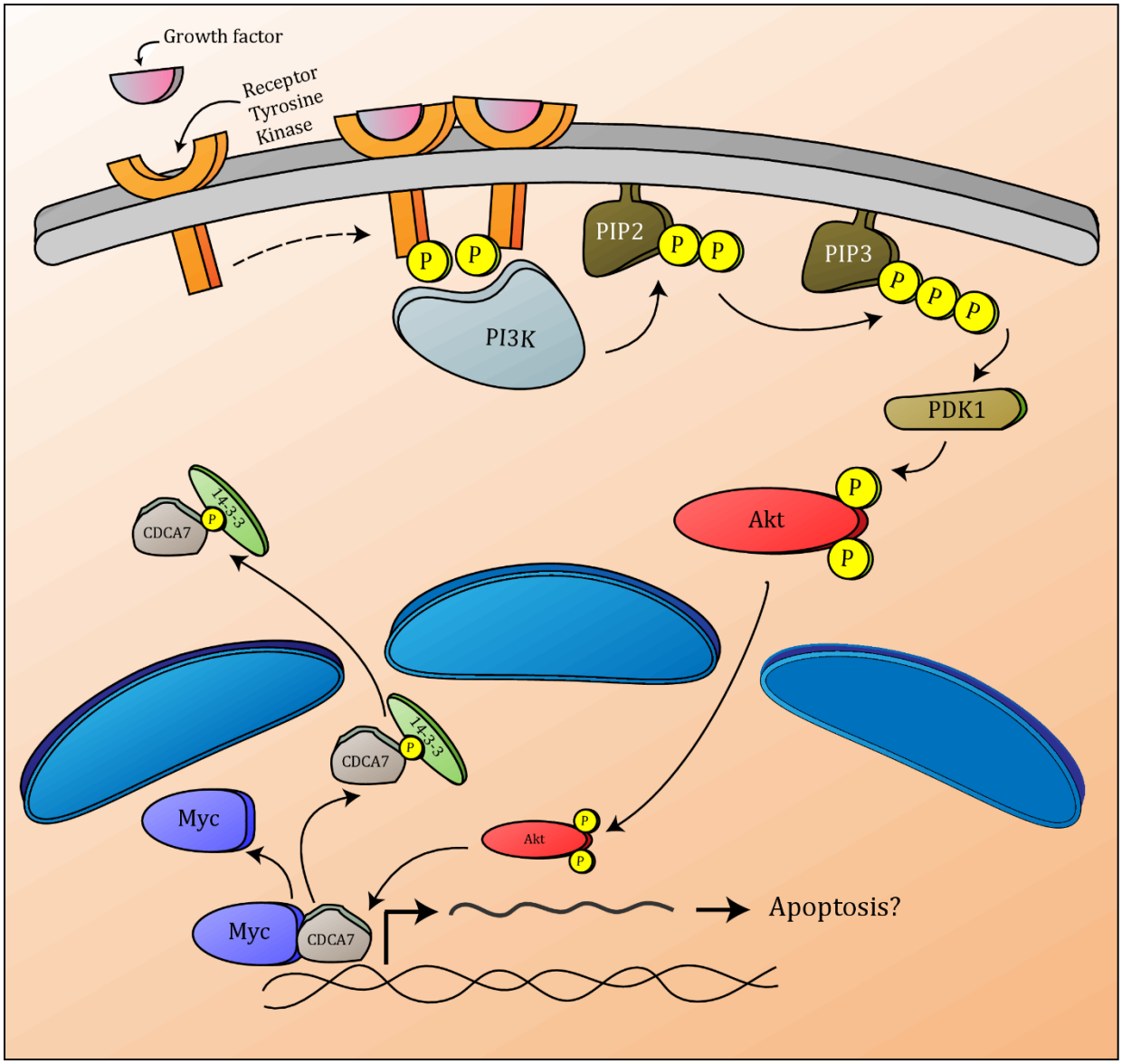

Figure 1.1: CDCA7 in relation to Myc, Akt and 14-3-3. The PI3K/Akt pathway is activated by mitogenic growth factors. Upon binding to receptor tyrosine kinases (RTKs), the kinases dimerize and are activated by autophosphorylation. The active RTKs recruit phosphoinositide-3-kinase (PI3K) to the cell membrane which then converts phosphoinositide-4,5-biphosphate (PIP2) to phosphoinositide-3,4,5-triphosphate (PIP3). PIP3 recruits phosphoinositide-dependent kinase 1 (PDK1) to the cell membrane and fully activates Akt kinase. Akt then localizes to the nucleus. CDCA7 and Myc reside in the nucleus and may interact with one another to potentially drive transcription of proapoptotic genes. Akt phosphorylates CDCA7 at threonine (T) 163 which can then be bound by 14-3-3. After 14-3-3 interaction, CDCA7-Myc interaction is weakened and the proteins dissociate from each other. CDCA7 bound to 14-3-3 has its nuclear localization sequence (NLS) concealed. Without the NLS, CDCA7 is shuttled to and sequestered in the cytoplasm.

CDCA7 Overexpression Promotes Tumorigenesis

In soft agar colony growth assays, stable expression of CDCA7 in Rat1a fibroblasts (Rat1a-CDCA7) has lower transformation induction capabilities in comparison to Rat1a-Myc fibroblasts. A point mutation of tryptophan (W) at residue 135 to glutamic acid (E) in the Myc Box II domain of Myc cannot transform Rat1a fibroblasts when ectopically expressed. However, ectopic expression of W135E Myc in Rat1a-CDCA7 fibroblasts does induce transformation.[18] The CDCA7 homolog JPO2 also stimulates transformation with W135E Myc. JPO2 is overexpressed in the medulloblastoma cell line UW228 as well as medulloblastoma tumor patients.[22] Deletion of CDCA7's NLS abolishes its interaction with Myc and diminishes transformation in Rat1a-Myc fibroblasts. Knockdown of CDCA7 decreases the transformation ability of Rat1a-Myc fibroblasts as well.[25] So, CDCA7 expression and CDCA7-Myc interaction may be a requirement for Myc-induced oncogenesis.

Experiments with microarray analysis found overexpression of CDCA7 in a variety of cancers. The complementary DNA (cDNA) of tumor and normal tissue from the same patient was probed for CDCA7. Overexpression of CDCA7 was found in lung, stomach, uterus, ovary, colon and rectum cancers. Analysis of blood fractions from hematologic cancer patients found overexpression of CDCA7 in acute myeloid leukemia (AML) and chronic myeloid leukemia (CML). CDCA7 expression was highest in the blast crisis phase of CML. CDCA7 was placed under the influence of the H2-K promoter, which is only present in adaptive immune cells (B cells and T cells). Transgenic mice expressing this construct had more solid tumors

including pancreatic, mesenteric and thymic lymphomas.[33] The mRNA expression of CDCA7 is also elevated in retinoblastoma cells.[34]

Patients with esophageal squamous cell carcinoma (ESCC) have amplified regions of DNA with the CDCA7 gene. When tumor and normal tissue were compared, elevated levels of CDCA7 mRNA expression were found in ESCC patients. Knockdown of CDCA7 in ESCC cells has been shown to boost apoptosis, reduce cell growth and led to reductions in the phosphorylation of extracellular signal-regulated kinases 1/2 (ERK1/2). CDCA7 knockdown also decreased expression of fibroblast growth factor 21 (FGF21).[35] ERK1/2 is part of mitogen activated protein (MAP) kinase pathways and following phosphorylation of ERK1/2, the kinases activate transcription factors in the nucleus.[36] FGF21 promotes glucose uptake by stimulating ERK1/2 in adipocytes which leads to expression of the glucose transporter 1 gene.[37] In pancreatic β-cells, FGF21 stimulates ERK1/2 and the Akt pathway.[38] So, CDCA7 overexpression may promote FGF21 overexpression and lead to overstimulation of ERK1/2, which in turn promotes dysregulated cell growth, driving tumorigenesis.[35]

Knockdown of CDCA7 in ESCC cells leads to increases in apoptotic gene expression.[35] Cysteine-aspartic proteases (caspases) mediate apoptosis through the extrinsic (receptor-mediated) and intrinsic (mitochondrial) death pathways. Caspases are present in an inactive state (procaspases) and have a prodomain, p20 large subunit and p10 small subunit. Procaspases dimerize and remove the prodomain to produce active caspases. Initiator caspases respond to apoptotic stimuli and activate through autocatalytic activity. Then active initiator caspases cleave executioner caspases which then cleave and degrade cellular constituents, leading to cell death.[39] Knockdown of CDCA7 also increases mRNA expression

of Caspase 10 and Caspase 7.[35] Caspase 10 is an initiator caspase only present in humans that cleaves caspase-3 and caspase-7[40] while Caspase 7 is an executioner caspase[41]. Another gene expressed after CDCA7 knockdown is the tumor necrosis factor (TNF)-related apoptosis inducing ligand (TRAIL) receptor (R).[35] TRAIL-R mediates the extrinsic death pathway by binding TRAIL and leading to activation of caspases.[42] Thus, overexpression of CDCA7 in ESCC cells may drive tumorigenesis by repressing expression of proapoptotic genes.[35]

Roles in Development and Stem Cell Maintenance

The epithelial cells of the thymus play a major role in T cell differentiation and maturation. The Forkhead box protein N1 (Foxn1) transcription factor is integral for thymic development and Foxn1 null mice are athymic. In zebrafish embryos, knockdown of Foxn1 leads to deficits in T cell development. Foxn1 knockdown in zebrafish thymus also reduces the levels of CDCA7 mRNA expression. CDCA7 mRNA expression was readily detectable in zebrafish and mouse thymic epithelial cells (TECs) and in mouse TEC lines. Knockdown of CDCA7 also leads to decreased expression of T cell specific markers in zebrafish embryos. When CDCA7 is overexpressed in embryos that have been subjected to Foxn1 knockdown, expression of a few T cell markers increases and results in partial rescue from the Foxn1 knockdown phenotype. Thus, CDCA7 is regulated by Foxn1, is expressed in TECs and its expression is partially responsible for T cell development.[43]

Notch signaling occurs in a variety of contexts. In general, when the Notch receptor domain is bound by a ligand, several proteolytic cleavages lead to the release of the Notch intracellular domain (NICD).[44] The NICD then translocates to the nucleus and associates with recombination signal binding protein for immunoglobin kappa J (RBPJ), which binds to

target genes of the Notch family.[45] The NICD is also bound to the coactivator Mastermind (Mam). Together, the Notch-RBPJ-Mam complex drives the transcription of Notch target genes. Low intensity interaction between Notch1 and the Jagged ligand (JAG1) is paramount to the process of hematopoiesis and hematopoietic stem cell (HSC) specification.[44]

Aorta-gonad-mesonephros (AGM) tissue arises during murine embryonic development. Target genes of Notch1/RBPJ that are regulated by JAG1 in AGM tissue were assayed. Preceding the CDCA7 transcription start site (TTS) are two adjoining RBPJ binding sites. ChIP experiments of this region found enrichment of RBPJ, Notch1 and Mam. A construct linking these RBPJ binding sites to a luciferase reporter gene found that NICD activated the construct and NICD and Mam together increased this basal level of expression. Expression of CDCA7 was found in the aortic clusters of AGM tissue where HSCs reside. Knockdown of CDCA7 in AGM tissue led to hematopoietic differentiation. Thus, CDCA7 is a target gene of the Notch1 signaling pathway, is expressed in HSCs and is involved in maintaining the HSC pool during development.[46]

Radial glial cells at the luminal side of the neuroepithelial embryonic tissue express the paired box 6 (Pax6) transcription factor. This forms a region called the ventricular zone. The subventricular zone is located above this region and contains immediate progenitor cells (IPCs) which develop from radial glial cells below. After one to two cell divisions, IPCs become post mitotic neurons that move into the cortical plate above. IPCs give rise to two-thirds of all excitatory neurons within the cerebral cortex. IPCs do not express Pax6 but do express the T-box brain 2 (Tbr2) transcription factor while post mitotic neurons do not express Tbr2 but do express the T-box brain 1 (Tbr1) transcription factor.[47]

The telencephalon is an embryonic structure that can be subdivided into a dorsal and ventral portion. The dorsal telencephalon gives rise to the cerebral cortex and the ventral telencephalon gives rise to the basal ganglia.[48] Pax6 expression was found to peak within the dorsal telencephalon, around the boundary of the lateral cortex and ventral telencephalon. This is the region where lateral cortex neuroprogenitors preside. CDCA7 expression in this region was relatively low. Inversely, Pax6 expression was lowest in the ventral telencephalon whereas CDCA7 expression peaked in this region. In Pax6 null mice, CDCA7 expression increased in regions where lateral cortex neuroprogenitors are located. CDCA7 was overexpressed in lateral cortex neuroprogenitors via *in utero* electroporation. CDCA7 overexpression decreased the number of IPCs produced (cells expressing Tbr2) and consequently, few post mitotic neurons (cells expressing Tbr1) reached the cortical plate. So, CDCA7 expression maintains a stem-like state in lateral cortex neuroprogenitors and is negatively regulated by Pax6 expression, a fundamental requirement for lateral cortical development of the cerebrum.[49]

ICF Syndrome

Immunodeficiency, Centromeric instability and Facial anomalies (ICF) syndrome is a rare genetic disorder that displays an array of phenotypes. The disorder is typically marked by: gastrointestinal and respiratory infections that are lethal, lack of gamma globulin in the bloodstream even though B cells are present, facial abnormalities such as a flat nasal bridge and centromeric instability.[50] Centromeric instability is marked by hypomethylation of juxtacentromeric sequences for chromosomes 1, 9 and 16. These sequences occur at heterochromatin and are called satellite sequences with GGAAT repeats.[51] There are 77

verified cases of ICF split into 4 subdivisions. Mutations in DNMT3B, a DNA methyltransferase gene, accounts for 56% of all cases, 31% with mutations in the zinc finger and BTB binding domain containing 24 (ZBTB24) gene, 6.5% with mutations in the helicase, lymphoid specific (HELLS) gene and 6.5% with mutations in the CDCA7 gene.[52]

There are five known ICF syndrome patients with mutations in the CDCA7 gene. All of these mutations occur in the putative zinc finger DNA binding domain within the C-terminal of CDCA7. In MEFs, knockdown of CDCA7 led to hypomethylation at heterochromatin adjacent to centromeres.[50] Deletion of the ZBTB24 gene is embryonically lethal in mice. In mouse embryonic stem cells (mESCs), deletion of ZBTB24 decreases CDCA7 mRNA expression and then overexpression of ZBTB24 reestablishes CDCA7 expression. ZBTB24 binds to the CDCA7 promoter and a reduction in CDCA7 mRNA levels is present in ICF patients with ZBTB24 mutations.[53] Thus, CDCA7 mutations play a role in ICF syndrome, its expression is required for methylation of pericentromeric heterochromatin and CDCA7 may also be responsible for ICF patients with ZBTB24 mutations.[50,53]

TPX2

Protein Structure and Function

Targeting protein for Xenopus centrosomal kinesin-like protein 2 (Xklp2), also known as TPX2[54], is a scaffolding protein which consists of three domains. The N-terminal domain interacts with the kinase Aurora A[55], the C-terminal domain binds to branching networks of microtubules[56] and the internal domain contains an NLS. The NLS is monopartite and binds to importin alpha.[57] TPX2 is located at chromosome 20q.[58] TPX2

plays an integral role during mitosis and TPX2 null mice are not viable, arresting at the morula stage. Embryonic cells of TPX2 null mice are tetraploid and do not contain a bipolar spindle, suggesting inability to perform chromosome segregation due to deficits in spindle assembly.[59] Overexpression of TPX2 also induces polyploidy in somatic cells.[60] TPX2 localizes on spindle poles near centrosomes as well as kinetochores during mitosis.[61]

Microtubule Nucleation and Xklp2

Microtubules are structural filaments that are present as alpha (α) and beta (β) tubulin subunits. Heterodimerization of the α- and β- subunits form the microtubule protofilament and 13 protofilaments form one microtubule. The microtubule tip has GTP bound to it (GTP tubulin cap) which stabilizes the microtubule and allows growth. Polymerization of microtubule protofilaments or growth begins by subunits joining one another, the polymer initially resembles a flattened structure but GTP hydrolysis of protofilaments leads to the formation of a lattice structure. Microtubules may also depolymerize, a process known as catastrophe. Cycles between growth and catastrophe define the structural cycle of microtubules. The ends of microtubules can be defined as plus (exposure of β-tubulin) or minus (exposure of α-tubulin). The minus ends of microtubules are more stable than plus ends, grow gradually relative to plus ends and loss of the GTP tubulin cap does not destabilize it.[62]

The nucleation or *de novo* polymerization of microtubules during mitosis is performed by the gamma (γ) tubulin ring complex (γTuRC). During mitosis, microtubule nucleation occurs at the microtubule organization center (MTOC) of animal cells, known as the centrosome. At the centrosome, γTuRC binds to the minus ends of microtubules and

stabilizes this end. The plus ends extend from γTuRC.[63] In humans, the protein ninein localizes the γTuRC to the centrosome and absence of ninein results in the absence of centrosomal γTuRC. Ninein binds to the centriole with its C-terminal domain and the γTuRC with its N-terminal domain.[64] The model of microtubule nucleation that conforms best to evidence present in current scientific literature is the template model.[65]

The template model is supported by the crystal structures of the γTuRC. In this model, gamma tubulin complex protein (GCP) 1 and GCP2 each bind a γ-tubulin subunit in a longitudinal direction, while GCP1 and GCP2 interact with one another laterally. This small subunit is known as the gamma tubulin small complex (γTuSC). Six sets of γTuSC are held to one another by GCP4, GCP5 and GCP6. This positions 12 γ-tubulin subunits next to one another and leaves space for the thirteenth subunit to begin forming the microtubule protofilament. It is here that α-tubulin binds (minus end) and initiates nucleation.[65]

The nucleation of microtubules may also occur adjacent to already formed microtubules during mitosis. In this case, the original microtubule is the mother and resulting microtubules are daughters. As expected, reduction of γ-tubulin results in the nucleation of few microtubules. Supplementing existing microtubules with the Ras-like nuclear protein which is a guanosine triphosphate hydrolase (RanGTPase), and TPX2 results in microtubule nucleation, even without the presence of chromosomes and centrosomes.[56] Another component required for branching microtubule networks is the protein complex augmin. Augmin is composed of the dim γ-tubulin protein 2 (Dgt2), Dgt3, Dgt4, Dgt5 and Dgt6.[66] When TPX2 or Augmin is depleted, the time required for microtubule nucleation is prolonged and branching of microtubules is ablated. Thus, TPX2 induces microtubule

nucleation at preexisting microtubules and is a requirement for formation of microtubule branching networks.[56]

When daughter microtubules have a branching angle of 90° or less to the mother microtubule, they maintain the same orientation as the mother microtubule (same polarity). All daughter microtubules initiated by RanGTPase and TPX2 have the same polarity as the mother microtubule. Most are nucleated at low branch angles, with the majority having angles of less than 30°. The C-terminal region of TPX2 also directly interacts with microtubules. Thus, TPX2 along with RanGTPase initiates microtubule branching networks where all microtubules share the same polarity and TPX2 directly interacts with microtubules.[56]

The plus end directed kinesin called Xklp2 was discovered in Xenopus oocytes and has centrosomal localization during mitosis. Its motor domain is required for spindle assembly and bipolarity, as well as chromosome segregation. When the motor domain of Xklp2 is deleted, the spindle poles collapse into each other and only large monopolar spindles are present.[67] Movement of Xklp2 towards the minus ends of microtubules depends on the dynein/dynactin complex and is a requirement for microtubule nucleation during mitosis. However, Xklp2 cannot bind to microtubules and move toward the minus ends alone. On the other hand, the presence of TPX2 allows for this process. So, TPX2 promotes microtubule nucleation by mediating association and movement Xklp2 toward the minus ends of microtubules.[54]

RanGTP Regulation

The monopartite NLS of TPX2 binds to importin alpha, and this interaction is dependent on residue 284 of TPX2. Mutations of this domain lead to loss of importin alpha binding and when these mutants are added to mitotic extracts the resulting phenotype is constitutive microtubule assembly.[57] Importin alpha (α) associates with importin beta (β) and target proteins. The importin α/β complex shuttles cargo proteins across the nuclear envelope and in the nucleus RanGTP binds to importin beta, which destabilizes the importin α/β complex. The cargo protein is released when importin alpha dissociates from the complex and then importin beta remains bound to RanGTP.[68] This mode of regulation has been demonstrated for TPX2. Thus, TPX2 is imported into the nucleus by interacting with importin alpha and freely dissociates in the nucleus by virtue of RanGTP.[69]

All phases of the cell cycle consist of a RanGTP gradient. During interphase, cytoplasmic RanGTP is absent while high nuclear concentrations of RanGTP are present. During mitosis, the regions closest to the cell membrane are devoid of RanGTP while the highest concentrations of RanGTP are found near chromatin.[70] The subcellular localization of RanGTP depends on nuclear transport factor 2 (NTF2). While Ran bound to guanosine diphosphate (RanGDP) may move into the nucleus via diffusion, it has been shown to directly interact with NTF2 and be imported into the nucleus.[71] NTF2 itself shuttles cargo proteins by dimerizing and binding to nucleoporins. In particular, the nucleoporin p62, which is an O-linked glycoprotein is essential for NTF2 nuclear transport.[72] The GDP in RanGDP is replaced by GTP in the nucleus.[73]

The guanosine exchange factor (GEF) called regulator of chromosome condensation 1 (RCC1), replaces GDP with GTP on RanGTPase. As RCC1 localizes close to chromatin, RanGTP levels are highest at chromatin.[73] TPX2 localizes to spindle microtubules near kinetochores (chromosomal structure) and near centrosomes during mitosis.[61] These components are in close proximity to chromatin during spindle assembly.[74] Accordingly, TPX2 localization during spindle assembly is determined by the RanGTP gradient and in turn, the RanGTP gradient is mediated by RCC1 during spindle assembly.[73]

TPX2 Deregulation Drives Tumorigenesis

TPX2 is a well-known oncogene and is overexpressed in several types of cancers. This includes but is not limited to colon, liver, ovary, pancreas, mesothelium, cervix, lung, brain, salivary gland and oral squamous cell carcinomas.[75] As previously mentioned, TPX2 is localized to chromosome 20q, a region that is amplified in several cancers and this event is associated with progression of colorectal adenomas to invasive carcinomas. The protein levels of TPX2 are linked to the DNA copy number of chromosome 20q and knockdown of TPX2 expression hinders the invasiveness of colorectal carcinomas.[58] As stated, TPX2 is involved in microtubule assembly and ultimately chromosome segregation. Improper segregation of chromosomes leads to chromosomal/genomic instability, a trademark of cancer. In fact, when compared to 10,051 candidate genes, TPX2 had the strongest association to chromosome instability.[76] So, TPX2 is overexpressed in a variety of cancers, plays a role in colorectal carcinoma invasion and is a marker of genomic instability.

DNA Damage Response

The DNA damage response depends on the phosphorylation of histone 2AX (H2AX) at the residue serine (S) 139. This phosphorylated version is known as γ-H2AX. When double stranded (ds) breaks in DNA occur, the MRN complex is recruited to the region of injury. This complex contains nijmegen breakage syndrome protein 1 (NBS1), which then recruits the ataxia telangiectasia mutated (ATM) kinase. ATM kinase phosphorylates H2AX at S139, generating γ-H2AX. Recruitment of ATM kinase allows recruitment of mediator of DNA damage checkpoint 1 (MDC1). MDC1 will then recruit more ATM kinase. High levels of γ-H2AX recruit DNA damage response factors which ultimately decide cell fate following the dsDNA breaks.[77]

The residue serine 634 of TPX2 has been identified as a putative ATM kinase phosphorylation site.[78] When cells are exposed to ionizing radiation, dsDNA breaks occur and activate the DNA damage response. Following ionizing radiation, TPX2 expression was found to be correlated with the level of γ-H2AX. Downregulation of TPX2 expression resulted in more γ-H2AX while overexpression of TPX2 resulted in less γ-H2AX. TPX2 has been shown to interact with NBS1, ATM kinase and MDC1. TPX2 also colocalizes with γ-H2AX, an event that occurs only in interphase and not during mitosis. Thus, during interphase, TPX2 associates with γ-H2AX and other DNA damage response proteins and TPX2 expression decreases the levels of γ-H2AX, suggesting an inhibitory role during the DNA damage response.[79]

Aurora A Kinase

Protein Expression, Activity and Function

Aurora A kinase belongs to the Aurora family of mitotic kinases and is located on chromosome 20q.[58] In most tissue, Aurora A localization is restricted to the nucleus.[80] Expression of Aurora A is detected during the S phase, G2 phase and M phase of the cell cycle and centrosomal localization of Aurora A occurs during all three of these cell cycle stages.[81] The Aurora A gene contains a cell cycle dependent element (CDE) and a cell cycle homology region (CHR) in tandem. Mutation of these regions results in loss of cell cycle dependent expression. Expression and activity of Aurora A increases during S phase and peaks in G2 and M phase.[82] So, Aurora A expression and activity peaks during mitotic processes.

During mitosis, Aurora A localizes to the peripheral regions of centrosomes (prophase) and to the spindle microtubules (prometaphase and metaphase). Once spindle assembly has been established, expression of Aurora A at the centrosome is not necessary for proper cell division to occur. Expression of Aurora A is a fundamental requirement for bipolar spindle assembly.[81] The catalytic domain of Aurora A determines its localization during mitosis. A point mutation of glycine (G) to asparagine (N) at residue 198 of Aurora A results in localization to the inner centromere (prometaphase and metaphase) and midzone (anaphase). The localization of G198N Aurora A mimics Aurora B localization. In fact, G198N Aurora A binds to and phosphorylates the Aurora B targets Survivin and inner centromere protein (INCENP).[83] So, Aurora A is a nuclear kinase involved in mitotic processes at the centrosome and bipolar spindle apparatus and Aurora A localization is dependent on its glycine 198 residue.

Centrosomin, a centrosomal core constituent and γ-tubulin are recruited by Aurora A to the centrosome. Mutations in Aurora A results in the loss of centrosomin and γ-tubulin recruitment and consequently, centrosomal maturation does not occur. As a result, morphological spindle abnormalities manifest.[84] Overexpression of Aurora A leads to apparent centrosomal amplification but the kinase activity of Aurora A is not a requirement for this phenotype. Overexpression of Aurora A leads to polyploid cell populations (5N-8N). This occurs since overexpression leads to failure of cytokinesis. Cytokinesis failure is also responsible for multinucleation, as centrosomes accumulate due to failed cell division and result in the centrosome amplified phenotype. Over time, the polyploid population increases as more and more cells fail to divide. If the cell cycle is arrested in S phase however, this does not result and cells are prone to programmed cell death. Interestingly, this phenotype is common in p53 null cells as the presence of p53 would arrest the cells in the event of polyploidization and/or multinucleation.[85] Therefore, Aurora A is involved in centrosomal maturation and in the absence of p53, Aurora A overexpression leads to failure of cytokinesis which in turn results in centrosome amplification and polyploidy.

Aurora A null mice are not viable and have been found with missing spindles, suggesting inability to form the spindle apparatus. When MEFs that are lacking one Aurora A allele were assayed, an approximate increase of 70% was found for polyploid cell populations. Inhibition of Aurora A kinase also generated similar findings. Thus, Aurora A is integral for development and lack of Aurora A results in polyploidy.[86]

Transcriptional Regulation

The essential heterodimer in the E4 transcription factor 1 (E4TF1) complex consists of E4TF1-60 and E4TF1-53, and this heterodimer increases expression of the Aurora A gene. E4TF1 was also shown to directly bind to the Aurora A promoter through electromobility shift assays (EMSAs).[82] Thyroid hormone receptor-associated protein complex 220 kDa (TRAP220) has been shown to directly bind to the Aurora A gene via ChIP experiments. Expression of TRAP220 increases basal level of Aurora A mRNA expression and overexpression of TRAP220 leads to overexpression of Aurora A mRNA.[87] ChIP experiments have found that both epidermal growth factor receptor (EGFR) and signal transducer and activator of transcription 5 (STAT5) bind to the Aurora A promoter. Knockdown of either EGFR or STAT5 or both leads to decreases in Aurora A mRNA expression.[88] Therefore, E4TF1, TRAP220, EGFR and STAT5 directly bind to the Aurora A promoter and transcriptionally activate Aurora A gene expression.

Phosphorylation Targets

Aurora A kinase targets a large array of proteins which are involved in a variety of processes, typically during mitosis. For example, Aurora A associates with the large tumor suppressor, homolog 2 (Lats2) protein and phosphorylates it at its serine 83 residue. This targets Lats2 to the centrosome.[89] Other centrosomal proteins phosphorylated by Aurora A include but are not limited to aster-associated protein (ASAP)[90], nuclear distribution gene E homolog (A.nidulans)-like 1 (NDEL1)[91] and transforming acidic coiled-coil 3 (TACC3)[92]. Aurora A also phosphorylates a host of transcription factors including p53. Phosphorylation of p53 at serine 315 by Aurora A leads to ubiquitination and degradation of p53 by the mouse

double minute 2 homolog (mdm2).[93] Phosphorylation of p53 at serine 215 by Aurora A prevents p53 transactivation by disrupting p53's DNA binding abilities.[94] Other transcription factor phosphorylation targets of Aurora A include Ikβα[95] and cFos[96]. Thus, Aurora A phosphorylates a variety of target proteins including centrosomal proteins and transcription factors.

Aurora A Kinase Dysregulation Promotes Tumorigenesis

Amplification of chromosome 20q is associated with a range of cancers and is required for promotion of colorectal invasive carcinomas. The DNA copy number of chromosome 20q parallels Aurora A protein expression. Inhibition of Aurora A kinase expression results in regression of invasive colorectal carcinomas.[58] Aurora A overexpression is common in colorectal patients and upregulation of Aurora A was detected in 41 out of 79 colorectal tumors.[97] Deletion of one Aurora A kinase allele in mice increased tumor incidence by 3-fold when compared to control mice with both Aurora A kinase alleles. Major tumors were found in lung, liver, lymph node and thymus tissue.[86] Other cancers with Aurora A overexpression include but are not limited to gliomas, cervical cancer, esophageal carcinomas, lung cancer and breast cancer.[98] Hence, Aurora A is a common oncogene present in a plethora of cancer types.

TPX2/Aurora A Kinase (TPX2-AurA) Complex

TPX2-AurA Interaction Activates Aurora A Kinase and Promotes Neurite Extension

Aurora A kinase activation is mediated by interaction of Aurora A with other proteins. These interactors include TPX2[99], human enhancer of filamentation 1 (HEF1)[100] and Ajuba[101]. The most defined activator of Aurora A is TPX2. Aurora A autophosphorylates and activates itself, the residue in humans is threonine (T) 288.[102] Protein phosphatase 2A deactivates Aurora A but binding to TPX2 restores kinase activity to Aurora A.[99] The crystal structure of Aurora A with or without the Aurora A binding domain of TPX2 indicates a conformational change in the catalytic domain of Aurora A. The key residue T288 which is accessible in Aurora A alone is tucked away upon TPX2 binding.[103] Thus, TPX2 interaction activates and stabilizes Aurora A kinase.

Aurora A kinase and TPX2 play a role in neurite extension in developing mice. Dorsal root ganglia from post-natal mice depend on atypical protein kinase C (aPKC), the TPX2-AurA complex and NDEL1. Phosphorylation of Aurora A at threonine (T) 287 by aPKC promotes TPX2-AurA interaction and Aurora A kinase becomes active. This occurs at the neurite hillock. Active Aurora A phosphorylates and recruits NDEL1 to the neurite hillock. Inhibition of any of these components reduces microtubule nucleation and polymerization at the neurite hillock. So, the TPX2-AurA complex promotes neurite extension in developing mice.[104]

Microtubule Nucleation Requires the TPX2-AurA Complex

The RanGTP gradient that regulates localization of TPX2 also regulates Aurora A microtubule localization and localization of receptor for hyaluronic-mediated motility (RHAMM), the γTuRC and neural precursor cell expressed developmentally downregulated protein 1 (NEDD1). The TPX2 in the TPX2-AurA complex associates with RHAMM which associates with NEDD1 which associates and recruits the γTuRC.[105] NEDD1 is phosphorylated by Aurora A at the residue serine (S) 405. Knockdown of NEDD1 or mutation of S405 to alanine (A) results in reduction of microtubule nucleation and spindle assembly defects. Expression of a constitutively active form of NEDD1 with a mutation at S405 to aspartic acid (D) restores microtubule nucleation and compensates for spindle defects.[106] This process was also shown to be RanGTP dependent.[105] Therefore, the TPX2-AurA complex plays an integral role in microtubule nucleation. A basic overview of the TPX2-Aurora A complex and its consequences are outlined in Figure 1.2.

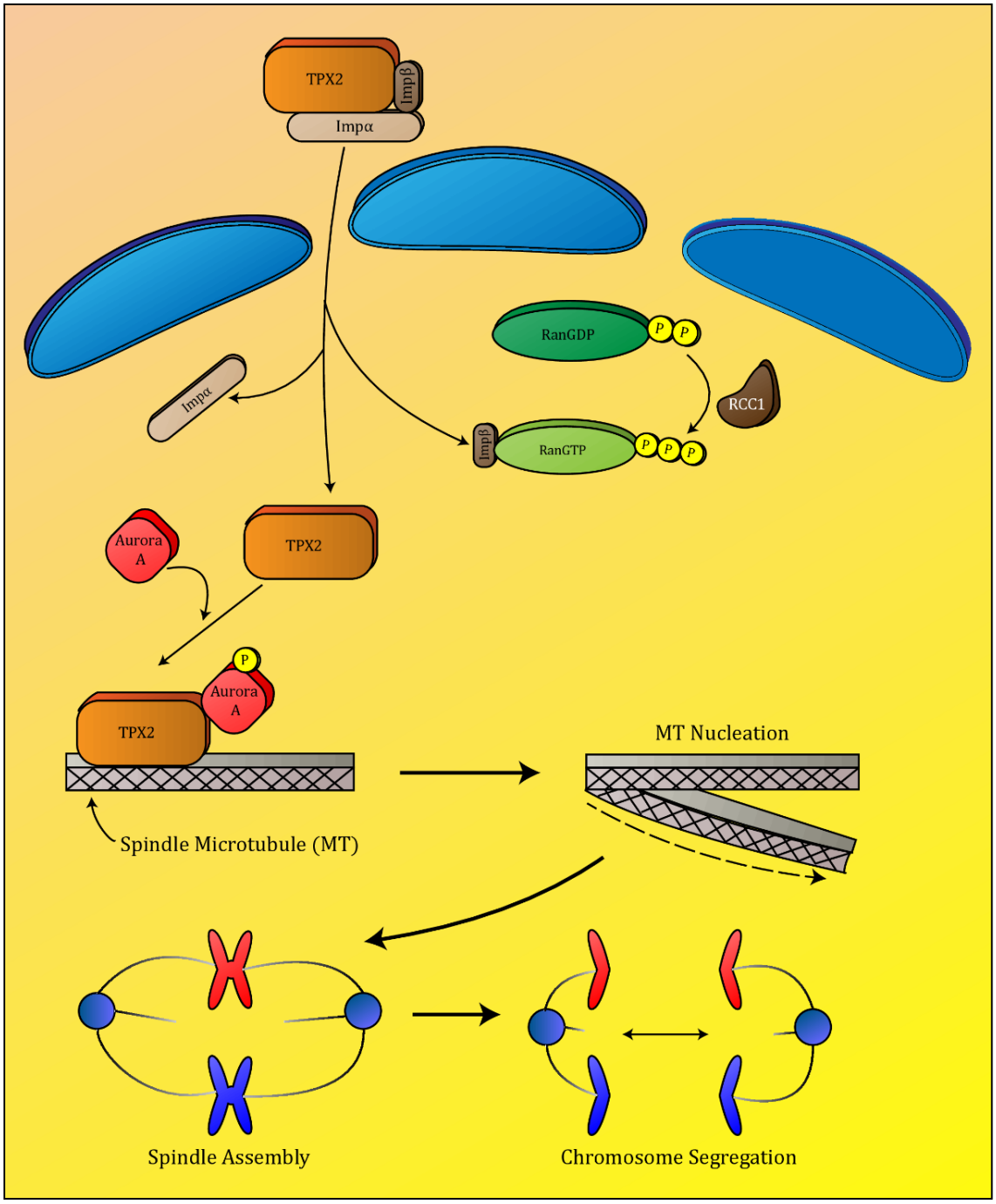

Figure 1.2: TPX2/Aurora A Pathway. TPX2 is bound to importin α (Impα) and importin β (Impβ) in the cytoplasm. Regulator of chromatin condensation1 (RCC1), a guanine exchange factor, replaces GDP with GTP on the Ran GTPase. Once the TPX2-Impα/Impβ complex translocates to the nucleus, RanGTP binds Impβ and weakens the Impα/Impβ complex bound to TPX2. Impα and TPX2 dissociate from each other. Free TPX2 binds to Aurora A kinase and Aurora A autophosphorylates and actives itself. The TPX2/Aurora A complex is localized to microtubules (MT), where Aurora A phosphorylates several factors which ultimately leads to MT nucleation. Eventually, the mitotic spindle is assembled and chromosome segregation ensues shortly after.

Dysregulation of TPX2 and Aurora A Kinase Magnify Oncogenic Progression

As previously stated, protein expression of Aurora A kinase and TPX2 are connected to the extent of chromosome 20q amplification. Both TPX2 and Aurora A are positively correlated with invasive colorectal carcinoma aggressiveness.[58] Aurora A and TPX2 are cooperatively overexpressed in a variety of cancers including but not limited to gastrointestinal, lung, liver, breast, kidney, ovary, prostate, head-neck and bladder cancers. Overexpression of both TPX2 and Aurora A suggests poor prognosis for patients.[75] TPX2 and Aurora A both induce polyploidy[60,86], which leads to chromosomal/genomic instability[76], one of the hallmarks of cancer. So, TPX2 and Aurora A work synergistically to drive several cancer types.

Biotin Identification (BioID)

A biotin ligase found in *Escherichia coli* is called bifunctional biotin-[acetylCoA carboxylase] holoenzyme synthetase/DNA-binding transcriptional repressor, bio-5'-AMP-binding (BirA).[107] BirA functions by binding to biotin molecules along with adenosine triphosphate (ATP), creating an intermediate molecule called biotinyl-adenosine monophosphate (bioAMP). When BirA comes into contact with primary amines on amino acids (lysine or a resonance structure of arginine), it tags the residue with biotin, releasing AMP. A mutant version of BirA, denoted as BirA*, has a mutation from arginine (R) at residue 118 to glycine (G). This R118G mutation decreases BirA's affinity for bioAMP which is then prematurely released.[108] Primary amines in the vicinity of BirA* will consequently be tagged with biotin.[109]

The promiscuous biotin ligase BirA* can be fused to a protein of interest and then be stably or transiently expressed in cell lines such as human embryonic kidney (HEK) 293T. Addition of biotin to media allows biotin to enter cells and the BirA* fusion protein will then tag proximal or interacting proteins with biotin.[109] In nature, one of the strongest noncovalent interactions is between biotin and streptavidin[110], so proteins tagged by the BirA* fusion protein can be purified on streptavidin-conjugated agarose beads[109]. These proteins can then be identified by mass spectrometry. This method of identifying potential interactors with a BirA* fusion protein is known as biotin identification (BioID).[109] Experiments on two subcomplexes of the nuclear pore complex suggest that a modest estimate of the BirA* labelling radius is 10 nanometers.[111]

Research Objectives

The initial goal was to perform BioID to identify novel interactors of CDCA7. Three constructs were generated: WT FLAG CDCA7-BirA*, T163A FLAG CDCA7-BirA* and Myc-BirA*. The protocol for BioID was then optimized for transient transfection of these constructs. Once an optimized protocol was established, potential interactors of CDCA7 were determined via BioID followed by mass spectrometry. A candidate interaction was then verified via coimmunoprecipitation of WT FLAG CDCA7 and the endogenous protein. Immunoprecipitation experiments, cell cycle synchronization experiments and immunofluorescence experiments were then employed to characterize the interaction.

Chapter II: Procedures, Protocols and Methodology

Cloning and Related DNA Procedures

Specifics details for cloning are present in the Appendix. Constructs that are not mentioned in the Appendix have been cloned for a previous publication[25] by other members of the Scheid lab. All constructs contain a carbenicillin resistance gene under a bacterial promoter. Unless stated otherwise, *E. coli* cells were grown in Lennox Luria Broth (LB) from Sigma Aldrich (Stock Keeping Unit/SKU L3022) supplemented with carbenicillin (100 µg/mL) from Sigma Aldrich (SKU C1613). *E. coli* cells are plated on LB-agar (1.5% w/v; Bacto™ Agar from Difco™ & BBL™, Catalog no. 214010) with carbenicillin (100 µg/mL). Cells are NEB® 5-alpha (DH5α strain) competent *E. coli* (subcoloning efficiency) cells (NEB Catalog# C2988). All cultures are incubated at 37°C, speed 5 on a VWR S-500 Orbital Shaker.

Polymerase Chain Reaction (PCR): The Q5 polymerase protocol was performed for all PCR reactions. First, volumes of all components were determined and then assembled on ice as follows: nuclease-free water (NEB Catalog# B9027), Q5 reaction buffer pack (NEB Catalog# B9027), Deoxynucleotide (dNTP) solution mix (NEB Catalog# N0447), reverse and forward primers, template DNA, and finally Q5 DNA polymerase (NEB Catalog# M0491). Reverse and forward primers are made in a master mix, where the primers have undergone a ten-fold dilution. Samples were placed on a thermocycler (Mastercycler® ep from Eppendorf), with the following settings: initial denaturation of 98°C for 30 seconds, 35 cycles and a final extension at 72°C for 2 minutes. Each cycle consists of denaturation (10 seconds, 98°C),

extension (30 seconds/kilo basepair, 50-72°C (based on melting temperature of primers)) and extension (25 seconds/kilo basepair, 72°C). PCR products have blunt ends.

Agarose Gel Electrophoresis: Agarose gels are 1% w/v agarose (BioRad #1613102) and made in TAE buffer, pH 8.3 (40 mM Tris, 20 mM acetic acid, 1 mM EDTA). The mixture is heated to dissolve the agarose and once it cools, SYBR® Green I nucleic acid gel strain (Sigma-Aldrich SKU S9430) is added. Gels are cast in an enclosed plastic tray where well-combs are added. Agarose gels are then placed in the Sub-Cell GT Cell apparatus from BioRad and TAE buffer is added to until the unit reaches full capacity. After samples are loaded, gels are run at constant voltage (175 volts) for 60 minutes. Current is provided through a VWR AccuPower Model 300 electrophoresis power supply unit.

Restriction Enzyme Digestion: Components of the reaction mixture first had their volumes established and were then assembled on ice as follows: nuclease-free water, buffer, restriction enzymes and finally template DNA. Reaction mixtures are made with the recommended enzymes buffers and incubated at the appropriate temperatures for the indicated time periods, as mentioned in the manufacturer's protocol (New England Biolabs Inc.). Sequential digests were based on the salt concentrations of the reaction buffers, with low concentrations digested first and higher concentrations after.

Transformation: DH5α *E. coli* cells (50 µL) are thawed on ice and mixed with 1-5 µL of plasmid DNA with gentle agitation. The plasmid-bacteria mix is placed back on ice for 30 minutes. Cells are placed on the Eppendorf Thermomixer 5436 for 45 seconds at 42°C (heat shock) and then placed back on ice for 5 minutes. Then cells are resuspended in SOC Outgrowth Medium (NEB Catalog# B9020) and incubated at 37°C for at least one hour. The

cells are then resuspended and plated onto an LB-agar plate and placed inverted, overnight at 37°C. If colonies appear the next day, plates are stored at -4°C until further use.

Ligations: The volumes of the reaction mixture components were first determined and then the components were assembled on ice as follows: nuclease-free water, T4 DNA ligase buffer (NEB Catalog# B0202), vector DNA, insert DNA and finally T4 DNA ligase (NEB Catalog# M0202). The reaction mixture is incubated for at least 10 minutes at 25°C. The ligations are then transformed. Insert DNA to vector DNA ratios are typically done as 1:1 or 3:1, where the size of insert in nucleotides/size of vector in nucleotides multiplied by the amount of vector used determines the amount of insert DNA required for 1:1 reactions. A control where only vector DNA is used in the ligation is performed to account for the rate of vector DNA re-annealing to itself. Ideally, this is zero, but if colonies are present, there should be more colonies in the actual ligation reactions, in comparison to the vector control.

Gel Extraction: DNA was purified from agarose gel cut-outs with PureLink™ Quick Gel Extraction kit from ThermoFisher Scientific (Catalog no. K210012), according to the manufacturer's protocol.

Miniprep: After DNA is transformed onto LB-agar plates, a colony was picked and grown overnight in 2 mL of media. Cells are pelleted with an Eppendorf 5415D Centrifuge, at 4000 g, 4°C for 1 minute. The majority of the media is aspirated leaving 50-100 µL. Cells are resuspended via VWR Vortex Mixer (2 to 5 seconds). Then 300 µL of TENS lysis buffer (10 mM Tris-HCl (pH 10.5), 1mm EDTA, 150 mM NaCl, 0.5% SDS w/v) is added and cells are vortexed for 2 to 5 seconds. Next, 150 uL of sodium acetate (3 M) is added and lysates are vortexed for 2 to 5 seconds. Cell debris and chromosomal DNA is pelleted at 12,000 g, room

temperature (RT) for 4 minutes. The supernatant is transferred to a new tube and mixed with 900 µL of 95% ethanol. DNA is pelleted at 16,000 g, RT for 10 minutes. The supernatant is aspirated, and pelleted DNA is washed twice with 70% ethanol. The DNA pellet is then resuspended in TE buffer with 100 µg/mL of RNase A (from the PureLink™ HiPure Plasmid Midiprep kit (Catalog no. K210004)).

Midi/Maxiprep: After DNA is transformed onto LB-agar plates, a colony was picked and grown overnight in 100 mL of media. DNA was purified from the overnight cultures of DH5α *E. coli* cells with PureLink™ HiPure Plasmid Midiprep kit (Catalog no. K210004) or PureLink™ HiPure Plasmid Filter Maxiprep kit (Catalog no. K210017) or GeneJET Plasmid Midiprep kit (Catalog no. K0481), according to the manufacturer's protocol. All kits are from ThermoFisher Scientific.

Sequence Verification: After DNA is midi/maxiprepped, plasmid DNA is sent for sequencing at Bio Basic Inc. or TCGA Facilities (Sick Kids Hospital) along with associated sequencing primers for the construct. The sequence reads are compared to the sequence of the gene insertion with the Nation Center for Biotechnology Information (NCBI) tool called Align Sequences Nucleotide BLAST. BLAST stands for Basic Local Alignment Search Tool.

Cell line and Cell Culture Conditions

Cell lines: Human Embryonic Kidney (HEK) 293T cells were obtained from American Type Cell Culture Collection and HeLa cells (cervical cancer cells) were a gift from the McDermott lab at York University. NIH 3T3 mouse embryonic fibroblast cells were purchased from Sigma-Aldrich.

Cell culture: Cells were cultured in Dulbecco's modified Eagle's medium (DMEM) from ThermoFisher Scientific (Catalog no. 11995065) which also contained 10% fetal bovine serum (FBS) from ThermoFisher Scientific (Catalog no. 10438026). Media also contained the antibiotics streptomycin and penicillin (Catalog no. 15140163) and a derivative of L-glutamine called GlutaMAX™ (Catalog no. 35050061), both from ThermoFisher Scientific. Cells are incubated at 37°C, 5% CO_2 in a Sanyo MCO-18AIC UV Double Stack Incubator.

Passaging: When cells reach 70-80% confluency in a 100 mm dish, media is aspirated and then cells are washed once with 10 mL of phosphate-buffered saline (1X) from Corning™ (Catalog no. 21-040-CV). Then cells are incubated with 2 mL of Trypsin-EDTA solution from Sigma-Aldrich (Stock Keeping Unit/SKU T4299) at 37°C, 5% CO_2 for either 1 minute (HEK 293T cells) or 5 minutes (HeLa cells). Then cells are resuspended with 8 mL of media and plated to the desired dilution.

Long-term storage: One 100 mm dish that is 70-80% confluent is washed once with PBS, trypsinized and then cells are collected through centrifugation (100 g, room temperature for 1 minute). Media is aspirated and then cells are resuspended in 4 mL of storage media. Storage media consists of DMEM with 10% dimethyl sulfoxide (DMSO) from BioShop Canada

(DMS666), 20% FBS and antibiotics. Next, 1 mL of cells is added to a total of four Corning™ externally threaded cryogenic vials from Fisher Scientific (Catalog no. 09-761-71) and stored at -80°C until further use.

Thawing: Cells in a cryogenic vial are placed in a water bath at 37°C until nearly thawed. One mL of DMEM is added drop wise to the cells and then cells are plated in a 100 mm dish with 8 mL of media. A second 100 mm dish, diluted ten-fold, is plated from the first dish. The next day, media is replaced with fresh cell culture media.

Transfection

Cells are seeded so that plates are 70-80% confluent on the day of transfection. Before transfection, all components must be at room temperature (RT). An Axygen® 1.5mL MaxyClear Snaplock Microcentrifuge Tube (Corning™ Catalog no. MCT-150-C) is filled with 200 µL, 1 mL or 2 mL of Opti-MEM™ I reduced serum medium from ThermoFisher Scientific (Catalog no. 31985070) for 35 mm, 100 mm or 150 mm dishes, respectively. Next, 3 µg, 8 µg or 21µg of plasmid DNA are added to the tubes for 35 mm, 100 mm or 150 mm dishes, respectively. Then, polyethylenimine (PEI) from Polysciences (cat# 23966-2) is added so that the DNA-PEI ratio is 1:3 w/w. The DNA-PEI mixture is vortexed and then incubated at RT for 30 minutes. The mixture is then diluted in 800 µL, 3 mL or 6 mL of tissue culture media for 35 mm, 100 mm or 150 mm dishes, respectively. Media is aspirated from cells and then the DNA-PEI mixture is added to cells, overnight at 37°C, 5% CO_2. Cells are then subjected to treatments or immediately lysed.

Sodium Dodecyl Sulfate Polyacrylamide Gel Electrophoresis (SDS-PAGE)

Handcast Gels: Gels are cast in 1 mm integrated spacers. The separating gel is cast first, followed by the stacking gel with a 10 well-comb. Both the separating and stacking gels are made from 30% acrylamide from BioShop Canada (Catalog no. ACR010). The separating gel (10% acrylamide) was composed of 375 mM Tris (pH 8.8), 0.1% sodium dodecyl sulfate (SDS), 0.1% ammonium persulfate (APS) and the stacking gel (4% acrylamide) was composed of 125 mM Tris (pH 6.8), 0.1% SDS, 0.1% APS. APS was added immediately before the addition of Tetramethylethylenediamine (TEMED) from Bioshop Canada (Catalog no. TEM001). After gels are produced, they are assembled on the MiniPROTEAN® Tetra vertical electrophoresis cell from BioRad. The unit is filled to the required volume with running buffer, pH 8.6 (25 mM Tris, 192 mM glycine, 0.1% SDS w/v). After samples are loaded, the gel is run at constant voltage (175 volts) for 60 minutes. Current is provided through a VWR AccuPower Model 300 electrophoresis power supply unit.

Silver Stain Gels: Gels are cast in Hoefer™ glass plates (1.0 mm) for SE 600 Standard from Fisher Scientific (Catalog no. 36-100-3845). The compositions of the separating (12.5% acrylamide) and stacking (5% acrylamide) are 375 mM Tris (pH 8.8), 0.1% SDS, 0.1% APS and 125 mM Tris (pH 6.8), 0.1% SDS, 0.1% APS, respectively. APS was added immediately before the addition of TEMED. Once gels are produced, they are assembled on the Hoefer™ SE 600 vertical electrophoresis unit from Fisher Scientific. The unit is filled to the required volume with running buffer, pH 8.6. After samples are loaded, the gel is run at constant voltage (50 volts) for 15 hours. Current is provided through a VWR AccuPower Model 300 electrophoresis power supply unit.

Precast Gels: Criterion™ XT Precast 4-12% Bis-Tris gels from BioRad (Catalog no. 3450124) are assembled into the Criterion™ vertical electrophoresis cell (BioRad). The unit is filled with 500 mL of 1X MOPS buffer from BioRad (Catalog no. 1610788). After samples are loaded, the gel is run at constant voltage (150 volts) for 90 minutes. Current is provided through a VWR AccuPower Model 300 electrophoresis power supply unit.

Gel Staining

Coomassie Staining: All staining procedures used Coomassie brilliant blue G-250 dye from ThermoFisher Scientific (Catalog no. 20279). After electrophoresis, gels are placed in containers and completely covered in fixing solution (50% methanol, 10% acetic acid) for 30 minutes. Gels are then incubated in staining solution (Coomassie brilliant blue G-250 (0.05% w/v), 50% methanol, 10% acetic acid) for at least one hour. Finally, gels were destained for visualization with destaining solution (5% methanol, 7% acetic acid).

Silver Staining: Gels were visualized with silver staining with the ProteoSilver™ Silver Stain Kit from Sigma-Aldrich (Stock Keeping Unit/SKU PROTSIL1), according to the manufacturer's protocol.

Western Blot Procedures

Only Criterion™ XT Precast 4-12% Bis-Tris gels are used for western blotting procedures.

Transfer: Immobilon-P (PVDF) Membrane (Millipore Sigma Catalog no. IPVH00010) and Fisherbrand™ Pure Cellulose Chromatography Paper (transfer paper) from Fisher Scientific (Catalog no. 05-714-4) were cut out into rectangle pieces, based on the dimensions of the gel to be transferred. The polyvinylidene fluoride (PVDF) membrane is activated by completely immersing the membrane in 100% methanol for 10 minutes. The membrane is then soaked in transfer buffer, pH 7.2 (bicine 25 mM, Bis-Tris 25 mM, EDTA 1 mM, 10% methanol). Once the gel has finished running, the gel and transfer paper are soaked entirely in transfer buffer for 10 minutes. The components for transfer are assembled on a Semiphor Semi-dry transfer unit from Amersham Pharmacia Biotech. The order of the components are as follows: three pieces of transfer paper, PVDF membrane, gel and three more pieces of transfer paper. The transfer apparatus is run at constant current (50 milliamps/gel) for 108 minutes. The membrane is washed twice with ultrapure water, 5 minutes per wash, before blocking.

Block: Blocking buffer depends on the type of secondary antibody (fluorescent vs. horse radish peroxidase (HRP)). For fluorescent secondary antibodies, membranes are incubated in Odyssey® Blocking Buffer (TBS) from LI-COR (Product Number 927-50000) for at least 30 minutes, prior to incubation with primary antibody. For HRP secondary antibodies, membranes are incubated in 5% bovine serum albumin (BSA) for at least 30 minutes, prior to primary antibody incubation. BSA is from Sigma-Aldrich (Stock Keeping Unit/SKU A2153).

Blot: All antibody mixtures are made in tris-buffered saline (TBS), pH 7.4 (50 mM Tris-HCl, 150 mM NaCl) with 25% blocking buffer. Primary antibodies are added to the antibody mixture with 0.1% Tween®-20 from BioShop Canada (Catalog no. TWN510). The primary antibodies are incubated with the membrane in a glass tray for one hour at room temperature or overnight at 4°C. Next, membranes are washed three times, 5 minutes per wash, with 0.1% Tween®-20 in TBS (TBS-T). Secondary antibodies are added to the antibody mixture with 0.2% Tween®-20 and 0.01% SDS. Secondary antibodies are incubated in the dark for one hour at room temperature. Membranes are once again washed three times, 5 minutes per wash, with 0.1% TBS-T before being processed.

Odyssey: If fluorescent secondary antibodies are used, membranes are scanned on the Odyssey® Infrared Imaging System, Model 9120. The system can detect emission wavelengths at 700 nm and 800 nm.

Film: If HRP secondary antibodies are used, membranes are incubated in Pierce™ ECL western blotting substrate from ThermoFisher Scientific (Catalog no. 32106) for 5 minutes. In a dark room, the membrane, which is secured to an X-ray film cassette, has CL-XPosure™ film from Thermofisher Scientific (Catalog no. 34090) exposed to it for various time periods. The film is then developed and fixed manually by placing the film in the developing solution and then fixing solution, for as long as desired.

BioID

RIPA Buffer Protocol: Cells are lysed via sonication on ice in radioimmunoprecipitation assay (RIPA) buffer, pH 7.5 (50 mM Tris-HCl, 150 mM NaCl, 1% Triton-X100, 1% sodium deoxycholate, 2 mM EDTA, 0.1% SDS). Triton-X100 is from BioShop Canada (Catalog no. TRX506). Lysis buffer was supplemented with cOmplete™, EDTA-free Protease Inhibitor Cocktail from Sigma-Aldrich (Stock Keeping Unit/SKU 11873580001) and Benzonase from Sigma-Aldrich (SKU E1014). Sonication was performed on Qsonica XL-2000 sonic homogenizer, with 3 seconds bursts, followed by 10 second rests, at 5 watts output, until the solution became transparent. Cell debris is pelleted through centrifugation (16,100 g, 4°C for 15 minutes). Soluble lysate is incubated with streptavidin-conjugated agarose beads from Millipore Sigma (SKU 69203-3) at 4°C, overnight on a nutator. Next, the lysate is aspirated, and beads are washed 5 times with RIPA buffer. After each wash, beads are pelleted through centrifugation (400 g, 4°C for 1 minute). After the last wash is removed, cells are eluted in SDS sample buffer, pH 6.8 (50 mM Tris-HCl, 2% SDS, 10% glycerol, 1% β-mercaptoethanol, 12.5 mM EDTA, 0.02% bromophenol blue). β-mercaptoethanol is from BioShop Canada (Catalog no. MER002) and bromophenol blue is from Sigma-Aldrich (SKU B0126). Beads are then placed on a heat rack at 100°C for 10 minutes. Samples are stored at -20°C until further use.

Roux Protocol: Cells are lysed with sonication on ice in an SDS-based buffer, pH 7.4 (50 mM Tris, 500 mM NaCl, 0.4% SDS, 5 mM EDTA, 1 mM DTT), supplemented with protease inhibitor. Then Triton-X100 is added to a final concentration of 2% and cells are sonicated on ice. Next, 50 mM Tris, pH 7.4 is added to half the concentration of SDS and prevent

precipitation. Cells are lysed via sonication on ice and cell debris is pelleted through centrifugation (16,100 g, 4°C for 15 minutes). Soluble lysate is incubated with streptavidin-conjugated agarose beads at 4°C, overnight on a nutator. Next, the lysate is aspirated, and beads are washed, where each wash occurs for 8 minutes, 25°C on a nutator. After each wash, beads are pelleted through centrifugation (400 g, 4°C for 1 minute). Beads are washed twice with wash buffer 1 (2% SDS). The lysate is then washed once with wash buffer 2, pH 7.5 (50 mM Hepes, 150 mM NaCl, 1% Triton-X100, 1% sodium deoxycholate, 1 mM EDTA) and once with wash buffer 3, pH 8.1 (10 mM Tris, 250 mM LiCl, 0.5% NP-40, 0.1% deoxycholate, 1 mM EDTA). Beads are finally washed twice with wash buffer 4, pH 7.4 (50 mM Tris, 50 mM NaCl). After the last wash is removed, cells are eluted in SDS sample buffer saturated in biotin (50 μM) from Sigma-Aldrich (SKU B5401). Samples are stored at -20°C until further use.

Mass Spectrometry

Sample preparation, processing and analysis were done by Andrew Macklin, from the Centre for Research in Mass Spectrometry at York University.

Sample Generation: The volumes mentioned in this protocol are valid for one sample. After the sample is subjected to the BioID Roux protocol, streptavidin-conjugated beads are washed three times in 50 mM ammonium bicarbonate, pH 8.0. Each wash is followed by a centrifugation step at 400 g, room temperature (RT) for one minute. After the last wash is aspirated, beads are resuspended with 200 μL of 50 mM ammonium bicarbonate, pH 8.0 and agitated overnight at 37°C with 1 μg of Promega modified trypsin (Catalog no. V5111). After the overnight incubation, 0.5 μg of trypsin is added to the sample for two more hours, at 37°C with agitation. Next, beads are pelleted at 400 g, RT for two minutes and the supernatant is

shifted to a new tube. Two washes with ultrapure water (150 µL each) are applied to the beads and following each wash, beads are pelleted at 400 g, RT for one minute. The washes are pooled with the supernatant and the samples are lyophilized in an Eppendorf® Vacufuge concentrator at 4°C, overnight. Finally, samples are resuspended in 5% formic acid (10 µL) and sent for mass spectrometry. Formic acid is from Sigma-Aldrich (Stock Keeping Unit/SKU 106526).

Sample Preparation: Samples are desalted prior to separation via chromatography. Samples were bound to C18 ZipTip pipette tips from Millipore Sigma (Catalog no. ZTC18S096). Prior to binding samples, ZipTips are cleansed in acetonitrile and washed with water. Once the samples are bound, ZipTips are washed in 0.1% formic acid and then eluted with 80% acetonitrile. Samples are lyophilized overnight at 4°C and then resuspended in 0.1% formic acid.

Processing and Analysis: Samples are first subjected to reversed-phase chromatography and the eluted peptides are detected with a 10 µm PicoFrit emitter and scanned with an LTQ Orbitrap Elite mass spectrometer. The Proteome Discoverer 1.4 program was used to process the obtained data, and then the processed data was compared to the UniPort Data base for *Homo sapiens* in order to identify proteins. Proteins detected at a 10 ppm mass threshold, with two or more peptides per match were considered. Identified proteins are then ranked based on their score. Experimental and control samples are compared and proteins that are common among both are ruled out, along with typical contaminants.

Immunoprecipitation (IP)

Cells are lysed via sonication on ice in Nonidet P-40 (NP-40) lysis buffer, pH 7.4 (50 mM Tris-HCl, 150 mM NaCl, 1% NP-40). NP-40 is from BioShop Canada (Catalog no. NON505). Lysis buffer was supplemented with Pierce™ protease and phosphatase inhibitor mini-tablets, EDTA free from ThermoFisher Scientific (Catalog no. 88669). Sonication was performed with 3 seconds bursts, followed by 10 second rests, at 5 watts output, until the solution became transparent. Cell debris is pelleted through centrifugation (16,100 g, 4°C for 15 minutes). Soluble lysate is incubated with anti-FLAG M2 agarose beads from Sigma-Aldrich (Stock Keeping Unit/SKU A2220) at 4°C, overnight on a nutator. Next, the lysate is aspirated, and beads are washed 3 times with NP-40 lysis buffer. After each wash, beads are pelleted through centrifugation (400 g, 4°C for 1 minute). After the last wash is removed, cells are eluted in SDS sample buffer. Beads are then placed on a heat rack at 100°C for 10 minutes. Samples are stored at -20°C until further use.

GST Pulldown

Bacterial Culture: BL21-codon plus (DE3) – RIPL *E. coli* cells were transformed with a GST construct, following the same protocol for DH5α *E. coli* cells (refer to DNA Cloning subsection). A colony was picked and grown in 10 mL of LB media with carbenicillin (100 µg/mL) overnight at 37°C, speed 5 on a VWR S-500 Orbital Shaker. The next day, the overnight culture was diluted into 45 mL of LB media with carbenicillin and incubated for 1 hour. When the optical density (OD) of the culture reached 0.8-1 at 600 nm, 60 µL of lysate was taken as a non-induced sample. The culture was then split into two 25 mL cultures and

each culture was induced with a different source of isopropyl β-D-1-thioglactopyranoside (IPTG) at a final concentration of 1 mM, for 2 hours. IPTG was either from BioShop Canada (Catalog no. IPT002) or Sigma-Aldrich (Stock Keeping Unit/SKU I6758). The cultures were then spun down at 4000 g, 4°C for 20 minutes in an Eppendorf Centrifuge 5804. The pellets were immediately lysed or stored at -20°C until further use.

GST Lysate Preparation: Frozen pellets were thawed at room temperature and then resuspended in phosphate buffered saline(PBS), pH 7.4 (4.3 mM Na_2HPO_4, 1.47 mM KH_2PO_4, 137 mM NaCl, 2.7 mM KCl, 5 mM DTT). The solution was produced by adding dithiothreitol (DTT) to phosphate-buffered saline (1X) at a final concentration of 5 mM. The solution will be called 1X PBS. Cells were then lysed with six 10 second pulses at a final watt output of 5, alongside 10 second intervening rest periods. Cells were then centrifuged (16,100 g, 4°C for 15 minutes) and a sample of induced soluble lysate (60 µL) was taken. Next, 100 µL of Pierce™ Glutathione agarose beads (GSH beads) were washed three times with water and equilibrated with three washes of 1X PBS. Each wash is followed by a centrifugation step (400 g, 4°C for one minute).

GST Purification: The lysate is diluted 4-fold with 1X PBS and then 1 mL of diluted lysate is incubated at 4°C with GSH beads, on a nutator for 30 minutes. After incubation with GSH beads, the lysate is aspirated and the beads are subjected to seven washes in 1X PBS. Each wash is followed by a centrifugation step (400 g, 4°C for one minute). Then GSH beads are resuspended with 1X PBS and 20 µL of the resuspended resin is taken as a sample. The final wash is spun down at 400 g, 4°C for one minute and a 60 µL wash sample is taken. Finally, GSH beads are incubated in GST elution buffer (20 mM reduced glutathione, 50 mM Tris-HCl,

pH 9.0) for 10 minutes, and gently agitated every 2 minutes. Reduced glutathione was from Sigma-Aldrich (SKU G4251). The beads are then spun down at 2000 g, 4°C for 5 minutes. A sample of the elution (60 µL) was taken. All samples aside from the GSH resin are mixed with 20 µL of 4X SDS sample buffer. The GSH resin was pelleted (400 g, 4°C for one minute), 1X PBS was aspirated and the beads were eluted in 40 µL of 1X SDS sample buffer.

Synchronization

Double Thymidine Block: Following transfection, cell culture media is replaced with media containing 2 mM of thymidine and incubated for 19 hours. Cells are washed once in phosphate buffered saline (PBS), pH 7.4 and then incubated in fresh media without thymidine for 9 hours. Cells are once again incubated in media containing 2 mM of thymidine for 16 hours. Cells are either lysed immediately or released in media without thymidine for a desired time period. Thymidine was from Sigma-Aldrich (Stock Keeping Unit/SKU T9250)

RO3306 G2/M Block: Following transfection, cell culture media is replaced with media containing 10 µM of RO3306 and incubated for 18 hours. Cells are either lysed immediately or released in media without RO3306 for a desired time period. RO3306 was from Sigma-Aldrich (SKU SML0569).

Cell Cycle Examination

Sample preparation: Following transfection and desired treatments, cells are incubated with 2 mL of Trypsin-EDTA solution at 37°C, 5% CO_2 for 1 minute, resuspended in 8 mL of cell culture media and transferred to a 15 mL conical tube. Cells are spun down at 2000 g, room temperature for one minute and resuspended in phosphate buffered saline (PBS), pH 7.4. Cells spun down at 2000 g, 4°C for one minute, washed with PBS and pelleted again. The majority of the PBS is aspirated leaving 100 µL. Then the cells are placed on a vortex, agitated gently and 300 µL of 70% ethanol was added to the cells drop wise. After the addition of ethanol, cells are stored at -20°C overnight. The next day, cells are washed twice in PBS, each wash was followed by a centrifugation step (2000 g, 4°C, 1 minute). Then cells are resuspended in PBS and PureLink™ RNase A from ThermoFisher Scientific (Catalog no. 12091021) was added to a final concentration of 500 µg/mL. Cells were incubated in RNase A for 30 minutes at 37°C. Next, propidium iodide was added to cells at a final concentration of 40 µg/mL and samples were incubated at 37°C for 30 minutes. Propidium iodide was from ThermoFisher Scientific (Catalog no. P1304MP). Samples were then analyzed via flow cytometry.

Flow cytometry: Samples were loaded on a FACSCalibur flow cytometer and visualized through CellQuest™ Pro software. A forward scatter vs. side scatter plot determined that there was one only population of cells (no contamination from other cell types). A forward scatter plot was used to determine the population of singular cells. This channel was gated so that only singular cells would be accepted for DNA content analysis. Finally, the DNA

content of the cells were analyzed over 50,000 events where one event equates to the scanning of a singular cell. The data was further analyzed by Dr. Michael P. Scheid.

Microscopy

All experiments were performed jointly with Dr. Michael P. Scheid.

Sample Preparation: Cells are plated on no. 1 glass coverslips and fixed after transfection and desired treatments. Next, coverslips are washed in phosphate buffered saline (PBS), pH 7.4, and after the PBS is aspirated, coverslips are overlaid with 100% methanol at -20°C for 15 minutes to fix cells. Then, cells are washed twice with PBS. Following fixation, cells are blocked with 1% BSA in PBS for 30 minutes followed by incubation with primary antibody in 1% BSA PBS for 1-2 hours at room temperature. Slides are washed three times with 1% BSA PBS plus 0.025% Tween-20® (PBS-T). Secondary antibody in 1% BSA PBS-T is added for 1-2 hours, room temperature, in the dark. Coverslips are washed three times with 1% BSA PBS-T, twice with ultrapure water and then dried and mounted on Fisherbrand ™ Superfrost™ plus microscope slides from Fisher Scientific (Catalog no. 12-550-15) with Prolong™ Gold Antifade mountant with DAPI from ThermoFisher Scientific (Catalog no. P36935). Slides are sealed with nail polish and viewed the next day.

Fluorescence Microscopy: An Olympus microscope was used to visualize cells and images are procured with a QImaging 2000R camera linked to the QCapture Pro program.

Confocal Microscopy: Slides were visualized and images were taken at the Imaging Facility at York University.

List of Common Reagents

All aqueous acids, bases and alcohols were purchased from the store in Petrie Science and Engineering building at York University.

Table 2.1: Common reagents purchased from BioShop Canada.

Name	Catalog no.
Dithiothreitol	DTT002
Ethylenediaminetetraacetic acid (EDTA)	EDT002
Sodium Acetate ($NaCH_2COOH$)	SAA304
Sodium Chloride (NaCl)	SOD004
Sodium Dodecyl Sulfate (SDS)	SDS001
Tris (tris(hydroxymethyl)aminomethane)	TRS001
Tris-hydrochloride (HCl)	TRS004

Table 2.2: Common reagents purchased from Sigma-Aldrich. SKU is Stock Keeping Unit.

Name	SKU
Ammonium persulfate (APS)	A3678
Bicine	B3876
Bis-Tris	B9754
Glycine	G7126
Sodium deoxycholate	D6750

Chapter III: Discoveries, Findings and Results

Proximity-dependent Biotin Identification (BioID)

Abridged Version

The BioID protocol was optimized for the eGFP-3xNLS-BirA* and WT FLAG CDCA7-BirA* constructs.

Methods

Western Blot: Western blots followed the general protocol outlined in Chapter 2. For streptavidin pulldowns, biotinylated proteins were detected with IRDye® 680RD Streptavidin, which is streptavidin conjugated to an infrared (IR) fluorophore from LI-COR (Product Number 925-68079). FLAG constructs were detected with the mouse monoclonal anti-FLAG M2 antibody from Sigma-Aldrich (Stock Keeping Unit/SKU F1804). GFP constructs were detected with the GFP (D5.1) XP® rabbit monoclonal antibody from Cell Signaling Technology (Product Number 2956).

Results

An optimized BioID protocol tailored to CDCA7 needed to be established before determining potential protein interactors of CDCA7 through mass spectrometry. The initial objective was to clone the following three constructs: WT FLAG CDCA7-BirA*, T163A FLAG CDCA7-BirA* and c-Myc-BirA* (Appendix A). However, experiments were only performed on WT FLAG CDCA7-BirA*. A control plasmid to evaluate non-specific targets of biotinylation was generated by fusing enhanced green fluorescent protein (eGFP) with BirA*. To mimic

the nuclear localization of CDCA7, a coding region containing three tandem copies of the SV40 large T antigen nuclear localization sequence (NLS) was incorporated to generate eGFP-3xNLS-BirA. The construct eGFP-3xNLS-BirA* will be referred to as GFP-BirA* here after.

Two consecutive BioID protocols were investigated. The initial protocol is based in radioimmunoprecipitation assay (RIPA) buffer, which lyses both cytoplasmic and nuclear components of cells. Human embryonic kidney (HEK) 293T cells were transiently transfected with the GFP-BirA* or the WT FLAG CDCA7-BirA* construct for 24 hours. The cells were then left untreated or incubated in DMEM supplemented with 50 μM of biotin for 24 hours. Cells were then lysed in RIPA buffer supplemented with benzonase and protease inhibitor. Benzonase is an endonuclease that cleaves and degrades all forms of DNA and RNA, but has no proteolytic activity. The nuclease ensures that biotinylated DNA is not purified. The soluble lysate was incubated with streptavidin-conjugated agarose beads overnight on a nutator at 4°C. The beads were then washed five times in RIPA buffer prior to elution with sodium dodecyl sulphate (SDS) sample buffer.

Western blots of the lysates confirm that both GFP-BirA* and WT FLAG CDCA7-BirA* were expressed (Figure 3.1). Biotinylated proteins were identified by probing blots of streptavidin pulldowns with streptavidin IRDye followed by detection on a fluorescence scanner (Odyssey). Addition of biotin leads to an increase in the amount of purified biotinylated protein when BirA* constructs are expressed. However, the addition of biotin to untransfected cells has no effect on the amount of purified biotinylated protein (Figure 3.1). Furthermore, upon addition of biotin, the increase in biotinylated protein detected in the

streptavidin pulldowns is more evident for the GFP-BirA* control than for WT FLAG CDCA7-BirA*. There were also too many nonspecific interactors present in the absence of biotin (Figure 3.1). As a result, another protocol was considered.

The next protocol involved the use of an SDS-based lysis buffer and a series of 4 wash buffers designed to reduce nonspecific interactions. This protocol was developed by the Roux Lab at Sanford Research[109] and will be referred to as the BioID Roux protocol. The SDS-based lysis buffer also lyses both nuclear and cytoplasmic fractions of cells. HEK 293T cells were transiently transfected with GFP-BirA* or WT FLAG CDCA7-BirA* for 6 hours. The cells were then left untreated or incubated in DMEM supplemented with 50 μM of biotin for 24 hours. After lysis via sonication, the lysates were incubated with streptavidin-conjugated agarose beads, overnight on a nutator at 4°C. The beads were then washed with a series of buffers. The first wash buffer utilizes SDS, an ionic detergent, to harshly strip nonspecific interactors. The second wash buffer utilizes Triton-X100, a nonionic detergent, to strip nonspecific interactors that are still bound to the beads. The third wash buffer includes a high concentration of lithium chloride to strip any remaining nonspecific interactors. The last wash buffer removes detergents from the sample. Finally, the beads were eluted in SDS sample buffer saturated in biotin.

Streptavidin pulldowns were run on 12.5% polyacrylamide gels and silver stained in order to determine the total protein content of the pulldowns. The silver stains showed that the addition of biotin substantially increased the amount of protein purified by streptavidin-conjugated agarose beads. This result was apparent for both GFP-BirA* and WT FLAG CDCA7-BirA* (Figure 3.2). Both GFP-BirA* and WT FLAG CDCA7-BirA* are highly visible

following the addition of biotin (Figure 3.2). In the absence of biotin, few nonspecific interactors were detected (Figure 3.2). Since the BioID Roux protocol resolved the issues experienced with the RIPA buffer protocol, it was chosen for all future BioID experiments.

In order to increase the yield of protein required for mass spectra identification, an experiment was conducted where increasing amounts of lysate was applied to a set amount of streptavidin beads. Unlike previous experiments, which were carried out in 100 mm tissue culture dishes, the following experiment was carried out in 150 mm dishes. Either GFP-BirA* or WT FLAG CDCA7-BirA* was transfected into thirteen 150 mm dishes of HEK 293T cells, incubated with DMEM supplemented with 50 μM of biotin and each dish was lysed with 1 mL of lysis buffer. Then 50 μL of streptavidin-conjugated agarose beads were incubated with 1 mL, 4 mL or 8 mL of soluble lysate. The remainder of the procedure followed the BioID Roux protocol.

Streptavidin-conjugated beads were subjected to western blots that were probed with streptavidin IRDye or run on 12.5% polyacrylamide gels and silver stained. The western blots of the streptavidin pulldowns showed that the amount of biotinylated protein pulled down decreased as the volume of soluble lysate increased for both GFP-BirA* and WT FLAG CDCA7-BirA* (Figure 3.3). The silver stain also showed a decrease in the amount of protein pulled down by streptavidin-conjugated beads as the amount of soluble lysate increased for both GFP-BirA* and WT FLAG CDCA7-BirA* (Figure 3.3). Despite the odd trend, where increasing the volume of lysate decreased the amount of purified protein, it became evident that one 150 mm plate of HEK 293T cells lysed in 1 mL of lysis buffer pulled down a sufficient amount of protein for mass spectrometric analysis.

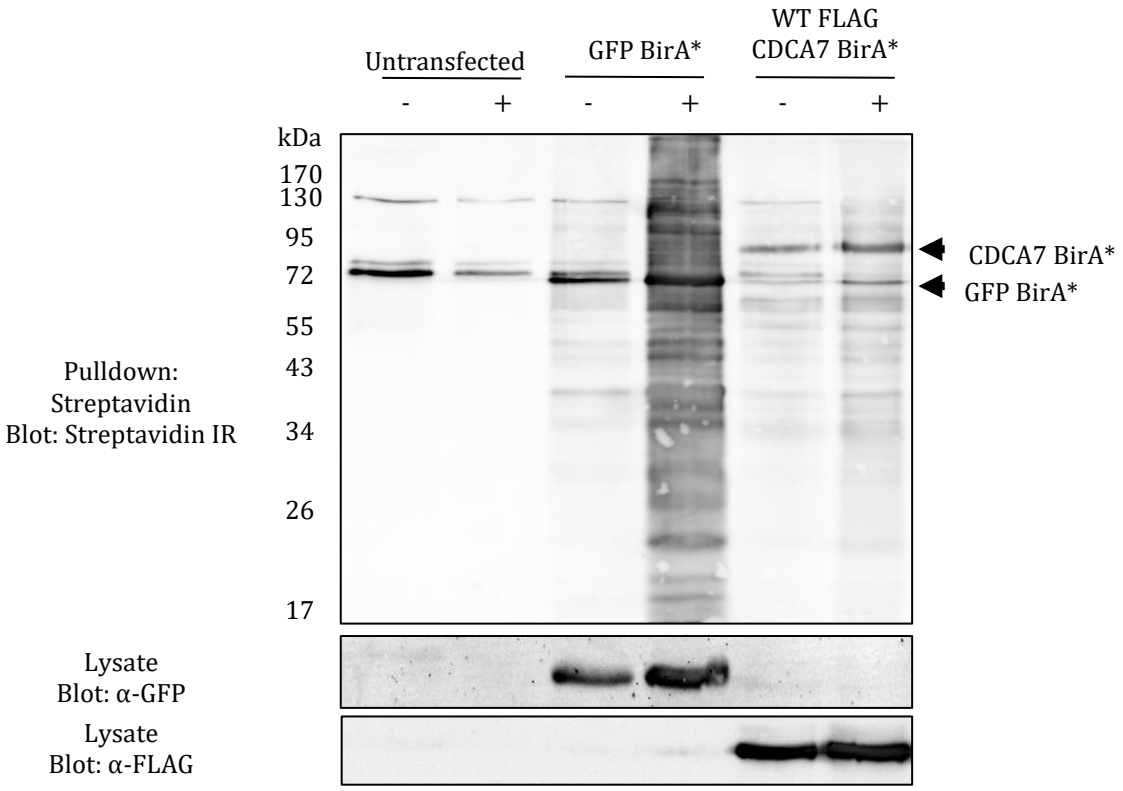

Figure 3.1: BioID of GFP-BirA* and WT FLAG CDCA7-BirA* Constructs (RIPA Buffer Protocol). HEK 293T cells were left untransfected (control) or transfected for 24 hours with GFP-BirA* or WT FLAG CDCA7-BirA*. Following transfection, the medium was replaced with control media or media that was supplemented with 50 μM of biotin for 24 hours. Cells were lysed in radioimmunoprecipitation assay (RIPA) buffer containing benzonase nuclease and protease inhibitor via sonication. The soluble lysate was incubated with streptavidin-conjugated beads overnight. Beads were washed five times with RIPA buffer and biotinylated proteins were eluted in SDS sample buffer. Top. Biotinylated proteins detected with streptavidin conjugated to an infrared (IR) fluorophore. Addition of biotin caused an increase in biotinylated proteins for transfected cells only. Several nonspecific interactors are detectable in the untreated lanes. Middle. Expression of the GFP-BirA* construct detected with a GFP antibody. Bottom. Expression of WT FLAG CDCA7-BirA* with a FLAG antibody.

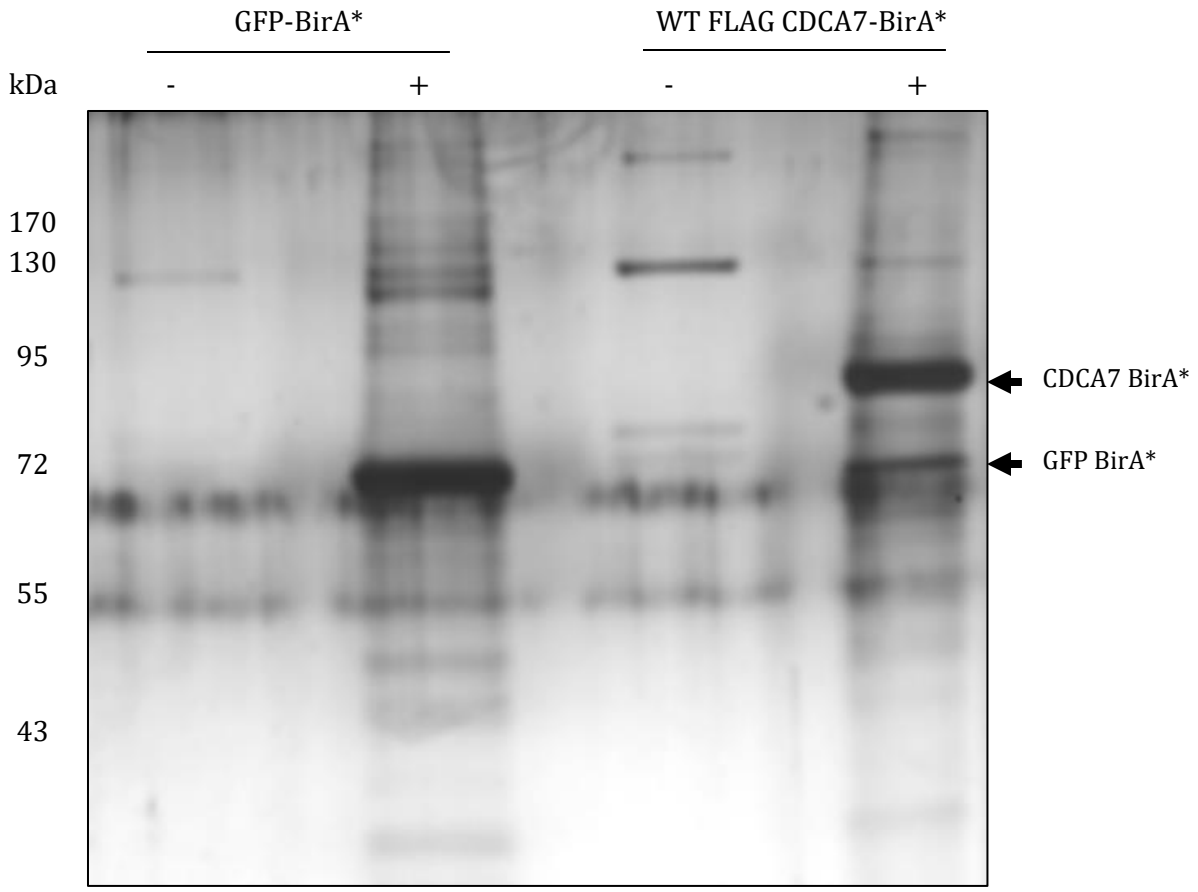

Figure 3.2: Silver stain for BioID of GFP-BirA* and WT FLAG CDCA7-BirA* Constructs (Roux Protocol). HEK 293T cells were transfected with GFP-BirA* or WT FLAG CDCA7-BirA* for 6 hours. Media was then swapped with control media or media containing 50 μM of biotin for 24 hours. Cells were lysed via sonication in the BioID lysis buffer with protease inhibitor. The soluble lysate was incubated with streptavidin-conjugated beads overnight. Beads were then washed with a series of 4 wash buffers and proteins were eluted with SDS sample buffer containing 50 μM of biotin. The silver stain here exhibits the total protein present in the streptavidin pulldowns. The pulldowns show a clear increase in the amount of protein detected when biotin is available in the media. The GFP-BirA* (70 kDa) and WT FLAG CDCA7-BirA* (85 kDa) constructs are noticeable following biotin addition (arrows indicate molecular weight position of constructs). Only a few non-specific protein interactors are visible when biotin is not present in the media.

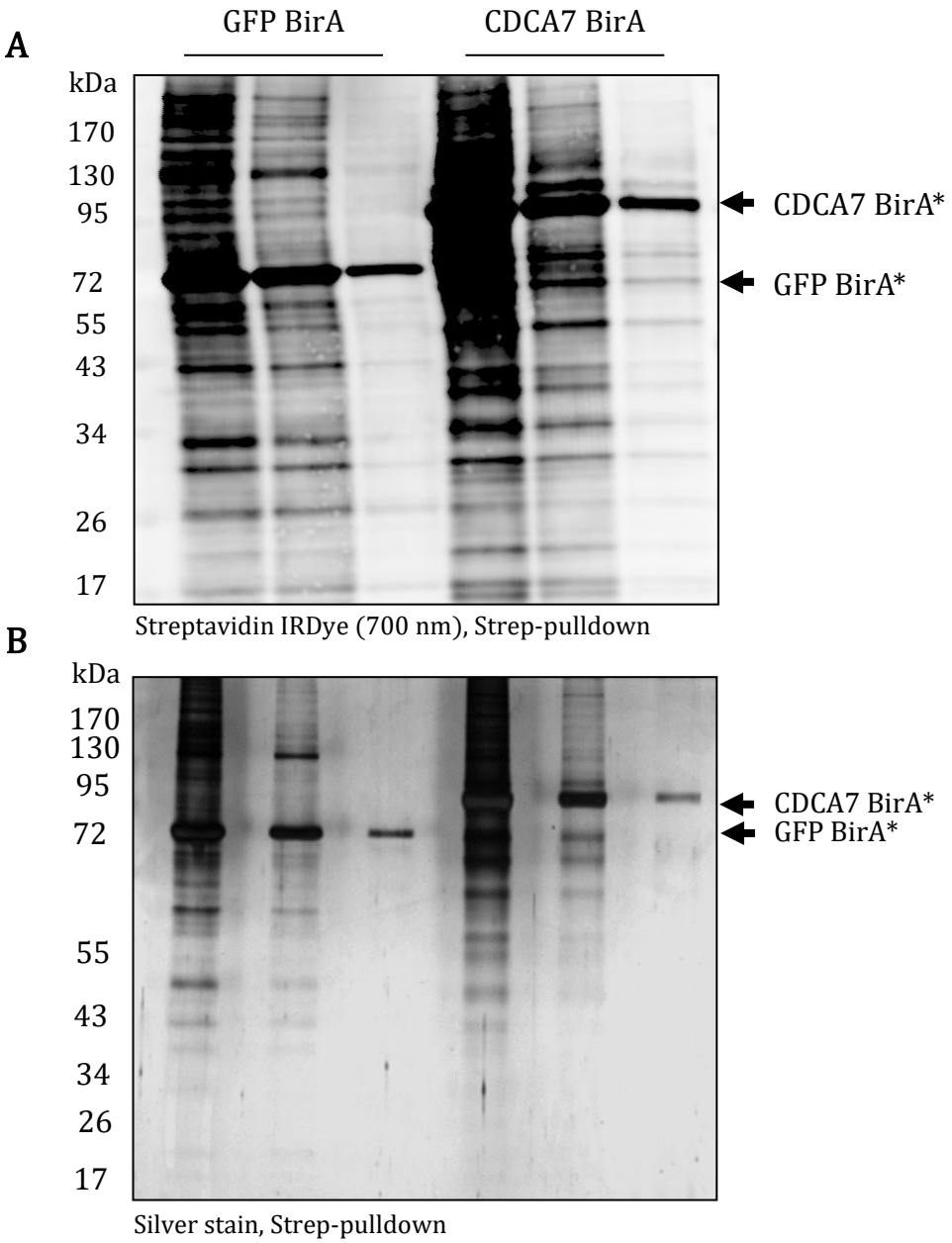

Figure 3.3: Optimization of BioID Roux Protocol. HEK 293T cells in thirteen 150 mm dishes were transfected with GFP-BirA* or WT FLAG CDCA7-BirA* and subjected to the BioID Roux Protocol, Cells were lysed with 1 mL of BioID lysis buffer per 150 mm dish. Streptavidin-conjugated beads (50 µL) were incubated in various volumes of soluble lysate (1 mL, 4 mL and 8 mL, respectively). One 150 mm dish of transfected HEK 293T cells, lysed in 1 mL of BioID lysis buffer was sufficient to saturate 50 uL of streptavidin-conjugated beads. Top. Western blot for streptavidin pulldowns of soluble lysates at 1 mL, 4 mL and 8 mL, respectively. Biotinylated proteins were detected with streptavidin conjugated to an infrared (IR) fluorophore. Bottom. Silver stain displaying total protein present in streptavidin pulldowns of soluble lysates at 1 mL, 4 mL and 8 mL, respectively.

Mass Spectrometry

Abridged Version

Mass spectrometry results indicate putative interactors of WT CDCA7. The most prominent interactor is TPX2.

Results

Once the protocol for BioID was established and fully optimized for CDCA7, mass spectrometry samples were generated. Samples were produced from one 150 mm dish of transiently transfected HEK 293T cells that were subjected to the BioID Roux protocol. Two replicates of GFP-BirA* and WT FLAG CDCA7-BirA* were sent for analysis. Common contaminants and nonspecific interactors (proteins found in both the GFP-BirA* and WT FLAG CDCA7-BirA* samples) were ruled out. Only proteins present in both replicates of WT FLAG CDCA7-BirA* are considered true potential interactors of CDCA7.

The results of the mass spectrometry experiment are displayed in Table 3.1. Wild-type (WT) CDCA7 ranks as the most common interactor of CDCA7. However, due to the nature of BioID, it cannot be considered as a potential interactor since WT FLAG CDCA7-BirA* may simply be biotinylating itself. As a result, the most common interactor following WT CDCA7 was considered. Consequently, TPX2 was chosen as the candidate interactor of CDCA7 that would be further investigated through coimmunoprecipitation (co-IP) experiments.

Table 3.1: Mass Spectrometry Results for BioID of WT FLAG CDCA7-BirA*. Following BioID of GFP-BirA* and WT FLAG CDCA7-BirA*, samples were prepared for mass spectrometry and sent for analysis at the Centre for Research in Mass Spectrometry at York University. Mass spectrometric experiments and analysis were performed by Andrew Macklin. Protein interactors that were present in two replicates and unique to WT FLAG CDCA7-BirA* are shown below. The protein name, accession code from the Human UniPort database, number of peptides detected, sequence coverage and score are provided. Interactors other than CDCA7 (red) are considered. TPX2 (blue) is the most prominent interactor found.

Name	Accession Number	Peptides	Coverage (%)	Score
CDCA7	B4DM13_HUMAN	6	17.5	198.7
TPX2	Q9ULW0_HUMAN	9	18.1	94.8
CDCA2	Q69YH5_HUMAN	8	15.3	53.7
SPDL1	Q96EA4_HUMAN	5	19.5	41.5
CFL1	G3V1A4_HUMAN	3	28.2	35.7
DLGAP5	Q15398_HUMAN	4	7.01	21.4
SAP30BP	J3KS14_HUMAN	3	42.3	19.2
SUGT1	A8K7W3_HUMAN	2	11.4	18.3
ATRX	P46100_HUMAN	4	2.8	17.8
RCC2	Q9P258_HUMAN	2	6.1	6.88
CDCA8	B4DXT3_HUMAN	2	13.9	5.32

WT CDCA7-TPX2 Interaction

Abridged Version

Interaction between CDCA7 and TPX2 is verified. The region of interaction is suggested to be residues 195-204 of CDCA7.

Methods

Western Blot: Western blots followed the general protocol outlined in Chapter 2. For streptavidin pulldowns, biotinylated proteins were detected with IRDye® 680RD Streptavidin, which is streptavidin conjugated to an infrared (IR) fluorophore from LI-COR (Product Number 925-68079). FLAG constructs were detected with the mouse monoclonal anti-FLAG M2 antibody from Sigma-Aldrich (Stock Keeping Unit/SKU F1804). Exogenous expression of TPX2 was accomplished with a generated TPX2 plasmid construct (Appendix B). Endogenous TPX2 and TPX2 constructs were detected with the TPX2 (D2R5C) XP® rabbit monoclonal antibody from Cell Signaling Technology (Product Number 12245).

Results

The candidate interactor of CDCA7 that was chosen for further investigation is TPX2. In order to validate TPX2 as a bonafide interactor of CDCA7, two experiments were performed. The first experiment included transfection of HEK 293T cells with either a FLAG vector construct or a WT FLAG CDCA7 construct. Cells were immunoprecipitated on agarose beads conjugated to a monoclonal FLAG antibody (anti-FLAG), and were analyzed after samples were western blotted. The second experiment involved transfection of HEK 293T cells with either GFP-BirA* or WT FLAG CDCA7-BirA* and then cells were subjected to the

BioID Roux protocol. SDS-PAGE and western blots were performed on the streptavidin pulldowns.

Both the immunoprecipitation experiment and BioID experiment were probed with a TPX2 antibody (Figure 3.4). TPX2 coimmunoprecipitates with WT FLAG CDCA7 but not the vector control and TPX2 is biotinylated by WT FLAG CDCA7-BirA* but not the GFP-BirA* control. Thus, TPX2 comes into proximity of and interacts with CDCA7 (Figure 3.4). Purified biotinylated proteins and the expression of WT FLAG CDCA7 and WT FLAG CDCA7-BirA* are also displayed (Figure 3.4).

The next objective was to determine whether certain mutations, substitutions or deletions would affect the interaction of TPX2 and CDCA7. HEK 293T cells were transfected with WT FLAG CDCA7 or mutations, substitutions and deletions of FLAG CDCA7. Cells were lysed, immunoprecipitated and subjected to western blots. Blots were probed for endogenous TPX2 with a TPX2 directed antibody. All mutations are point mutations and includes T163A CDCA7, which is a loss of function mutation for the AKT phosphorylation site within the nuclear localization sequence (NLS) of CDCA7. T234A, another loss of function mutation for a potential phosphorylation site on CDCA7, was also investigated. Substitutions include DE-CDCA7 and KK-CDCA7. DE-CDCA7 involved the replacement of CDCA7's NLS with a sequence that constitutively binds the 14-3-3 adapter protein. KK-CDCA7 is a mutated version of DE-CDCA7 that will not bind to 14-3-3. The constructs Δ156-187 CDCA7 and Δ1-234 CDCA7 are deletions of the NLS and N-terminal region of CDCA7, respectively.

The results of the experiment show that all FLAG CDCA7 constructs were successfully expressed and immunoprecipitated (Figure 3.5). When western blots were probed for endogenous TPX2, all the mutations, substitutions and deletions of FLAG CDCA7 bound to endogenous TPX2 with the exception of Δ1-234 CDCA7 (Figure 3.5). So, TPX2 does not bind within the NLS region of CDCA7 but does bind with the first 234 residues of CDCA7.

The subsequent objective was to narrow down the region of interaction of TPX2 and CDCA7. FLAG vector, WT FLAG CDCA7 or deletions of FLAG CDCA7 were transfected in HEK 293T cells, lysed and immunoprecipitated (IP). Western blots were performed on the IPs and endogenous TPX2 was detected with a TPX2 antibody. The deletions include the N-terminal deletion Δ1-234 CDCA7 and the C-terminal deletion Δ154-371 CDCA7. Deletions of the leucine zipper domain (Δ122-137 CDCA7) and the region adjacent to the leucine zipper domain and preceding the NLS (Δ138-164 CDCA7) were also examined. Finally, three consecutive internal deletions of 8 amino acids (Δ187-194 CDCA7), 10 amino acids (Δ195-204 CDCA7) and 10 amino acids (Δ205-214 CDCA7) were investigated. The internal deletions are adjacent to the NLS.

The experiment shows positive results for the expression and purification of all FLAG CDCA7 constructs (Figure 3.6). Endogenous TPX2 detected in western blots of the IPs verify that Δ1-234 CDCA7 (N-terminal deletion) does not bind to TPX2. The deletions of the leucine zipper or its adjacent region still immunoprecipitated TPX2 (Figure 3.6) and therefore TPX2 does not bind within residues 122-164 of CDCA7. The three internal deletions Δ187-194 CDCA7, Δ195-204 CDCA7 and Δ205-214 CDCA7 do not bind to TPX2 (Figure 3.6). Consequently, TPX2 binds within residues 187-214 of CDCA7. The C-terminal deletion does

bind to TPX2, which suggests that TPX2 binds within residues 1-152 of CDCA7 (Figure 3.6). However, this large deletion may compromise the three-dimensional (3D) conformation[112] of CDCA7. Whereas the smaller internal deletions are less likely to affect the 3D conformation.[112] Accordingly, the region adjacent to CDCA7's NLS (residues 187-214) was chosen for further investigation.

Finally, the residues 195-204 of CDCA7 were chosen as the potential binding region for TPX2. The region contains the sequence PMEEEEEEDK, which contains a string of acidic residues (6 residues of glutamic acid (E) and one residue of aspartic acid (D)). The string of acidic amino acids may interact with a basic domain on TPX2. To confirm if this region of CDCA7 interacts with TPX2, TPX2 was first cloned into a vector where it would be under the control of the cytomegalovirus (CMV) promoter (Appendix). Either FLAG vector, WT FLAG CDCA7 or Δ195-204 FLAG CDCA7 were cotransfected with TPX2 in HEK 293T cells. Ectopic expression of TPX2 was used in order consistently express similar amounts of TPX2 in all samples. Cells were lysed and immunoprecipitated. Both lysates and IPs underwent western blot procedures.

The western blots of the lysates were used as loading controls. Equivalent amounts of TPX2 protein were expressed in all samples (Figure 3.7a). The IPs also displayed similar expression of WT FLAG CDCA7 and Δ195-204 FLAG CDCA7 (Figure 3.7a). When western blots of the IPs were probed for coimmunoprecipitation (co-IP) of the FLAG constructs and ectopically expressed TPX2, all constructs tested positive for TPX2 interaction. There is significantly more TPX2 bound to WT FLAG CDCA7 in comparison to the vector control, while

there is no visible difference in the amount of TPX2 bound to the FLAG vector and Δ195-204 FLAG CDCA7 (Figure 3.7a). Thus, TPX2 interacts within residues 195-204 of CDCA7.

The next objective was to determine if this sequence containing a string of acidic amino acids is evolutionarily conserved. Examination of similar regions in other species was performed with the Clustal Omega multiple sequence alignment program from the European Bioinformatics Institute. The sequences were obtained from the National Center for Biotechnology Information (NCBI) protein database and converted into the FASTA format prior to analysis.

The sequence PMEEEEEEDK from residues 195-204 of human CDCA7 is highly conserved in primates with identical sequences present in the west lowland gorilla (*Gorilla gorilla gorilla*), chimpanzee (*Pan troglodytes*), olive baboon (*Papio anubis*) and rhesus macaque (*Macaca mulatta)*, refer to Figure 3.7b. Similar sequences are present in other mammals such as mouse (*Mus musculus*), rat (*Rattus norvegicus*), bovine (*Bos taurus*), horse (*Equus caballus*) and pig (*Sus scrofa*), refer to Figure 3.7b. The region of interaction seems to follow the sequence PXE_nDK. Here, P stands for Proline, X (any amino acid, methionine (M) in primates and T (threonine) in other mammals), a string of glutamic acid (E) residues, one aspartic acid (D) residue at the penultimate residue and finally lysine (K). The degree of conservation decreases in avian and ichthyoid (fish-like) species. For chicken (*Gallus gallus*) and zebrafish (*Danio rerio*), residue X is not present, and the string of acidic amino acids immediately follows the proline. For chicken, the final residue is the basic residue arginine (R) rather than the basic residue lysine, refer to Figure 3.7b.

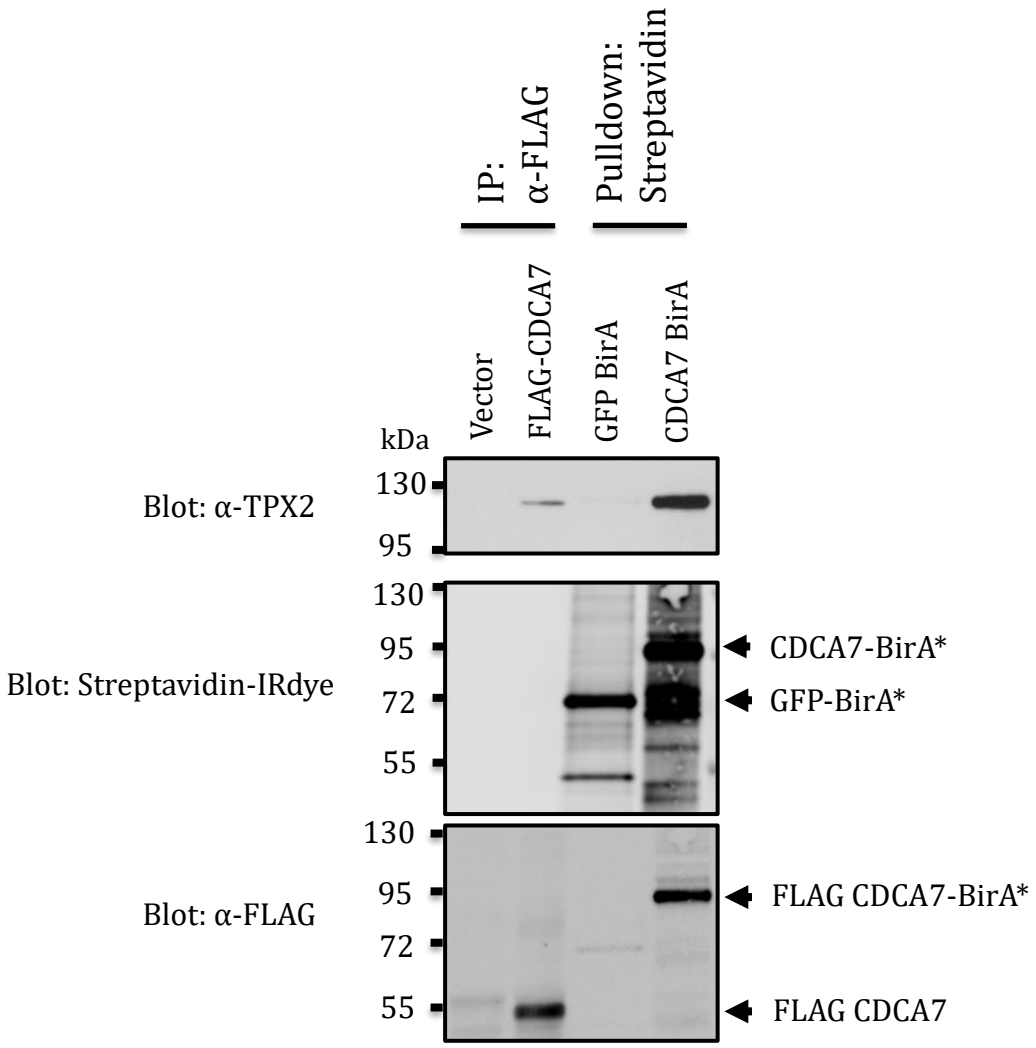

Figure 3.4: CDCA7 and TPX2 are in proximity to one another and interact. Flag vector (p3xFLAG-CMV-10), WT FLAG CDCA7, GFP-BirA* or WT FLAG CDCA7-BirA* were transfected in HEK 293T cells. Cells transfected with the FLAG vector or WT FLAG CDCA7 constructs were lysed and immunoprecipitated (IP) on anti-FLAG conjugated beads. Cells transfected with the BirA* constructs were incubated in media with 50 μM of biotin for 24 hours, lysed and then biotinylated proteins were purified via streptavidin-conjugated beads. Top. Endogenous TPX2 was detected with anti-TPX2 immunoblotting. TPX2 is only present in the WT FLAG CDCA7 IP and not in the FLAG vector control. TPX2 is only present in the WT FLAG CDCA7-BirA* streptavidin pulldown and not in the GFP-BirA* control. Middle. Biotinylated proteins were identified with a streptavidin-conjugated infrared (IR) fluorophore. Bottom. Ectopically expressed FLAG constructs were identified with anti-FLAG immunoblotting.

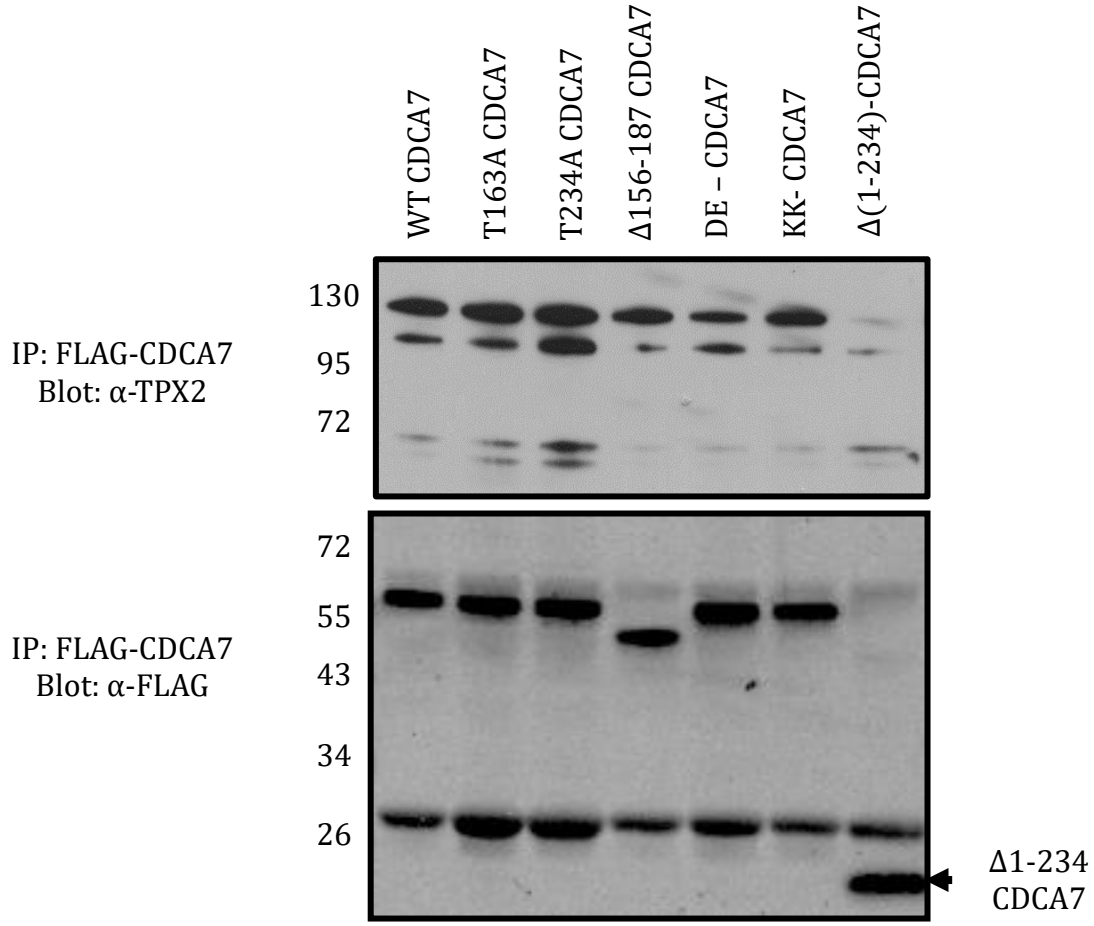

Figure 3.5: TPX2 interacts within the first 234 residues of CDCA7. WT FLAG CDCA7 or the indicated point mutations, substitutions or deletions were transfected in HEK 293T cells, lysed and immunoprecipitated (IP) on anti-FLAG conjugated beads. Roles of mutations, substitutions or deletions: T163A (mutation of AKT phosphorylation site), Δ156-187 (nuclear localization sequence), DE (constitutive 14-3-3 interactor), KK (constitutive 14-3-3 non-binder) and Δ1-234 (N-terminal deletion). Top. Endogenous TPX2 was detected with anti-TPX2 immunoblotting. TPX2 is absent in the Δ1-234 FLAG CDCA7 IP. Bottom. Ectopically expressed FLAG constructs were identified with anti-FLAG immunoblotting.

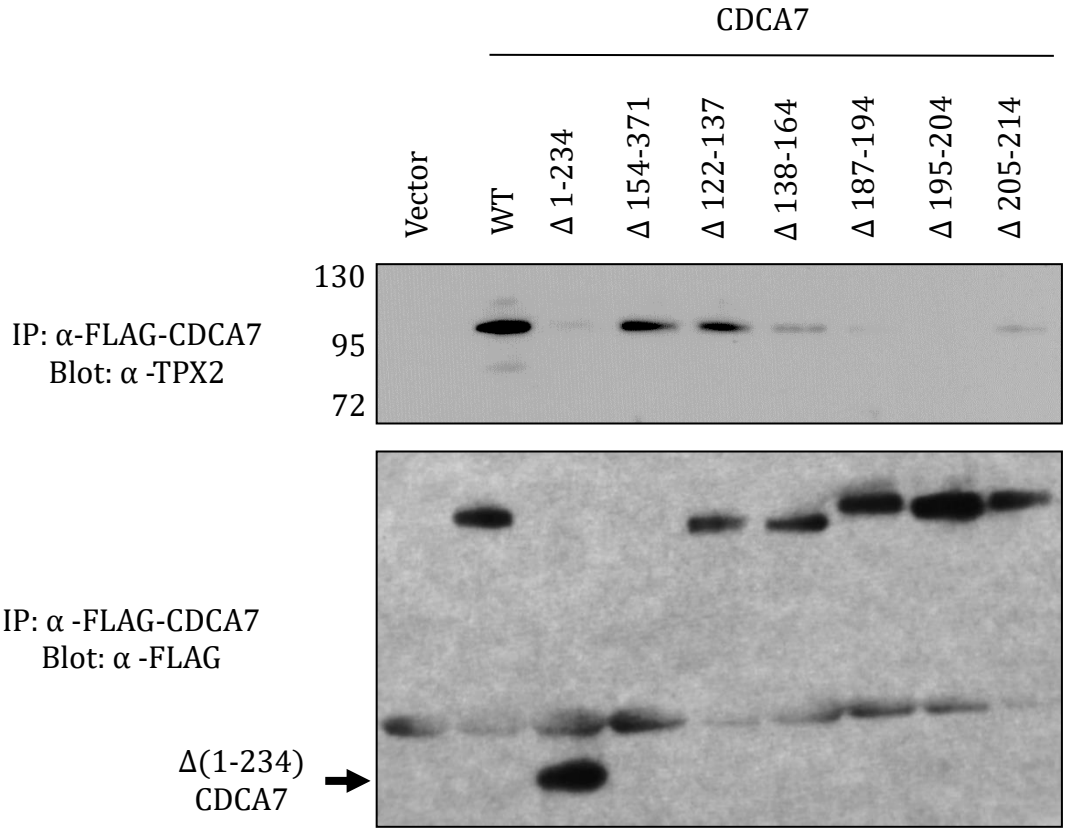

Figure 3.6: TPX2 interacts within residues 187-214 of CDCA7. WT FLAG CDCA7 or the indicated deletions were transfected in HEK 293T cells, lysed and immunoprecipitated (IP) on anti-FLAG conjugated beads. Roles of deletions: Δ1-234 (N-terminal deletion), Δ154-371 (C-terminal deletion), Δ122-137 (Leucine zipper domain), Δ138-164 (region between leucine zipper domain and nuclear localization sequence/NLS), Δ187-194, Δ195-204 and Δ205-214 (regions adjacent NLS). Top. Endogenous TPX2 was detected with anti-TPX2 immunoblotting. TPX2 is absent in the Δ187-194 FLAG CDCA7, Δ195-204 FLAG CDCA7 and Δ205-214 FLAG CDCA7 IPs. Bottom. Ectopically expressed FLAG constructs were identified with anti-FLAG immunoblotting.

A

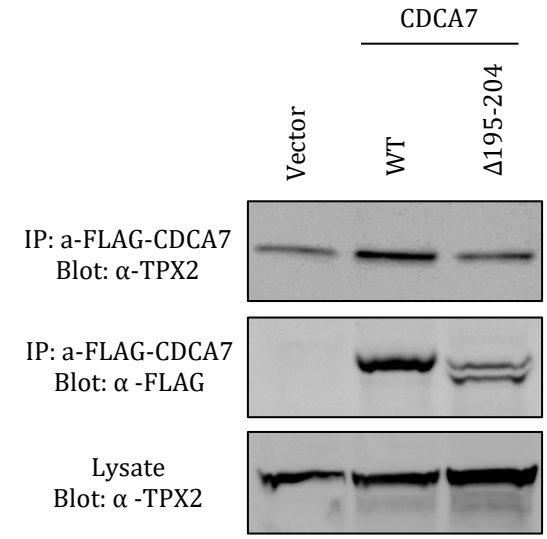

Overexpression of ectopic TPX2

B

```
Zebrafish    208 SRSLVDGPPSPPPED-------EEEDKYSLVRRSRGYEDVDEEEKEPRRRSYNSSLTIPH 260
Chicken      224 SRSLIEGPPTPLPEE-------EDDDRYLLVRRRKMSGEDLEHDAQTPRRGHRGAMALPH 276
Mouse        190 SRSRILGSLGALPTEEEEEEEEEEEDKYMLVRQRKSMDSYMNDDDVPRSRRP-GSMTLPH 248
Rat          186 SRSRILGSLGALPTEEEED-EEEEEDKYMLVRRRKSVDGYMNDDDVSRSRRP-GSMTLPH 243
Baboon       183 SRSRILGSLDALPMEEE-----EEEDKYMLVRKRKTMDGYMNEDDLPRSRRSRSSMTLPH 237
Macaque      183 SRSRILGSLDALPMEEE-----EEEDKYMLVRKRKTMDGYMNEDDLPRSRRSRSSMTLPH 237
Gorilla      183 SRSRILRSLDALPMEEE-----EEEDKYMLVRKRKTMDGYMNEDDLPRSRRSRSSVTLPH 237
Human        183 SRSRILGSLDALPMEEE-----EEEDKYMLVRKRKTVDGYMNEDDLPRSRRSRSSVTLPH 237
Chimpanzee   183 SRSRILGSLDALPMEEE-----EEEDKYMLVRKRKTMDGYMNEDDLPRSRRSRSSVTLPH 237
Horse        290 SRSRILGSLSALPTEEEEE-EEEEDDKYVLVRKRKAVDGYMNGDDVPRGRRP-GSMTLPH 348
Cow          183 SRSRVLGSLSALPTEEEEE-EEEEEDKYMLVRKRKSMVGYMNEDDMPRSRRP-GPMTLPH 240
Pig          183 SRSRVLGSLGALPTEEEEE--EEEEDKYMLVRKRKPTDGYLNEDDMPRSRRP-GSMTLPH 239
                 *** :       * :       *::*:* ***: :      : :     *   . :::**
```

Figure 3.7: TPX2 interacts within residues 195-204 of CDCA7. A) Flag vector (p3xFLAG-CMV-10), WT FLAG CDCA7 or Δ195-204 FLAG CDCA7 were co-transfected with TPX2 into HEK 293T cells, lysed and immunoprecipitated (IP) on anti-FLAG conjugated beads. Top. Endogenous TPX2 was detected with anti-TPX2 immunoblotting. The amount of TPX2 in the vector IP is compared with the amount of TPX2 present in either WT or Δ195-204 FLAG CDCA7 IP. There is a significant difference in the amount of TPX2 when the vector control is compared to WT FLAG CDCA7, but there is no difference when the vector control is compared to Δ195-204 FLAG CDCA7. Middle. Ectopically expressed FLAG constructs were identified with anti-FLAG immunoblotting. Bottom. The amount of TPX2 in the soluble lysates were used as a loading control. B) The residues 195-204 in human CDCA7 contains amino acids PMEEEEEEDK. This region containing a string of acidic amino acids, mainly glutamic acid (E) is evolutionarily conserved (black). The region is highly conserved in primates and is also conserved between mammals. Asterisks (*) denote identical amino acid matches while colons (:) indicate similar matches.

Phosphorylation of CDCA7 by Aurora A Kinase

Abridged Version

Residue T163 of CDCA7 matches the Aurora A kinase phosphorylation consensus motif. Inhibition of Aurora A kinase decreases phosphorylation of T163 along with CDCA7-14-3-3β interaction.

Methods

Western Blot: Western blots followed the general protocol outlined in Chapter 2. FLAG constructs were detected with the mouse monoclonal anti-FLAG M2 antibody from Sigma-Aldrich (Stock Keeping Unit/SKU F1804). Phospho-T163 (pT163) CDCA7 was detected with a pT163 CDCA7 polyclonal rabbit antibody, produced via GenScript Corporation (CA). A rabbit polyclonal antibody of 14-3-3β from Santa Cruz (catalog Number sc-628) was used to detect endogenous 14-3-3β. Aurora A Inhibitor I is from Sigma-Aldrich (SKU SML0882) and MLN8237 is from APExBIO (Catalog no. A4110).

Results

The previous section verified the interaction between CDCA7 and TPX2. As mentioned above, TPX2 is a well-known interactor and regulator of Aurora A kinase. Based on sequence analysis of CDCA7 performed on the phosphorylation motif application Scansite 3.0, the residue T163, which was previously shown to be phosphorylated by Akt, was also a very high match for the consensus phosphorylation site of Aurora A. The consensus motif of Aurora A is [R/K/N]-R-X-S/T-B, where [R/K/N] indicates that the first residue is either arginine (R), lysine (K) or asparagine (N). The second residue is arginine (R), followed by X

(any amino acid), serine or threonine (S/T) and finally B (any hydrophobic amino acid other than proline)[113], refer to Figure 3.8a. Residues 160 to 164 within the nuclear localization sequence (NLS) of CDCA7 perfectly match the Aurora A consensus motif, with the sequence R-R-R-T-F (Figure 3.8a). Accordingly, experiments investigating this region were conducted.

To determine whether Aurora A kinase phosphorylates CDCA7 at threonine 163, experiments using inhibitors of Aurora A kinase were conducted. First, an inhibitor designed by Sigma Aldrich, Aurora A Inhibitor I, was used to determine if inhibition of Aurora A kinase affects the level of phospho-T163 (pT163). HEK 293T cells were transfected with WT FLAG CDCA7 and then cells were left untreated or were incubated with 1 μM of Aurora A Inhibitor I for a set period of time (3, 6, 9, 12 or 24 hours). Cells were then lysed, immunoprecipitated (IP) on anti-FLAG conjugated beads and the IPs were subjected to western blotting. The same experiment was performed with 5 μM of Aurora A Inhibitor I. Cells were not treated with inhibitor for 24 hours at the 5 μM concentration, but a control was included where cells were transfected with FLAG vector and left untreated.

The expression of WT FLAG CDCA7 was confirmed by probing the IPs with an anti-FLAG antibody. All samples transfected with WT FLAG CDCA7 had similar levels of expression (Figure 3.8b and Figure 3.8c). The IPs were also probed for pT163 CDCA7 and all samples expressing WT FLAG CDCA7 tested positive of T163 phosphorylation (Figure 3.8b and Figure 3.8c). The ratio of pT163 CDCA7 to total WT FLAG CDCA7 for each sample was determined. The ratio of the untreated WT FLAG CDCA7 sample was set to one-fold and all other ratios were divided by the untreated ratio to determine their fold. After three hours of incubation with Aurora A Inhibitor I at 1 μM, the pT163 CDCA7 levels had decreased by more

than 50% when compared to the untreated sample (Figure 3.8b). A greater than 80% decrease in the pT163 level occurred following incubation of cells with Aurora A Inhibitor I at 5 μM, in comparison to the untreated sample (Figure 3.8c). Thus, inhibition of Aurora A kinase decreases the amount of phosphorylation for T163 CDCA7.

The concentrations of Aurora A Inhibitor I were relatively high (μM scale) for detectable decreases in pT163 CDCA7 levels. These high concentrations may be nonspecifically inhibiting other kinases, which in turn leads to the detected decrease in pT163 CDCA7 levels. In order to confirm that Aurora A specifically affects the phosphorylation status of T163 CDCA7, the inhibitor MLN8237 was used. This inhibitor was described in the literature to exclusively inhibit Aurora A kinase.[98] HEK 293T cells were transfected with FLAG vector and left untreated. Cells were also transfected with WT FLAG CDCA7, left untreated or treated with MLN8237 over a range of concentrations (20 nM, 100 nM, 200 nM or 500 nM) or treated with Aurora A Inhibitor I at 5 μM. Treatment with inhibitor was set to one hour. Then cells were lysed, immunoprecipitated and both lysates and IPs underwent western blotting procedures.

Lysates were probed with an anti-FLAG antibody in order to determine WT FLAG CDCA7 expression. All samples that were transfected with WT FLAG CDCA7 successfully expressed the construct at comparable levels (Figure 3.9). Lysates were also probed for pT163 CDCA7, which was also positive when WT FLAG CDCA7 was expressed (Figure 3.9). IPs were probed for 14-3-3β and was positive for samples where WT FLAG CDCA7 was expressed (Figure 3.9). Folds were determined in the same manner as the Aurora A Inhibitor I experiments performed in Figure 3.8b and 3.8c. Decreases of approximately 50% and 70%

occurred for the 14-3-3β-CDCA7 interaction following treatment with MLN8237 (100 nM) and Aurora A Inhibitor I (5 μM), respectively (Figure 3.9). When cells were incubated with 100 nM of MLN8237 for one hour, a greater than 40% drop in the pT163 level occurred, as compared to the untreated sample (Figure 3.9). Higher concentrations of MLN8237 (200 nM and 500 nM) did not have a similar effect, however. A similar decrease (50%) in the pT163 CDCA7 level took place after cells were incubated with Aurora A Inhibitor I for 1 hour at 5 μM (Figure 3.9). Low concentrations of an Aurora A specific inhibitor (MLN8237) produced similar drops in the pT163 CDCA7 level as high concentrations of Aurora A Inhibitor I. This provides strong support for the notion that CDCA7 is phosphorylated by Aurora A kinase at residue T163.

The next objective would be to verify if CDCA7 can be phosphorylated by Aurora A kinase in vitro. First, GST-WT FLAG CDCA7 and a GST control were subjected to purification on GSH beads. Non-induced lystes and induced lysates from two different sources of IPTG were obtained. Comparison between noninduced and induced lysates was done to verify expression of the GST constructs. The wash sample is a control which will indicate whether a GST construct is/is not eluted prior to the elution step. The resin is a control that verifies if a GST construct bound to reduced glutathione (GSH) beads to begin with and the elution indicates whether a GST construct has been purified off the GSH beads. Samples were subjected to SDS-PAGE and proteins were detected with Coomassie stain. While the GST control construct was successfully purified, GST-WT FLAG CDCA7 could not be expressed and consequently lead to failed purification (Figure 3.10). As a result, in vitro kinase assays with GST-WT FLAG CDCA7 and Aurora A kinase were not possible.

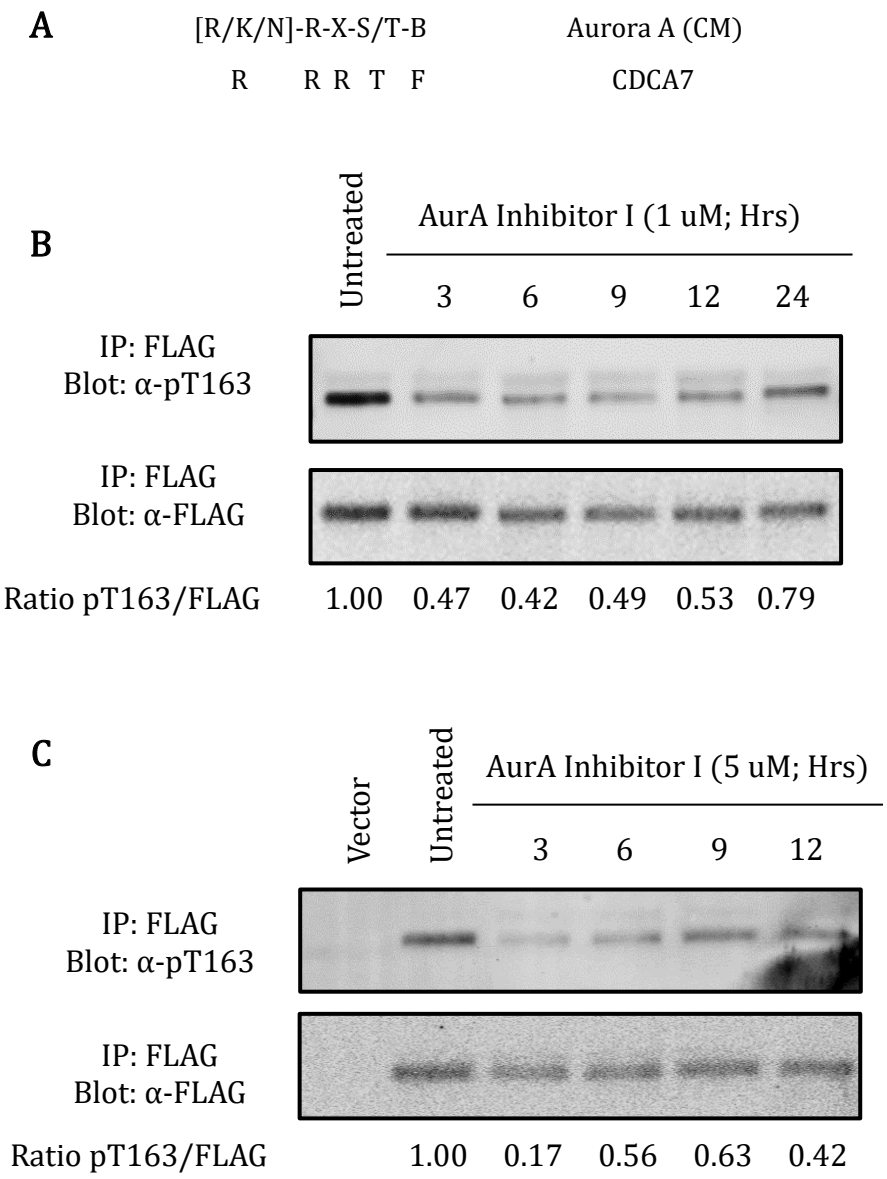

Figure 3.8: Phosphorylation of T163 CDCA7 via Aurora A Kinase. All experiments were done in HEK 293T cells. A) Consensus motif (CM) for Aurora A is compared to residues 160-164 of CDCA7. This region of CDCA7 matches the CM of Aurora A completely. B) Following transfection of WT FLAG CDCA7, cells are left untreated or subjected to Aurora A Inhibitor I (1 μM) for the indicated time (in hours), lysed and immunoprecipitated (IP) on anti-FLAG conjugated beads. Top. Phosphorylation of T163 (pT163) is detected with anti-pT163 CDCA7 immunoblotting. Bottom. Ectopically expressed FLAG constructs were identified with anti-FLAG immunoblotting. The ratio of pT163 CDCA7/FLAG CDCA7 is provided and this ratio in untreated cells in set to one-fold. Over 3 hours there is a greater than 50% drop in pT163 levels. C) Same as in B expect Aurora A inhibitor I concentration is 5 μM. Flag vector (p3xFLAG-CMV-10) is added as an additional control. Over 3 hours there is a greater than 80% drop in pT163 levels. Abbreviations. AurA is Aurora A Kinase.

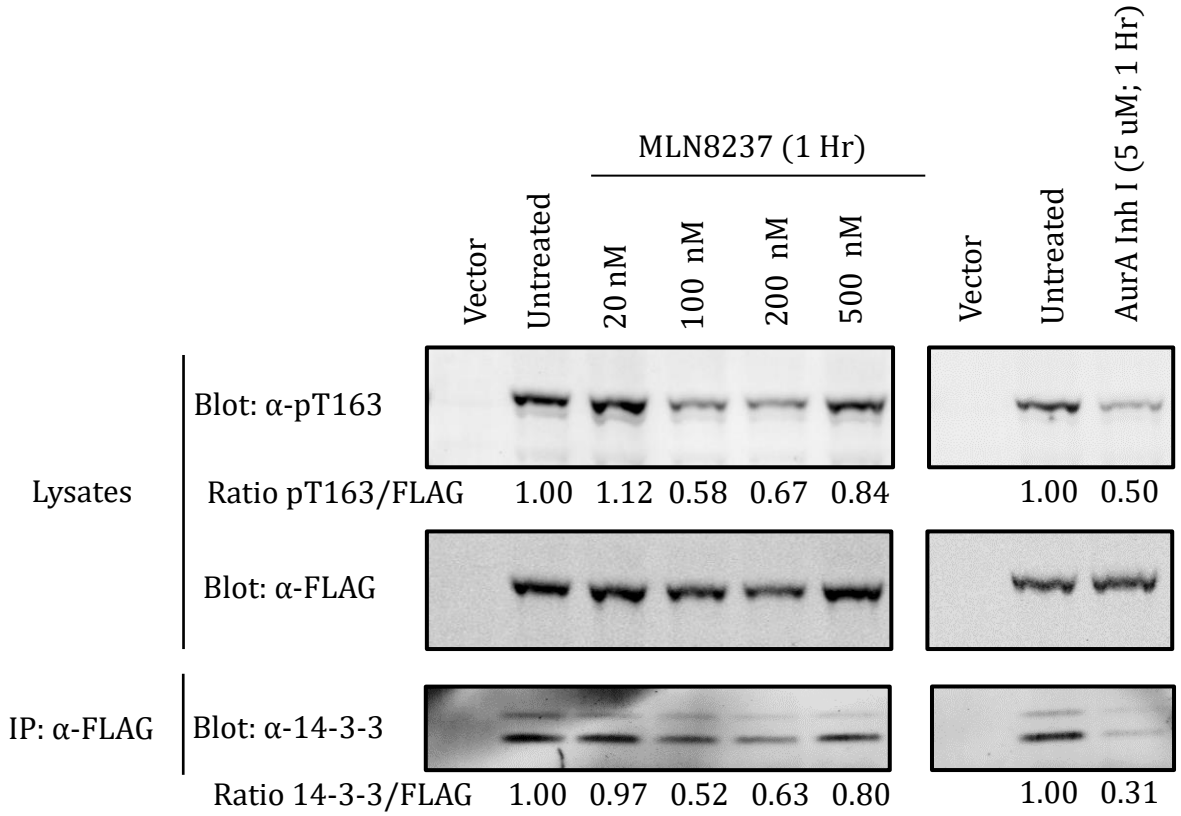

Figure 3.9: Aurora A Kinase specifically phosphorylates T163 CDCA7. Following transfection with either Flag vector (p3xFLAG-CMV-10) or WT FLAG CDCA7, HEK 293T cells are left untreated or incubated in the indicated concentrations (nM) of MLN8237 or in 5 μM of Aurora A Inhibitor I for 1 hour. Cells are then lysed and immunoprecipitated (IP) on anti-FLAG conjugated beads. Top. Phosphorylation of T163 (pT163) is detected with anti-pT163 CDCA7 immunoblotting. Middle. Ectopically expressed FLAG constructs were identified with anti-FLAG immunoblotting. Bottom. Endogenous 14-3-3β is detected with anti-14-3-3β immunoblotting. The ratio of pT163 CDCA7/FLAG CDCA7 is provided and this ratio in untreated cells is set to one-fold. The ratio of 14-3-3β/FLAG CDCA7 is provided and this ratio in untreated cells in set to one-fold. Over the span of 1 hour, there is a 50% drop in pT163 levels with Aurora A Inhibitor I (5 μM), whereas a comparable drop of 40% in pT163 levels occurs with 100 nM of MLN8237. Abbreviations. AurA Inh I is Aurora A Inhibitor I.

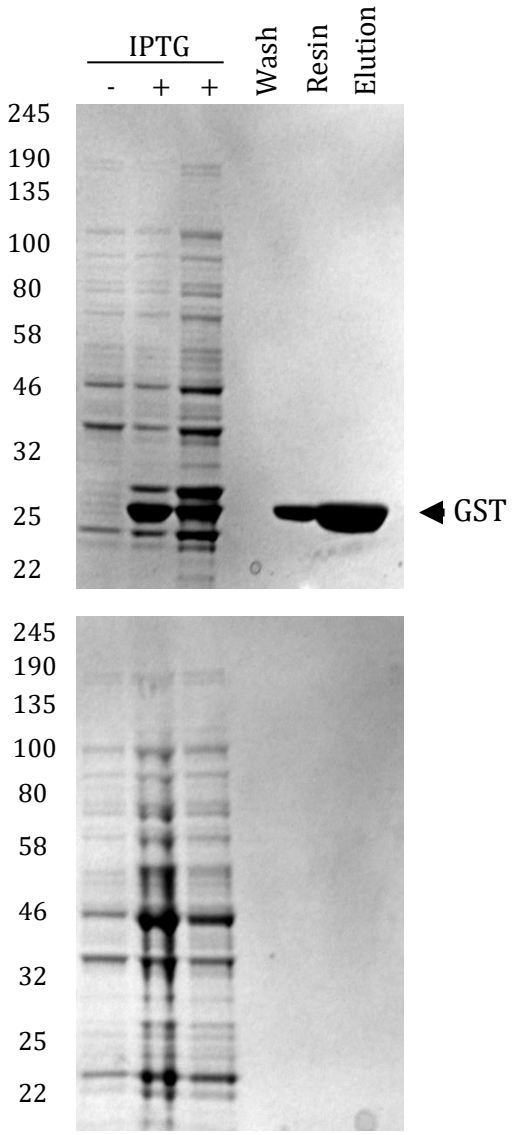

Figure 3.10: Purification of GST-WT FLAG CDCA7 (Negative Result). Two colonies of either GST or GST-WT FLAG CDCA7 (GWC) in BL21-codon plus (DE3) – RIPL *E. coli* cells were grown in LB supplemented with carbenicillin. Cells were induced with two different sources of isopropyl β-D-1-thiogalactopyranoside (ITPG) for 3 hours, pelleted, lysed via sonication and incubated on reduced glutathione (GSH) beads. The beads were then washed seven times in wash buffer (1X PBS, pH 7.4). Prior to elution, a sample of the resin was stored. This sample verifies that the GST construct bound to the resin in the first place. Finally, the beads were eluted in 20 mM of GSH in Tris-HCl, pH 9.0. The order of lanes are as follows: non-induced lysate, induced lysates from IPTG sources 1 and 2, respectively, wash, resin and elution. Top. The GST construct (26 kDa) was purified following elution. Bottom. The GWC construct was not expressed since a prominent band of ~76 kDa is not present in the induced lysates. Failure to purify GWC made in vitro kinase assays with GWC and Aurora A kinase impossible.

Cell Cycle Modulation of CDCA7 and CDCA7 Interactors

Abridged Version

Cells are synchronized to the G1/S boundary and then released. The interaction between 14-3-3β and WT CDCA7 and the phosphorylation status of residue T163 for CDCA7 coincide with one another. CDCA7-TPX2 interaction continually decreases over the cell cycle.

Methods

Western Blot: Western blots followed the general protocol outlined in Chapter 2. FLAG constructs were detected with the mouse monoclonal anti-FLAG M2 antibody from Sigma-Aldrich (Stock Keeping Unit/SKU F1804). Phospho-T163 (pT163) CDCA7 was detected with a pT163 CDCA7 polyclonal rabbit antibody, produced via GenScript Corporation (CA). A rabbit polyclonal antibody of 14-3-3β from Santa Cruz (catalog Number sc-628) was used to detect endogenous 14-3-3β. Endogenous TPX2 was detected with the TPX2 (D2R5C) XP® rabbit monoclonal antibody from Cell Signaling Technology (Product Number 12245).

Results

The previous two sections confirmed interaction of CDCA7 and TPX2, and highlighted CDCA7 as a potential target for Aurora A phosphorylation. The changes in the degree of interaction for CDCA7-14-3-3β or CDCA7-TPX2 and the changes in the phosphorylation status of T163 CDCA7, over the cell cycle, were investigated. HEK 293T cells were transfected with FLAG vector or WT FLAG CDCA7 and synchronized to the G1/S checkpoint via double thymidine block[114]. Cells were either stained with propidium iodide (PI) and analyzed

following flow cytometry or cells were lysed, immunoprecipitated (IP) and the IPs were subjected to western blotting.

Data from synchronized cells subjected to flow cytometry was analyzed and graphically represented by Dr. Michael P. Scheid. Following synchronization, cells were released over various timepoints (0, 2, 4, 6, 8, 10, 12, 14 or 16 hours) prior to being harvested. The cell cycle profile of these timepoints are displayed in Figure 3.11. The y-axis of each graph represents the number of cells and the x-axis represents the DNA content. Units are arbitrary for both axes and for the x-axis, 50 units denotes cells in G1, 100 units denotes cells in G2, and any cells within 50-100 are in S phase (Figure 3.11). Prior to release (0 hours), the majority of cells are at the G1/S boundary (Figure 3.11). After 4 hours of release, a population of the cells have moved into the G2 phase and by 8 hours of release, cells have again moved to G1 or S phase (Figure 3.11). This graphical representation shows that cells subjected to double thymidine block are synchronized and remain synchronized for the 16 hours of release displayed.

The expression and purification of WT FLAG CDCA7 was confirmed by probing IPs with an anti-FLAG antibody. When WT FLAG CDCA7 is transfected, the construct can be detected, and all samples of WT FLAG CDCA7 have similar levels of expression (Figure 3.12). The IPs were also probed for phospho-T163 (pT163) CDCA7, endogenous 14-3-3β or endogenous TPX2. The ratios of either pT163 CDCA7, endogenous 14-3-3β or endogenous TPX2 and total WT FLAG CDCA7 were determined. The ratio at zero hours of release was normalized to one-fold and the other ratios were divided by this ratio to determine their fold. Both pT163 CDCA7 and 14-3-3β levels decrease after the zero hour release point and are at

their lowest after 8 hours of release. Then both pT163 CDCA7 and 14-3-3β levels undergo a recovery period between 10 hours and 16 hours of release, where levels rise close to their original folds (Figure 3.12). TPX2 levels on the other hand continually decrease over time (Figure 3.12).

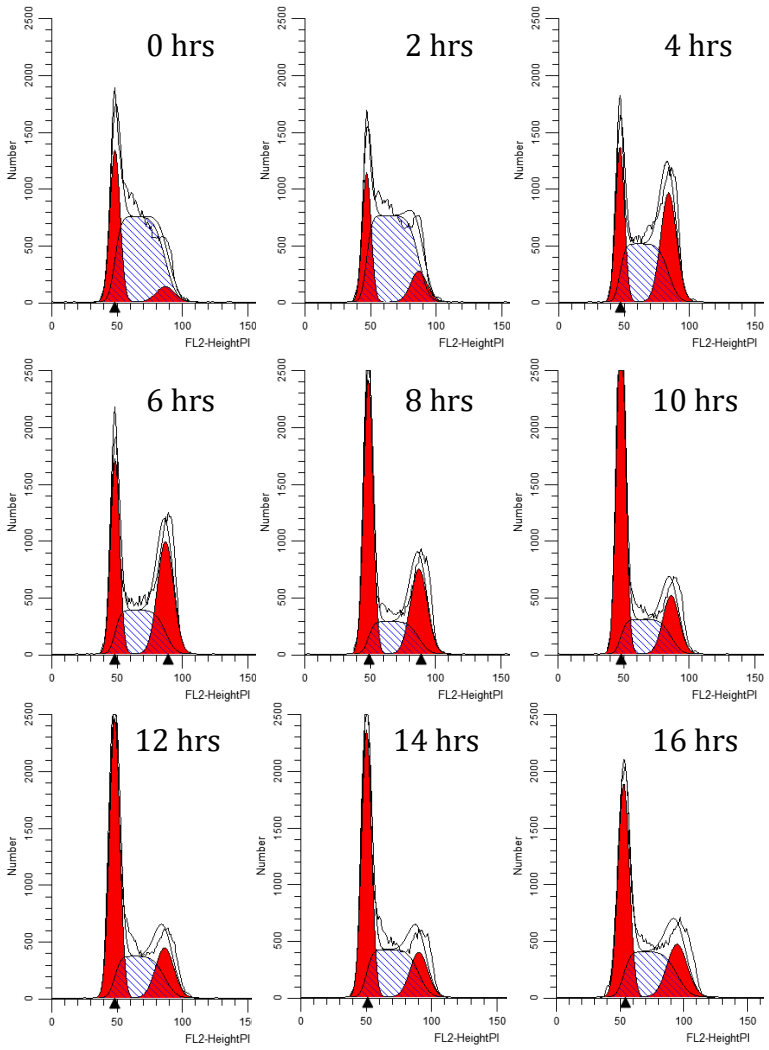

Figure 3.11: Cell cycle profile of synchronized HEK 293T cells obtained from flow cytometry. Following double thymidine block, cells are synced to the G1/S checkpoint. The cells are then released for the indicated durations. DNA was stained with propidium iodide. The progression of cells through the cell cycle is clearly visible over this 16-hour interval. The x-axis denotes DNA content, cells at 50 units are in G1, cells at 100 units are in G2 and cells between 50 and 100 units are in S phase. The y-axis denotes the number of cells. Units are arbitrary.

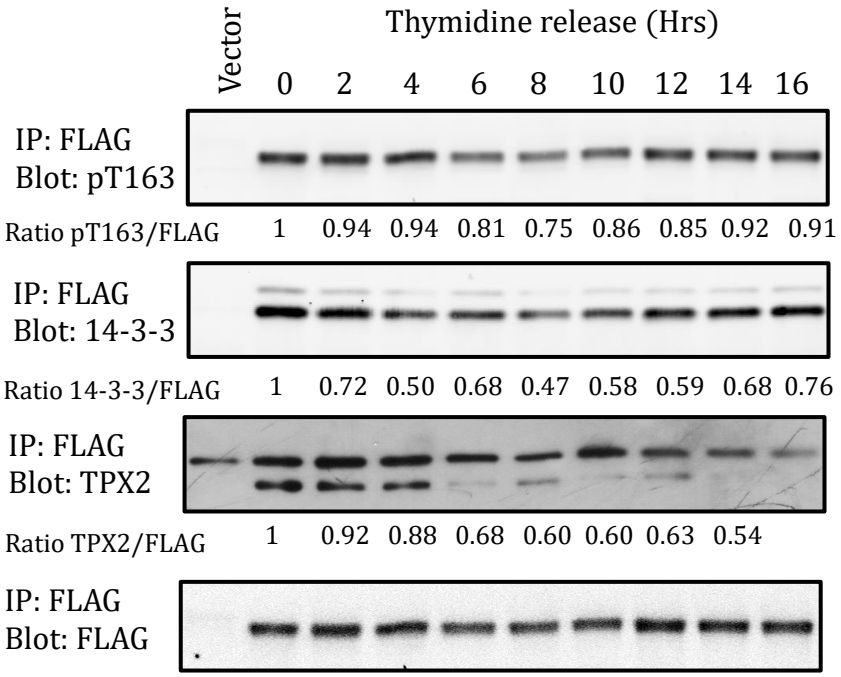

Figure 3.12: TPX2, pT163 CDCA7 and 14-3-3β protein levels vary throughout the cell cycle. HEK 293T cells were transfected with Flag vector (p3xFLAG-CMV-10) or WT FLAG CDCA7, subjected to thymidine double block synchronization, and released at indicated time points (in hours). Cells were lysed and immunoprecipitated (IP) on anti-FLAG conjugated beads. Top. Phosphorylation of T163 (pT163) is detected with anti-pT163 CDCA7 immunoblotting. Second row. Endogenous 14-3-3β is detected with anti-14-3-3β immunoblotting. Third row. Endogenous TPX2 is detected with anti-TPX2 immunoblotting. Bottom. Ectopically expressed FLAG constructs were identified with anti-FLAG immunoblotting. Ratio of pT163 CDCA7/FLAG CDCA7, 14-3-3β/FLAG CDCA7 and TPX2/FLAG CDCA7 is provided and these ratios at zero hours of release are set to one-fold. Both pT163 and 14-3-3β levels decrease and then recover over the 16 hour interval whereas TPX2 levels continuously decrease over the 16 hour interval.

CDCA7 and Mitosis

Abridged Version

During mitosis CDCA7 localizes to the centrosomes where it is phosphorylated at residue threonine (T) 163. CDCA7 also colocalizes with TPX2 during mitosis and phosphorylation of residue T163 CDCA7 increases throughout mitosis.

Methods

Western Blot: Western blots followed the general protocol outlined in Chapter 2. FLAG constructs were detected with the mouse monoclonal anti-FLAG M2 antibody from Sigma-Aldrich (Stock Keeping Unit/SKU F1804). Phospho-T163 (pT163) CDCA7 was detected with a pT163 CDCA7 polyclonal rabbit antibody, produced via GenScript Corporation (CA). Endogenous CDCA7 was detected with a monoclonal rabbit antibody from Sigma-Aldrich (SKU HPA005565)

Results

The previous sections have demonstrated that CDCA7 interacts with TPX2 and is a candidate substrate for Aurora A phosphorylation. Both TPX2 and Aurora A kinase play important roles in spindle assembly and regulation as well as centrosomal regulation, during mitosis.[74, 81] Accordingly, it is expected that CDCA7 may also play a role during the mitotic phase of the cell cycle. A series of immunofluorescence experiments were performed to examine CDCA7 within the context of mitosis. All microscopy experiments were performed jointly with Dr. Michael P. Scheid.

The first experiment was done in asynchronous cells. HEK 293T cells were transiently transfected with WT FLAG CDCA7. Ectopically expressed CDCA7 was found in prophase (nuclear envelope disappears and spindles begin to form) and metaphase (chromosomes line up along the metaphase plate), refer to Figure 3.13. During prophase, WT FLAG CDCA7 and its phosphorylated version phospho-T163 (pT163) CDCA7 were detected and appear as spherical, bright foci. There are several foci present during prophase (Figure 3.13). During metaphase, WT FLAG CDCA7 is found as two concentrated regions located adjacent to the DNA lined up at the metaphase plate (Figure 3.13). The regions of localization for WT FLAG CDCA7 during metaphase resemble that of centrosomes.

For all subsequent experiments within this section, cells are synchronized with compound RO3306, a Cyclin-dependent kinase 1 (CDK1) inhibitor that synchronizes cells to the G2/M checkpoint[115]. This increases the number of cells captured in the mitotic phase. The previous experiments have indicated that ectopically expressed CDCA7 localizes to regions in the same manner as centrosomes. The next objective was to determine if endogenous CDCA7 does colocalize with known centrosomal markers. Gamma (γ) tubulin is a known marker of centrosomes and is used to determine if CDCA7 localizes to the centrosomes. HeLa cells are synchronized with RO3306, released for 40 minutes and prepared for immunofluorescence. Cells are probed for endogenous CDCA7 and γ-tubulin and imaged after confocal microscopy. Cells in metaphase/anaphase (sister chromatids have just begun to pull apart from the metaphase plate) show that endogenous CDCA7 and endogenous γ-tubulin colocalize (Figure 3.14a). Thus, endogenous CDCA7 localizes at the centrosomes during mitosis.

The residue threonine (T) 163 of CDCA7 has been noted as a potential phosphorylation target of the centrosomal kinase Aurora A. So, the phosphorylation status of T163 CDCA7 at the centrosomes was investigated next. The mouse embryonic fibroblast cell line NIH 3T3 was synchronized with RO3306, released for 45 minutes and prepared for immunofluorescence. Cells are probed for endogenous phospho (p) T163 CDCA7 and γ-tubulin and then imaged after fluorescence microscopy. Cells found in metaphase and early anaphase (sister chromatids at the metaphase plate or sister chromatids that have just begun to pull apart from the metaphase plate) show that endogenous pT163 CDCA7 and endogenous γ-tubulin colocalize (Figure 3.14b). Thus, CDCA7 is phosphorylated on residue T163 at the centrosomes during mitosis.

TPX2 localizes with microtubule spindles during mitosis, and is highly concentrated near the spindle poles (centrosomes). Previous sections have also demonstrated interaction between TPX2 and CDCA7. So, TPX2 and CDCA7 may colocalize with one another during mitosis. Transiently transfected HEK 293T cells were analyzed after synchronization with RO3306, release for one hour and immunofluorescence preparation. Cells found in metaphase/anaphase show colocalization of CDCA7 and TPX2 (Figure 3.14c). However, CDCA7 appears to also localize as distinct foci at regions adjacent to the centrosomes in HEK 293T cells (Figure 3.14c). Thus, CDCA7 colocalizes with TPX2 in the mitotic phase of the cell cycle.

Finally, the phosphorylation status of T163 CDCA7 was investigated during mitosis. HEK 293T cells that were transfected with WT FLAG CDCA7 were either left asynchronized or were synchronized with RO3306 to the G2/M checkpoint. Synchronized cells were then released over various timepoints (0, 0.5, 1, 2 or 3 hours). Samples were either prepared for immunofluorescence or lysed, immunoprecipitated (IP) and subjected to western blotting.

At zero hours of release, there is no detectable pT163 CDCA7 signal, but after one hour of release, pT163 CDCA7 is clearly visible as round foci (Figure 3.15a). Expression and purification of WT FLAG CDCA7 was detected with an anti-FLAG antibody. WT FLAG CDCA7 was successfully expressed in all samples, at similar levels (Figure 3.15b). The IPs were also positive for pT163 CDCA7 (Figure 3.15b). The ratio of pT163 CDCA7 to total FLAG CDCA7 was determined for all samples. The ratio at zero hours of release is set to one-fold and the other ratios are divided by the ratio at zero hours of release to determine their folds. Within 30 minutes of release from the G2/M checkpoint, the pT163 CDCA7 level increases by 2-fold (Figure 3.15b). Thus, the pT163 CDCA7 level increases as cells progress through mitosis.

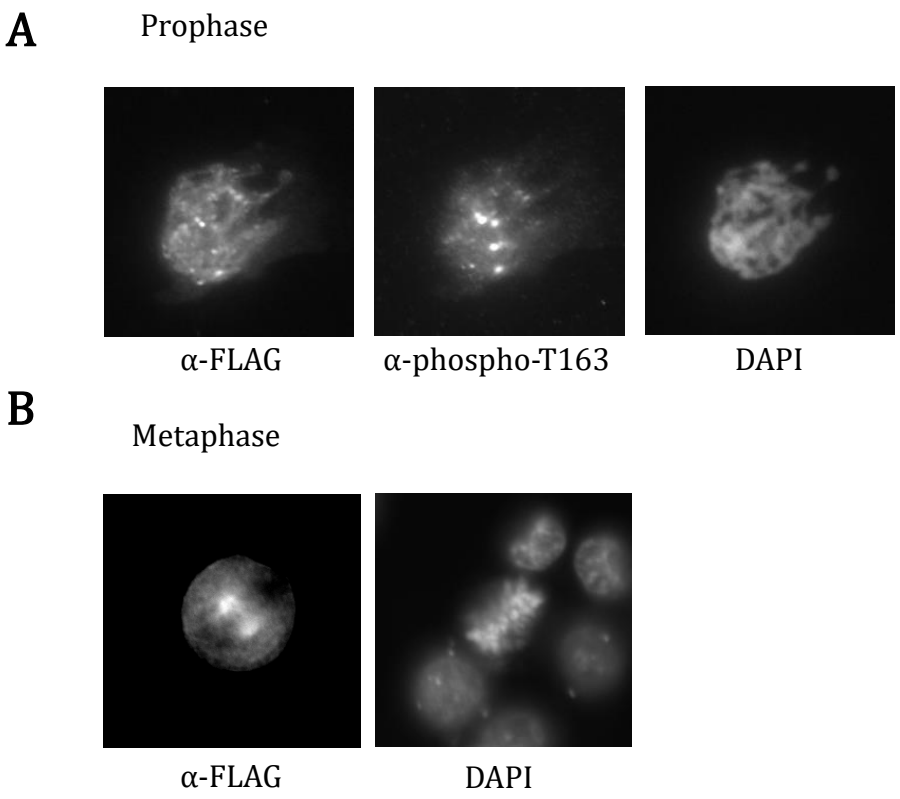

Figure 3.13: Localization of WT FLAG CDCA7 during mitosis. HEK 293T cells were transfected on glass coverslips with WT FLAG CDCA7 for 24 hours. The next day, cells were fixed and probed with the indicated antibodies and stained with 4',6-diamidino-2-phenylindole (DAPI). Slides were examined via fluorescence microscopy and photographed through a camera. A) Cell found to be in prophase where the nuclear envelope has disappeared, and spindles are beginning to form (DAPI image). Staining of FLAG CDCA7 and phospho-T163 CDCA7 is prominent, these regions appear as concentrated foci. B) Cell found in metaphase, DNA can be seen lining up at the metaphase plate (DAPI image). FLAG CDCA7 appears to localize at concentrated regions adjacent to the DNA, similar to centrosomes.

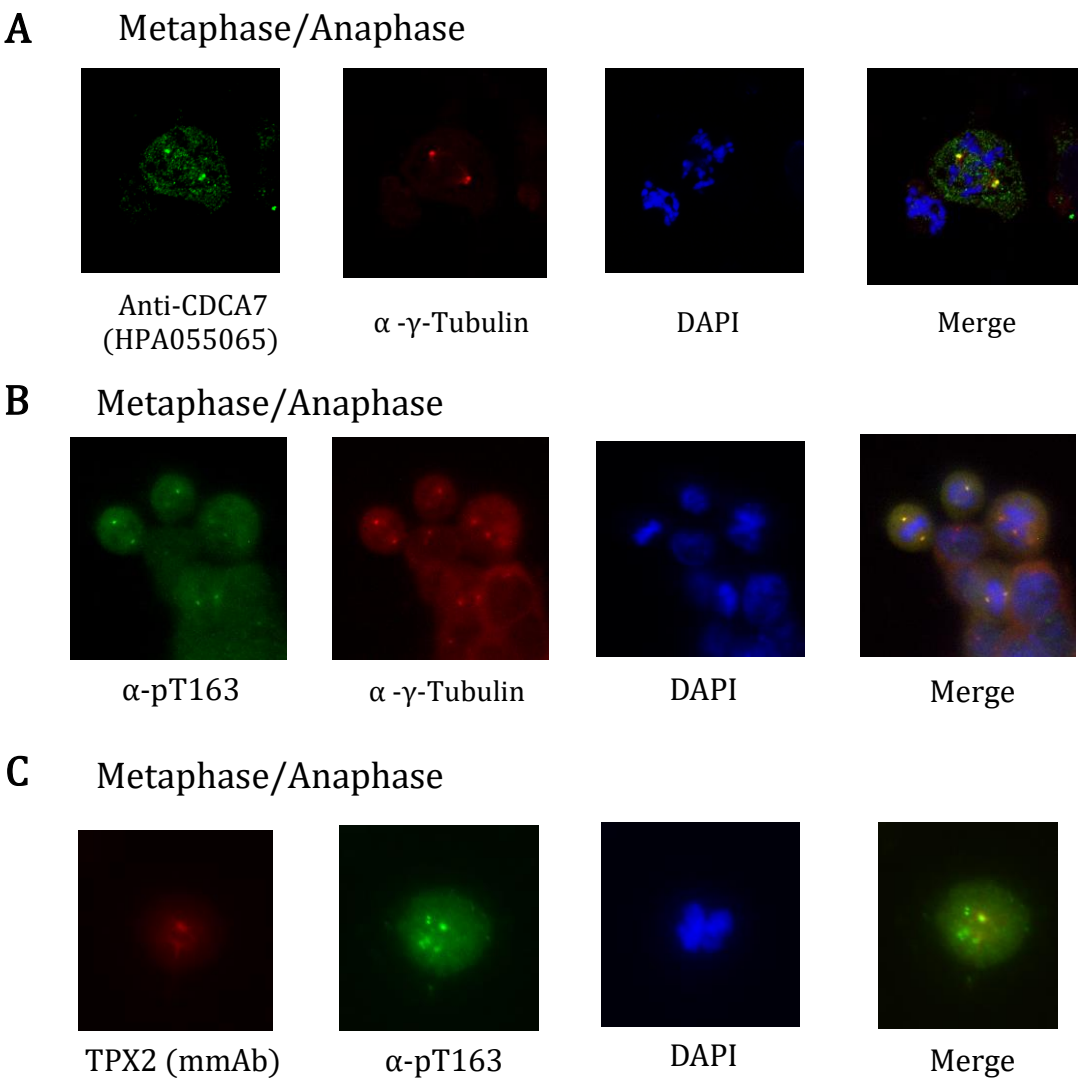

Figure 3.14: CDCA7 colocalization studies during mitosis. HeLa cells (A), NIH 3T3 cells (B) or HEK 293T cells transfected with WT FLAG CDCA7 for 24 hours (C) were plated on glass coverslips. Cells were incubated with RO3306 for 18 hours to synchronize to the G2/M checkpoint. Following synchronization, cells were released for either 40 minutes (A), 45 minutes (B) or 60 minutes (C) and then fixed. Cells were later probed with the indicated antibodies and stained with 4',6-diamidino-2-phenylindole (DAPI). Slides were examined via confocal microscopy (A) or fluorescence microscopy (B and C) and photographed through a camera. Images are all false colored. A) Cell found to be transitioning between metaphase and anaphase, sets of DNA are beginning to separate at the metaphase plate (DAPI image). Endogenous CDCA7 and γ-tubulin, a centrosomal marker, colocalize. Thus, CDCA7 localizes to the centrosomes. B) Cells found at metaphase and early anaphase (DAPI image). Endogenous phospho-threonine 163 (pT163) and γ-tubulin colocalize. Therefore, CDCA7 is phosphorylated at the centrosome. C) Cell found to be transitioning between metaphase and anaphase (DAPI image). Endogenous TPX2 and pT163 CDCA7 colocalize near the regions where spindles branch out from the centrosomes (TPX2 image and merge image). Here pT163 CDCA7 also localizes as concentrated foci in regions adjacent to TPX2.

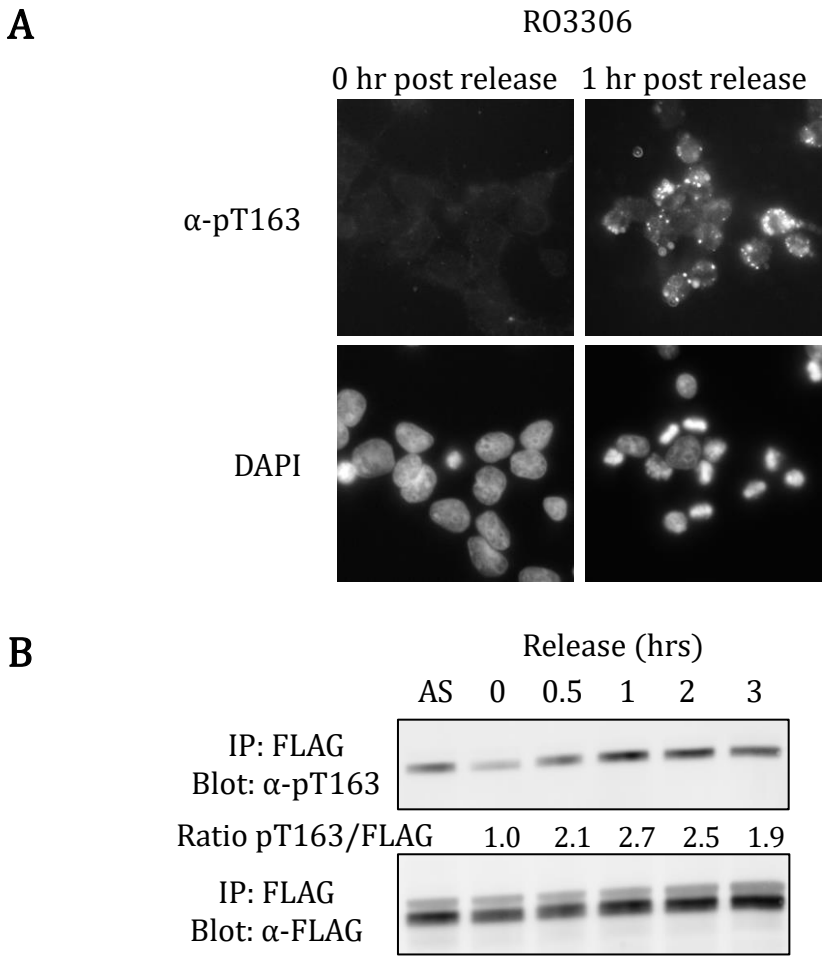

Figure 3.15: Changes in phosphorylation of T163 CDCA7 during mitosis. A) HEK 293T cells were transfected on glass coverslips with WT FLAG CDCA7 for 24 hours. Cells were incubated with RO3306 for 18 hours to synchronize to the G2/M checkpoint. Following synchronization, cells were either fixed immediately or released for one hour and then fixed. Cells were later probed with anti-phospho-T163 (anti-pT163) and stained with 4',6-diamidino-2-phenylindole (DAPI). Slides were examined via fluorescence microscopy and photographed through a camera. At the G2/M checkpoint (0 hours) pT163 staining is not detectable but after one hour of release, pT163 staining becomes prominent (anti-pT163 image). B) WT FLAG CDCA7 was transfected in HEK 293T cells, left untreated or synchronized for 18 hours with RO3306 and released at the indicated time points. Cells were then lysed and immunoprecipitated (IP) on anti-FLAG conjugated beads. Top. Here pT163 CDCA7 was detected with anti-pT163 CDCA7 immunoblotting. Bottom. Ectopically expressed FLAG constructs were identified with anti-FLAG immunoblotting. The ratio of pT163 CDCA7/FLAG CDCA7 is provided and this ratio at zero hours of release is set to one-fold. Within 30 minutes, pT163 levels increase by two-fold. Abbreviations. AS is asynchronous.

Chapter IV: Discussion, Future Directions and Conclusion

Discussion and Future Directions

CDCA7 was originally defined as a Myc target gene.[18] CDCA7 has been shown to be overexpressed in a variety of cancers[33] and plays a role in neoplastic growth[18]. Expression of CDCA7 is regulated by E2F transcription factors and the C-terminal domain of CDCA7 contains transcriptional abilities.[20] CDCA7 and Myc interact and this interaction is a requirement for colony formation and for apoptosis under serum starved conditions. The CDCA7-Myc interaction is regulated by Akt phosphorylation and 14-3-3 binding.[25] Understanding the roles CDCA7 plays within the cell may shed light on its oncogenic properties. This study focused on identifying novel interactors of CDCA7 through BioID and mass spectrometry. The next objective was to verify and characterize a candidate interaction through various cell and molecular biology methods.

The BioID protocol was optimized for both WT FLAG CDCA7-BirA* and the GFP-BirA* control. The experiments were done via transient transfection, however Amber L. Couzens, an associate at the Anne-Claude Gingras lab advised the use of stably transfected cell lines, which are found to substantially reduce background interactions detected during mass spectrometry. Amber L. Couzens has used BioID and immunoprecipitation (IP) experiments to map 599 novel interactions.[116] The candidate interactor TPX2 was verified through IP experiments and the region of interaction was mapped to residues 195-204 of CDCA7. Another experiment that can be performed centers around generation of various CDCA7-

BirA* deletion constructs that are subjected to BioID. Ideally, these experiments would find loss of TPX2 biotinylation when residues 195-204 of CDCA7-BirA* are deleted.

The residue threonine (T) 163 of CDCA7 conforms to the Aurora A phosphorylation consensus site and inhibition of Aurora A kinase was also found to reduce the levels of T163 phosphorylation. This suggests that CDCA7 is an Aurora A phosphorylation target. One question to ask is whether Aurora A phosphorylation impacts the interaction between CDCA7 and TPX2. Coexpression of CDCA7 and TPX2 in the presence and absence of Aurora A inhibitors may provide answers to this question. Verification of CDCA7 as an Aurora A phosphorylation target failed since GST-WT FLAG CDCA7 could not be purified. CDCA7 can be cloned with a 6xHis tag and be purified via ion-metal immobilized chromatography (IMAC). Once CDCA7 can be purified, in vitro kinase assays can be performed with Aurora A.

The phosphorylation of CDCA7 increases during mitosis and this suggests a role for CDCA7 during the M phase of the cell cycle. Other cell division cycle associated protein (CDCA) family members including CDCA1[117], CDCA2[118], CDCA3[119], CDCA5[120] and CDCA8[121] are involved in mitosis. Since CDCA7 interacts with TPX2 and is a potential Aurora A phosphorylation target, CDCA7 may play a role in microtubule spindle assembly. Consequently, dysregulation of CDCA7 may result in spindle assembly defects, genomic instability and account for the oncogenic phenotype seen with CDCA7 overexpression.

CDCA7 may instead be a phosphorylation target of Aurora B. Mass spectrometry results generated from WT FLAG CDCA7-BirA* have identified several Aurora B associated proteins. This includes CDCA2/protein phosphatase 1γ (PP1γ)/Repo-Man. CDCA2 dephosphorylates histone 3 (H3) at threonine (T) 3, and this dephosphorylation targets

Aurora B to chromosomes.[122] Another potential interactor, human Spindly, localizes to kinetochores via Aurora B.[123]

The putative interactor of CDCA7 called regulator of chromatin condensation 2 (RCC2) shares homology with RCC1 and is a guanine exchange factor (GEF). RCC2 activates Ras-like protein A (RalA) which is a GTPase. Interactions between kinetochores and microtubules are regulated by Aurora B, RCC2 and RalA and reduction of RCC2 or RalA protein downregulates Aurora B activity.[124] CDCA8 may also interact with CDCA7. CDCA8 is part of the chromosome passenger complex (CPC) and binds with Aurora B interactors Survivin and INCENP. Knockdown of CDCA8 leads to deregulation of kinetochore-chromosome attachment which leads to defects in chromosome segregation.[121] TPX2 also mediates Aurora B activation. Immunodepletion of TPX2 reduces the Aurora B-Survivin or Aurora B-INCENP interactions, while TPX2 overexpression has the opposite effect.[125] Thus, experiments investigating the effects of Aurora B on CDCA7 should be considered.

The localization pattern of Aurora B is chromosomal (prophase), centromeric (metaphase) and midzone (anaphase).[126] CDCA7 on the other hand localizes at centrosomes during prophase, metaphase and anaphase and is phosphorylated at the centrosomes. The localization of CDCA7 coincides more with Aurora A[81], so CDCA7 is more likely to be an Aurora A kinase phosphorylation target. However, CDCA7 localizes at the centrosomes while the TPX2-AurA complex localizes to branching microtubules[81]. How can this complex phosphorylate CDCA7 at the centrosome? This may be contingent on the mitotic phase where CDCA7 is phosphorylated. For example, during prometaphase, the centrosomes (CDCA7) and branching microtubules (TPX2-AurA complex), where microtubule nucleation

events occur, are in close proximity.[74] During this time, CDCA7 may interact with the TPX2-AurA complex. Aurora A can then phosphorylate CDCA7 at T163. Several centrosomal target proteins of Aurora A cannot be phosphorylated in the absence of TPX2. One example is the transforming acid coiled coil 3 protein (TACC3).[127] Thus, the TPX2-AurA complex likely regulates the phosphorylation status of residue T163 of CDCA7, based on the evidence provided in this study and findings in scientific literature.

Aurora A phosphorylation targets were also identified through mass spectrometry such as cofilin-1[128]. The putative interactor DLGAP5, also known as hepatoma Up-regulated protein (HURP), is a known oncogene that plays a role in hepatocellular carcinomas.[129] HURP localization is RanGTP dependent[130] and HURP is a TPX2-AurA complex regulated protein[131]. Aurora A phosphorylation stabilizes HURP.[131] Overexpression of HURP also leads to spindle defects and HURP can arrest cells at the spindle checkpoint. The N- and C-terminal domains of unphosphorylated HURP interact and this interaction is disrupted by phosphorylation of HURP at the C-terminal by Aurora A. The N-terminal domain of HURP then binds to microtubules and stabilizes them. Dysregulation of HURP permits spindle checkpoint evasion and is thought to be a major cause of TPX2-AurA complex mediated oncogenesis.[132] So, verification of CDCA7-HURP interaction would provide another line of evidence for CDCA7 regulation via the TPX2-AurA complex.

CDCA7 has been defined as a phosphorylation target of Akt.[25] Active Akt, phosphorylated at threonine (T) 308, also localizes to centrosomes during mitosis. The levels of phospho-T308 Akt increase during prophase, peak at metaphase and return to basal levels following chromosome segregation.[133] The effect of Akt inhibition on the phosphorylation

status of residue T163 of CDCA7 should be considered. The possibility of Akt and CDCA7 colocalization during mitosis should also be investigated.

A theory postulates that target genes of Myc lead to the phenotypic outcomes of Myc expression, including tumorigenesis.[33] CDCA7 is an established target gene of Myc.[18] ChIP experiments have shown direct interaction between Myc and the Myc E-box at the transcription start site (TTS) of the Aurora A promoter. Myc also positively regulates Aurora A gene expression.[134] Myc is correlated with 70% of cancers.[15] Amplification of chromosome 20q where Aurora A and TPX2 genes reside coincide with amplification of chromosome 8q where the Myc gene resides, in colorectal cancers. In assays for colony growth in soft agar, overexpression of Aurora A, TPX2 and Myc results in violent anchorage-independent growth.[135]

CDCA7 has also been shown to be overexpressed in numerous cancers including colorectal cancer. Upregulation of CDCA7 and Myc has been demonstrated in colorectal cancer patients.[33] The human protein atlas (HPA) has reported CDCA7 dysregulation in 597 colorectal cancer cases. While 124 patients have passed away (21%), 473 patients are still alive (79%). Unfortunately, 64% of remaining patients have low probability of survival (301 cases).[136] Accordingly, future experiments should investigate the effects of Myc, Aurora A kinase and TPX2 on CDCA7 in the context of colon carcinoma (HCT116) and adenoma (DLD-1) cell lines.

In hepatocellular carcinomas (HCCs), ChIP experiments have demonstrated binding of Myc to the Aurora A promoter and Myc also transcriptionally activates Aurora A in HCCs. Aurora A has also been shown to bind to the Myc gene. Aurora A binds to the nuclear

hypersensitive element III(1) and increases Myc expression.[137] However, NHEIII(1) has been shown to negatively regulate Myc expression[138], so Aurora A may negatively regulate this region[137]. Expression of Aurora A and Myc are linked and increasing concentrations of Aurora A kinase in the nucleus lead to increases in Myc mRNA expression.[137] TPX2 is also overexpressed in HCCs and inhibition of TPX2 expression results in decreases in cell proliferation and invasion.[139]

Interestingly, while mRNA analysis of CDCA7 in HCCs has not been directly reported, the HPA has identified dysregulation of CDCA7 as a poor prognosis marker for liver cancers. There are 365 documented cases of CDCA7 deregulation in liver cancer patients. Out of the 365 reported cases found in the HPA, only 64% of patients are currently alive and 36% of patients are dead. From the remaining 235 cases, 79% of patients have low predicted probability of survival.[136] Consequently, CDCA7 regulation and expression with respect to Myc, Aurora A kinase and TPX2 in HCC cell lines such as HepG2 and BEL-7402 should be considered.

Conclusion

Aurora A kinase and its activator TPX2 play integral roles during mitosis.[105] Null mice of Aurora A and TPX2 are embryonically lethal and have defects in spindle assembly and chromosome segregation.[59,86] Both Aurora A and TPX2 are potent oncogenes that promote genomic instability and drive tumorigenesis.[75] The TPX2-AurA complex is regulated by the RanGTP gradient and localizes to microtubules where Aurora A phosphorylates target proteins. The phosphorylation targets of Aurora A mediate microtubule nucleation and leads to spindle assembly, chromosome segregation and ultimately proper cell division.[105]

Discerning the roles of the TPX2-AurA complex targets is required to delineate the process of spindle assembly and its dysregulation.

The study presented here has demonstrated that CDCA7 and TPX2 directly interact with each other. The acidic amino acid residues within residues 195-204 of CDCA7 may provide the mode of interaction between these two proteins. Inhibitor experiments suggest that Aurora A kinase phosphorylates CDCA7 at the residue T163. CDCA7 has been shown to localize to the centrosome during mitosis and is phosphorylated at the centrosomes. CDCA7 has been shown to colocalize with TPX2 around the centrosomes. Thus, during mitosis, CDCA7 at the centrosome may interact with TPX2 at branching microtubules. Interaction of CDCA7 and TPX2 brings active Aurora A near CDCA7. Aurora A can then phosphorylate CDCA7 at T163. Figure 4.1 provides an overview of this study's findings and theories.

Future experiments should consider the significance of CDCA7 T163 phosphorylation during mitosis. As CDCA7 interacts with TPX2 and is potentially regulated by Aurora A, it may be involved in spindle assembly. Interaction of CDCA7 with other TPX2-AurA complex targets should be investigated. The effect of CDCA7 knockdown or the effect of loss of function mutant T163A CDCA7 on spindle assembly should be considered. The possibility of Aurora B or Akt regulation of CDCA7 during mitosis should also be examined. Finally, the effects of Myc, Aurora A kinase and TPX2 on CDCA7 should also be studied in colorectal and liver cancers. These findings shed light on the interactions and regulation of CDCA7 and define the CDCA7 protein in normal physiological contexts. The information here will facilitate points of reference when investigating the role of CDCA7 in dysregulated processes, such as tumorigenesis.

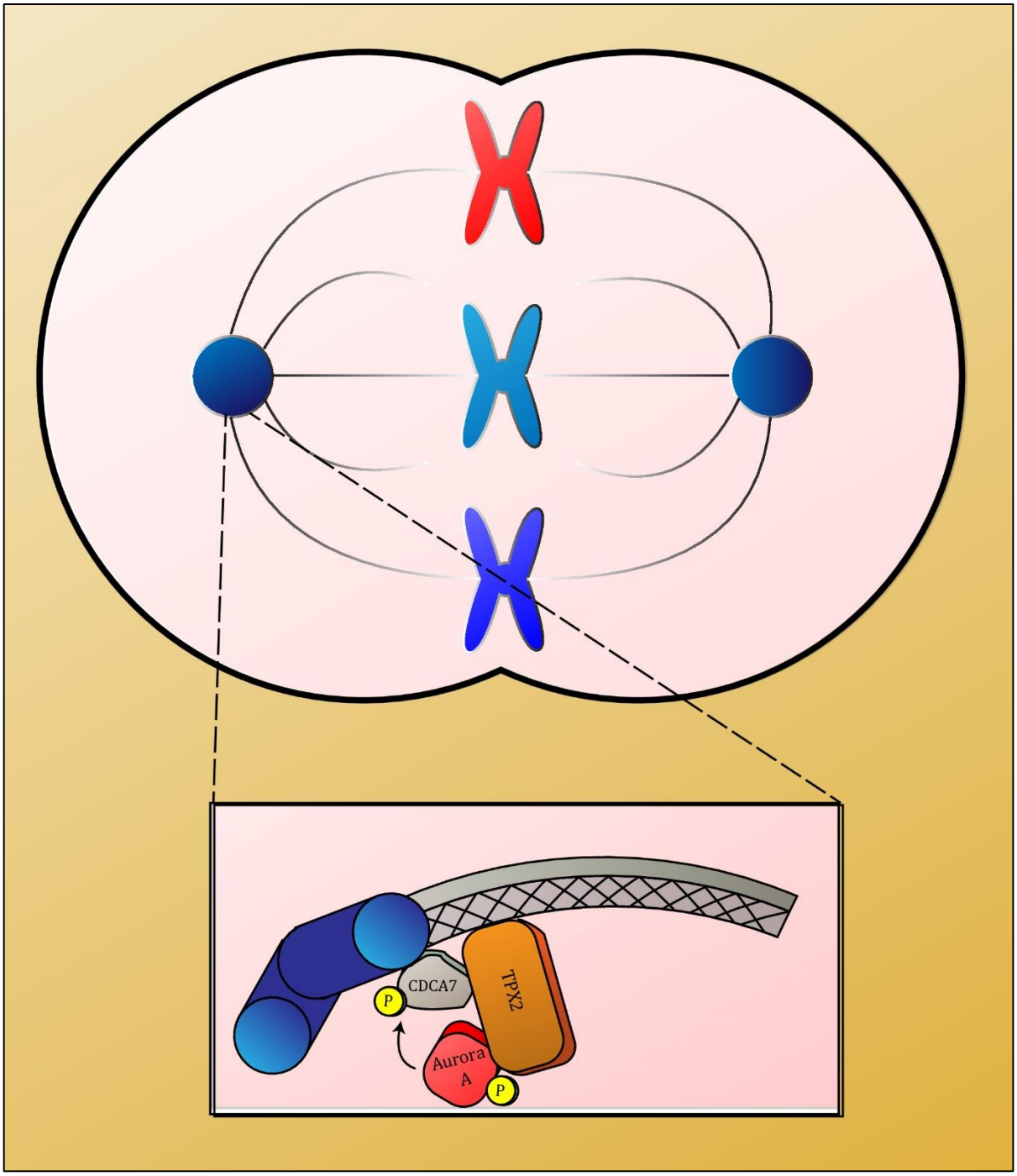

Figure 4.1: CDCA7, TPX2 and Aurora A model. Zoomed out. Cell in the mitotic phase of the cell cycle. Zoomed in. During mitosis, CDCA7 localizes to the centrosomes. TPX2 bound to microtubules also binds with Aurora A. TPX2 binding allows Aurora A to autophosphorylate and activate itself. TPX2 also directly interacts with CDCA7. Aurora A, complexed with TPX2, phosphorylates CDCA7 at threonine (T) 163.

Bibliography

1. Ferlay J, Soerjomataram I, Dikshit R, Eser S, Mathers C, Rebelo M, Parkin DM, Forman D, Bray F. 2015. Cancer incidence and mortality worldwide: Sources, methods and major patterns in GLOBOCAN 2012. Int. J. Cancer. 136:E359–E386.
2. Bray F, Soerjomataram I. 2015. The Changing Global Burden of Cancer: Transitions in Human Development and Implications for Cancer Prevention and Control. In: Gelband H, Jha P, Sankaranarayanan R, et al., editors. Cancer: Disease Control Priorities, Third Edition (Volume 3). Washington (DC): The International Bank for Reconstruction and Development / The World Bank. Chapter 2.
3. Canadian Cancer Society's Advisory Committee on Cancer Statistics (CCSACCS). 2015. Canadian Cancer Statistics 2015. Toronto, ON: Canadian Cancer Society.
4. Tansey WP, P. W. 2014. Mammalian MYC Proteins and Cancer. New J. Sci. 2014:1–27.
5. Dang C V., O'Donnell KA, Zeller KI, Nguyen T, Osthus RC, Li F. 2006. The c-Myc target gene network. Semin. Cancer Biol. 16:253–264.
6. Zeller KI, Zhao X, Lee CWH, Chiu KP, Yao F, Yustein JT, Ooi HS, Orlov YL, Shahab A, Yong HC, et al. 2006. Global mapping of c-Myc binding sites and target gene networks in human B cells. Proc. Natl. Acad. Sci. U. S. A. 103:17834–9.
7. Dominguez-sola D, Gautier J. 2014. MYC and the Control of DNA Replication. Cold Spring Harb Perspect Med. 4(6): a014423
8. Rahl PB1, Young RA. 2014. MYC and transcription elongation. Cold Spring Harb Perspect Med. 1;4(1): a020990.
9. van Riggelen J, Yetil A, Felsher DW.2010. MYC as a regulator of ribosome biogenesis and protein synthesis. Nat Rev Cancer. 10(4):301-309.
10. Baudino TA, McKay C, Pendeville-Samain H, Nilsson JA, Maclean KH, White EL, Davis AC, Ihle JN, Cleveland JL. 2002. c-Myc is essential for vasculogenesis and angiogenesis during development and tumor progression. Genes Dev. 16:2530–2543.
11. Casey SC, Baylot V, Felsher DW. 2017. MYC: Master Regulator of Immune Privilege. Trends Immunol. 38:298–305.
12. Dang CV. 2013. MYC, metabolism, cell growth, and tumorigenesis. Cold Spring Harb Perspect Med. 3(8): a014217.
13. Nilsson JA, Cleveland JL. 2003. Myc pathways provoking cell suicide and cancer. Oncogene. 22:9007–9021.
14. Gabay M, Li Y, Felsher DW. 2014. MYC activation is a hallmark of cancer initiation and maintenance. Cold Spring Harb Perspect Med. 4(6): a014241.
15. Dang C V. 2012. MYC on the path to cancer. Cell. 149:22–35.

16. Marinkovic D, Marinkovic T, Kokai E, Barth T, Möller P, Wirth T. 2004. Identification of novel Myc target genes with a potential role in lymphomagenesis. Nucleic Acids Res. 32:5368–5378.
17. Lewis BC, Shim H, Li Q, Wu CS, Lee LA, Maity A, Dang C V. 1997. Identification of putative c-Myc-responsive genes: characterization of rcl, a novel growth-related gene. Mol. Cell. Biol. 17:4967–78
18. Prescott JE, Osthus RC, Linda A, Lewis BC, Shim H, John F, Guo Q, Hawkins AL, Griffin CA, Dang C V, et al. 2013. A Novel c-Myc - responsive Gene , JPO1 , Participates in Neoplastic Transformation. J Biol Chem. 276:48276–48284.
19. Haggerty TJ, Zeller KI, Osthus RC, Wonsey DR, Dang C V. 2003. A strategy for identifying transcription factor binding sites reveals two classes of genomic c-Myc target sites. Proc. Natl. Acad. Sci. U. S. A. 100:5313–5318.
20. Goto Y, Hayashi R, Muramatsu T, Ogawa H, Eguchi I, Oshida Y, Ohtani K, Yoshida K. 2006. JPO1/CDCA7, a novel transcription factor E2F1-induced protein, possesses intrinsic transcriptional regulator activity. Biochim. Biophys. Acta - Gene Struct. Expr. 1759:60–68.
21. Lukas J, Petersen BO, Holm K, Bartek J, Helin K. 1996. Deregulated expression of E2F family members induces S-phase entry and overcomes p16INK4A-mediated growth suppression. Mol. Cell. Biol. 16:1047–1057.
22. Huang A, Ho CSW, Ponzielli R, Barsyte-Lovejoy D, Bouffet E, Picard D, Hawkins CE, Penn LZ. 2005. Identification of a novel c-Myc protein interactor, JPO2, with transforming activity in medulloblastoma cells. Cancer Res. 65:5607–5619.
23. Chen K, Ou XM, Chen G, Si HC, Shih JC. 2005. R1, a novel repressor of the human monoamine oxidase A. J. Biol. Chem. 280:11552–11559.
24. Whitfield ML, Sherlock G, Saldanha AJ, Murray JI, Ball CA, Alexander KE, Matese JC, Perou CM, Hurt MM, Brown PO, Botstein D. 2002. Identification of genes periodically expressed in the human cell cycle and their expression in tumors. Mol. Cell. Biol. 13(6):1977-2000.
25. Gill RM, Gabor T V, Couzens AL, Scheid MP. 2013. The MYC-associated protein CDCA7 is phosphorylated by AKT to regulate MYC-dependent apoptosis and transformation. Mol. Cell. Biol. 33:498–513.
26. Alessi DR, Caudwell FB, Andjelkovic M, Hemmings BA, Cohen P. 1996. Molecular basis for the substrate specificity of protein kinase B; comparison with MAPKAP kinase-1 and p70 S6 kinase. FEBS Lett 399:333–338.
27. Johnson C, Crowther S, Stafford MJ, Campbell DG, Toth R, MacKintosh C. 2010. Bioinformatic and experimental survey of 14-3-3-binding sites. Biochem. J. 427:69–78.
28. Hoffman B, Liebermann DA. 2008. Apoptotic signaling by c-MYC. Oncogene. 27(50): 6462-72.

29. Veitia RA. 2007. Exploring the Molecular Etiology of Dominant-Negative Mutations. Plant Cell Online 19:3843–3851.
30. Wang B, Yang H, Liu YC, Jelinek T, Zhang L, Ruoslahti E, Fu H. 1999. Isolation of high-affinity peptide antagonists of 14-3-3 proteins by phage display. Biochemistry 38:12499–12504.
31. Song G, Ouyang G, Bao S. 2005. The activation of Akt/PKB signaling pathway and cell survival. J Cell Mol Med 9:59–71.
32. Gharbi SI, Zvelebil MJ, Shuttleworth SJ, Hancox T, Saghir N, Timms JF, Waterfield MD. 2007. Exploring the specificity of the PI3K family inhibitor LY294002. Biochem. J. 404:15–21.
33. Osthus RC, Karim B, Prescott JE, Smith BD, Mcdevitt M, Huso DL, Dang C V. 2005. The Myc Target Gene JPO1 / CDCA7 Is Frequently Overexpressed in Human Tumors and Has Limited Transforming Activity In vivo in Human Tumors and Has Limited Transforming Activity In vivo. 65(13):5620–5627.
34. Wang QL, Chen X, Zhang MH, Shen QH, Qin ZM. 2015. Identification of hub genes and pathways associated with retinoblastoma based on co-expression network analysis. Genet. Mol. Res. 14:16151–16161
35. Cheng C, Zhou Y, Li H, Xiong T, Li S, Bi Y, Kong P, Wang F, Cui H, Li Y, et al. 2016. Whole-Genome Sequencing Reveals Diverse Models of Structural Variations in Esophageal Squamous Cell Carcinoma. Am. J. Hum. Genet. 98:256–274.
36. Zhang W, Liu HT, Tu LIU H. 2002. MAPK signal pathways in the regulation of cell proliferation in mammalian cells. Cell Res. 12:9–18.
37. Ge X, Chen C, Hui X, Wang Y, Lam KSL, Xu A. 2011. Fibroblast growth factor 21 induces glucose transporter-1 expression through activation of the serum response factor/Ets-like protein-1 in adipocytes. J. Biol. Chem. 286:34533–34541.
38. Wente W, Efanov AM, Brenner M, Kharitonenkov A, Köster A, Sandusky GE, Sewing S, Treinies I, Zitzer H, Gromada J. 2006. Fibroblast growth factor-21 improves pancreatic beta-cell function and survival by activation of extracellular signal-regulated kinase 1/2 and Akt signaling pathways. Diabetes 55:2470–2478.
39. Li J, Yuan J. 2008 Caspases in apoptosis and beyond. Oncogene. 27: 6194-6206.
40. Wachmann K, Pop C, Van Raam BJ, Drag M, MacE PD, Snipas SJ, Zmasek C, Schwarzenbacher R, Salvesen GS, Riedl SJ. 2010. Activation and specificity of human caspase-10. Biochemistry 49:8307–8315.
41. Lamkanfi M, Kanneganti TD. 2010. Caspase-7: A protease involved in apoptosis and inflammation. Int. J. Biochem. Cell Biol. 42:21–24.
42. Johnstone RW, Frew AJ, Smyth MJ. 2008. The TRAIL apoptotic pathway in cancer onset, progression and therapy. Nat Rev Cancer. 8(10):782-98.
43. Ma D, Wang L, Wang S, Gao Y, Wei Y, Liu F. 2012. Foxn1 maintains thymic epithelial cells to support T-cell development via mcm2 in zebra fish.Proc Natl Acad Sci U S A.2012:2–7.

44. Bray SJ. 2006. Notch signalling in context. Nat Rev Mol Cell Biol. 17(11):722-735.
45. Castel D, Mourikis P, Bartels SJJ, Brinkman AB, Tajbakhsh S, Stunnenberg HG. 2013. Dynamic binding of RBPJ is determined by notch signaling status. Genes Dev. 27:1059–1071.
46. Guiu J, Bergen DJM, De Pater E, Islam ABMMK, Ayllón V, Gama-Norton L, Ruiz-Herguido C, González J, López-Bigas N, Menendez P, et al. 2014. Identification of Cdca7 as a novel Notch transcriptional target involved in hematopoietic stem cell emergence. J. Exp. Med. 211:2411–2423.
47. Englund C. 2005. Pax6, Tbr2, and Tbr1 Are Expressed Sequentially by Radial Glia, Intermediate Progenitor Cells, and Postmitotic Neurons in Developing Neocortex. J. Neurosci. 25:247–251.
48. Hébert JM, Fishell G. 2008. The genetics of early telencephalon patterning: some assembly required. Nat Rev Neurosci. 9(9):678-685.
49. Huang YT, Mason JO, Price DJ. 2017. Lateral cortical Cdca7 expression levels are regulated by Pax6 and influence the production of intermediate progenitors. BMC.Neurosci. 18:47.
50. Thijssen PE, Ito Y, Grillo G, Wang J, Velasco G, Nitta H, Unoki M, Yoshihara M, Suyama M, Sun Y, et al. 2015. Mutations in CDCA7 and HELLS cause immunodeficiency–centromeric instability–facial anomalies syndrome. Nat. Commun. 6:7870.
51. Walton E, Francastel C, Velasco G. 2014. Dnmt3b Prefers Germ Line Genes and Centromeric Regions: Lessons from the ICF Syndrome and Cancer and Implications for Diseases. Biology (Basel). 3:578–605.
52. van den Boogaard ML, Thijssen PE, Aytekin C, Licciardi F, Kiykim AA, Spossito L, Dalm VASH, Driessen GJ, Kersseboom R, de Vries F, et al. 2017. Expanding the mutation spectrum in ICF syndrome: Evidence for a gender bias in ICF2. Clin. Genet.:380–387.
53. Wu H, Thijssen PE, de Klerk E, Vonk KKD, Wang J, den Hamer B, Aytekin C, van der Maarel SM, Daxinger L. 2016. Converging disease genes in ICF syndrome: ZBTB24 controls expression of CDCA7 in mammals. Hum. Mol. Genet. 25:4041–4051.
54. Wittmann T, Boleti H, Antony C, Karsenti E, Vernos I. 1998. Localization of the kinesin-like protein Xklp2 to spindle poles requires a leucine zipper, a microtubule-associated protein, and dynein. J. Cell Biol. 143:673–685.
55. Kufer TA, Silljé HH, Körner R, Gruss OJ, Meraldi P, Nigg EA. 2002. Human TPX2 is required for targeting Aurora-A kinase to the spindle. J. Cell Biol. 158:617–623.
56. Petry S, Groen AC, Ishihara K, Mitchison TJ, Vale RD. 2013. Branching microtubule nucleation in xenopus egg extracts mediated by augmin and TPX2. Cell 152:768–777.

57. Schatz CA, Santarella R, Hoenger A, Karsenti E, Mattaj IW, Gruss OJ, Carazo-Salas RE. 2003. Importin α-regulated nucleation of microtubules by TPX2. EMBO J. 22:2060–2070.
58. Sillars-Hardebol AH, Carvalho B, Tijssen M, Beliën JA, de Wit M, Delis-van Diemen PM, Pontén F, van de Wiel MA, Fijneman RJ, Meijer GA. 2012. TPX2 and AURKA promote 20q amplicon-driven colorectal adenoma to carcinoma progression. Gut. 61(11):1568-1575.
59. Bird AW, Hyman A, Ca M, Castro IP De, Malumbres M. 2012. Tpx2 Controls Spindle Integrity , Genome Stability , and Tumor Development. 72:1518–1529.
60. Heidebrecht HJ, Adam-Klages S, Szczepanowski M, Pollmann M, Buck F, Endl E, Kruse ML, Rudolph P, Parwaresch R. 2003. repp86: A human protein associated in the progression of mitosis. Mol Cancer Res 1:271–279.
61. Ma N, Tulu US, Ferenz NP, Fagerstrom C, Wilde A, Wadsworth P. 2010. Poleward transport of TPX2 in the mammalian mitotic spindle requires dynein, Eg5, and microtubule flux. Mol. Cell. Biol. 21(6):979-88.
62. Akhmanova A, Steinmetz MO. 2015. Control of microtubule organization and dynamics: two ends in the limelight. Nat Rev Mol Cell Biol. 16(12):711-26.
63. Raynaud-Messina B, Merdes A. 2007. Gamma-tubulin complexes and microtubule organization. Curr Opin Cell Biol. 19(1):24-30.
64. Delgehyr N, Sillibourne J, Bornens M. 2015. Microtubule nucleation and anchoring at the centrosome are independent processes linked by ninein function. J Cell Sci. 118(Pt 8):1565-1575.
65. Kollman JM, Merdes A, Mourey L, Agard DA. 2011. Microtubule nucleation by γ-tubulin complexes. Nat Rev Mol Cell Biol. 12(11):709-21.
66. Goshima G, Mayer M, Zhang N, Stuurman N, Vale RD. 2008. Augmin: A protein complex required for centrosome-independent microtubule generation within the spindle. J. Cell Biol. 181:421–429.
67. Boleti H, Karsenti E, Vernos I. 1996. Xklp2, a novel Xenopus centrosomal kinesin-like protein required for centrosome separation during mitosis. Cell 84:49–59.
68. Rexach M, Blobel G. 1995. Protein import into nuclei: association and dissociation reactions involving transport substrate, transport factors, and nucleoporins. Cell 83:683–692.
69. Gruss OJ, Carazo-Salas RE, Schatz CA, Guarguaglini G, Kast J, Wilm M, Le Bot N, Vernos I, Karsenti E, Mattaj IW. 2001. Ran induces spindle assembly by reversing the inhibitory effect of importin α on TPX2 activity. Cell 104:83–93.
70. Kaláb P, Pralle A, Isacoff EY, Heald R, Weis K. 2006. Analysis of a RanGTP-regulated gradient in mitotic somatic cells. Nature. 440(7084):697-701.
71. Smith A, Brownawell A, Macara IG. 1998. Nuclear import of Ran is mediated by the transport factor NTF2. Curr. Biol. 8:1403–1406.

72. Paschal BM, Gerace L. 1995. Identification of NTF2, a cytosolic factor for nuclear import that interacts with nuclear pore complex protein p62. J. Cell Biol. 129:925–937.
73. Carazo-Salas RE, Guarguaglini G, Gruss OJ, Segref A, Karsenti E, Mattaj IW. 1999. Generation of GTP-bound Ran by RCC1 is required for chromatin-induced mitotic spindle formation. Nature. 400(6740):178-181.
74. Kalab P, Heald R. 2008. The RanGTP gradient - a GPS for the mitotic spindle. J. Cell Sci. 121:1577–1586.
75. Asteriti IA, Rensen WM, Lindon C, Lavia P, Guarguaglini G. 2010. The Aurora-A/TPX2 complex: A novel oncogenic holoenzyme? Biochim. Biophys. Acta - Rev. Cancer. 1806:230–239.
76. Carter SL, Eklund AC, Kohane IS, Harris LN, Szallasi Z.2006. A signature of chromosomal instability inferred from gene expression profiles predicts clinical outcome in multiple human cancers. Nat Genet. 38(9):1043-8.
77. Shiloh Y, Ziv Y. 2013. The ATM protein kinase: regulating the cellular response to genotoxic stress, and more. Nat Rev Mol Cell Biol. 14(4):197-210.
78. Matsuoka S, Ballif BA, Smogorzewska A, McDonald ER, Hurov KE, Luo J, Bakalarski CE, Zhao Z, Solimini N, Lerenthal Y, et al. 2007. ATM and ATR Substrate Analysis Reveals Extensive Protein Networks Responsive to DNA Damage. Science. 316:1160–1166.
79. Neumayer G, Helfricht A, Shim SY, Le HT, Lundin C, Belzil C, Chansard M, Yu Y, Lees-Miller SP, Gruss OJ, et al. 2012. Targeting protein for Xenopus kinesin-like protein 2 (TPX2) regulates γ-histone 2AX (γ-H2AX) levels upon ionizing radiation. J. Biol. Chem. 287:42206–42222.
80. Burum-Auensen E, De Angelis PM, Schjølberg AR, Kravik KL, Aure M, Clausen OPF. 2007. Subcellular localization of the spindle proteins Aurora A, Mad2, and BUBR1 assessed by immunohistochemistry. J. Histochem. Cytochem. 55:477–486.
81. Roghi C, Giet R, Uzbekov R, Morin N, Chartrain I, Le Guellec R, Couturier a, Dorée M, Philippe M, Prigent C. 1998. The Xenopus protein kinase pEg2 associates with the centrosome in a cell cycle-dependent manner, binds to the spindle microtubules and is involved in bipolar mitotic spindle assembly. J. Cell Sci. 111(Pt 5):557–572.
82. Tanaka M, Ueda A, Kanamori H, Ideguchi H, Yang J, Kitajima S, Ishigatsubo Y. 2002. Cell-cycle-dependent regulation of human aurora A transcription is mediated by periodic repression of E4TF1. J. Biol. Chem. 277:10719–10726.
83. Fu J, Bian M, Liu J, Jiang Q, Zhang C. 2009. A single amino acid change converts Aurora-A into Aurora-B-like kinase in terms of partner specificity and cellular function. Proc. Natl. Acad. Sci. U. S. A. 106:6939–6944.
84. Berdnik D, Knoblich JA. 2002. Drosophila Aurora-A is required for centrosome maturation and actin-dependent asymmetric protein localization during mitosis. Curr. Biol. 12:640–647.

85. Meraldi P, Honda R, Nigg EA. 2002. Aurora-A overexpression reveals tetraploidization as a major route to centrosome amplification in p53-/- cells. EMBO J. 21:483–492.
86. Lu LY, Wood JL, Ye L, Minter-Dykhouse K, Saunders TL, Yu X, Chen J. 2008. Aurora A is essential for early embryonic development and tumor suppression. J. Biol. Chem. 283:31785–31790.
87. Udayakumar TS, Belakavadi M, Choi KH, Pandey PK, Fondell JD. 2006. Regulation of Aurora-A kinase gene expression via GABP recruitment of TRAP220/MED1. J. Biol. Chem. 281:14691–14699.
88. Hung LY, Tseng JT, Lee YC, Xia W, Wang YN, Wu ML, Chuang YH, Lai CH, Chang WC. 2008. Nuclear epidermal growth factor receptor (EGFR) interacts with signal transducer and activator of transcription 5 (STAT5) in activating Aurora-A gene expression. Nucleic Acids Res. 36(13):4337-4351.
89. Toji S, Yabuta N, Hosomi T, Nishihara S, Kobayashi T, Suzuki S, Tamai K, Nojima H. 2004. The centrosomal protein Lats2 is a phosphorylation target of Aurora-A kinase. Genes Cells. 9(5):383-397.
90. Venoux M, Basbous J, Berthenet C, Prigent C, Fernandez A, Lamb NJ, Rouquier S. 2008. ASAP is a novel substrate of the oncogenic mitotic kinase Aurora-A: phosphorylation on Ser625 is essential to spindle formation and mitosis. Hum Mol Genet. 17(2):215-24.
91. Mori D, Yano Y, Toyo-oka K, Yoshida N, Yamada M, Muramatsu M, Zhang D, Saya H, Toyoshima YY, Kinoshita K, et al. 2007. NDEL1 Phosphorylation by Aurora-A Kinase Is Essential for Centrosomal Maturation, Separation, and TACC3 Recruitment. Mol. Cell. Biol. 27:352–367.
92. Kinoshita K, Noetzel TL, Pelletier L, Mechtler K, Drechsel DN, Schwager A, Lee M, Raff JW, Hyman AA. 2005. Aurora A phosphorylation of TACC3/maskin is required for centrosome-dependent microtubule assembly in mitosis. J. Cell Biol. 170:1047–1055.
93. Katayama H, Sasai K, Kawai H, Yuan ZM, Bondaruk J, Suzuki F, Fujii S, Arlinghaus RB, Czerniak BA, Sen S. 2004. Phosphorylation by aurora kinase A induces Mdm2-mediated destabilization and inhibition of p53. Nat Genet. 36(1):55-62.
94. Liu Q, Kaneko S, Yang L, Feldman RI, Nicosia S V., Chen J, Cheng JQ. 2004. Aurora-A abrogation of p53 DNA binding and transactivation activity by phosphorylation of serine 215. J. Biol. Chem. 279:52175–52182.
95. Briassouli P, Chan F, Savage K, Reis-Filho JS, Linardopoulos S. 2007. Aurora-A Regulation of Nuclear Factor-κB Signaling by Phosphorylation of IκBα. Cancer Res. 67:1689–1695.
96. Yu CT, Wu JC, Liao MC, Hsu SL, Huang CY. 2008. Identification of c-Fos as a mitotic phosphoprotein: regulation of c-Fos by Aurora-A. J Biomed Sci. 15(1):79-87.

97. Bischoff JR, Al. E. 1998. A homologue of Drosophila is oncogenic and amplified in human colorectal cancers. EMBO J. 17:3052–3065.
98. Yan M, Wang C, He B, Yang M, Tong M, Long Z, Liu B, Peng F, Xu L, Zhang Y, Liang D, Lei H, Subrata S, Kelley KW, Lam EW, Jin B, Liu. 2016. Aurora-A Kinase: A Potent Oncogene and Target for Cancer Therapy. Med Res Rev. 36(6):1036-1079.
99. Piast M, Kustrzeba-Wójcicka I, Matusiewicz M, Banaś T. 2005. Molecular evolution of enolase. Acta Biochim. Pol. 52:507–513.
100. Eyers PA, Erikson E, Chen LG, Maller JL. 2013. A novel mechanism for activation of the protein kinase Aurora A. Curr Biol. 13(8):691-697.
101. Hirota T, Kunitoku N, Sasayama T, Marumoto T, Zhang D, Nitta M, Hatakeyama K, Saya H. 2003. Aurora-A and an interacting activator, the LIM protein Ajuba, are required for mitotic commitment in human cells. Cell. 114:585–598.
102. Littlepage LE, Wu H, Andresson T, Deanehan JK, Amundadottir LT, Ruderman J V. 2002. Identification of phosphorylated residues that affect the activity of the mitotic kinase Aurora-A. Proc. Natl. Acad. Sci. U. S. A. 99:15440–15445.
103. Bayliss R, Sardon T, Vernos I, Conti E. 2003. Structural basis of Aurora-A activation by TPX2 at the mitotic spindle. Mol. Cell 12:851–862.
104. Mori D, Yamada M, Mimori-Kiyosue Y, Shirai Y, Suzuki A, Ohno S, Saya H, Wynshaw-Boris A, Hirotsune S. 2009. An essential role of the aPKC-Aurora A-NDEL1 pathway in neurite elongation by modulation of microtubule dynamics. Nat Cell Biol. 11(9):1057-1068.
105. Scrofani J, Sardon T, Meunier S, Vernos I. 2015. Microtubule nucleation in mitosis by a RanGTP-dependent protein complex. Curr. Biol. 25:131–140.
106. Pinyol R, Scrofani J, Vernos I. 2013. The role of NEDD1 phosphorylation by aurora a in chromosomal microtubule nucleation and spindle function. Curr. Biol. 23:143–149.
107. Streaker ED, Beckett D. 1999. Ligand-linked structural changes in the Escherichia coli biotin repressor: the significance of surface loops for binding and allostery. J Mol Biol. 292(3):619-632.
108. Kwon K, Beckett D. 2000. Function of a conserved sequence motif in biotin holoenzyme synthetases. Protein Sci. 9(8):1530-1539.
109. Roux KJ, Kim DI, Raida M, Burke B. 2012. A promiscuous biotin ligase fusion protein identifies proximal and interacting proteins in mammalian cells. J. Cell Biol. 196:801–810.
110. Chivers CE, Koner AL, Lowe ED, Howarth M. 2011. How the biotin–streptavidin interaction was made even stronger: investigation via crystallography and a chimaeric tetramer. Biochem. J. 435:55–63.
111. Kim DI, KC B, Zhu W, Motamedchaboki K, Doye V, Roux KJ. 2014. Probing nuclear pore complex architecture with proximity-dependent biotinylation. Proc. Natl. Acad. Sci. 111:E2453–E2461.

112. Nicolas A, Lucchetti-Miganeh C, Yaou RB, Kaplan JC, Chelly J, Leturcq F, Barloy-Hubler F, Le Rumeur E. 2012. Assessment of the structural and functional impact of in-frame mutations of the DMD gene, using the tools included in the eDystrophin online database. Orphanet J Rare Dis. 7:45.
113. Ferrari S, Marin O, Pagano MA, Meggio F, Hess D, El-Shemerly M, Krystyniak A, Pinna LA. 2005. Aurora-A site specificity: a study with synthetic peptide substrates. Biochem J. 390(Pt 1):293-302.
114. Jackman J, O'Connor PM. 2001. Methods for synchronizing cells at specific stages of the cell cycle. In: Current Protocols in Cell Biology. New York: Wiley Online Library. Chapter 8: Unit 8.3.
115. Vassilev LT. 2006. Cell cycle synchronization at the G2/M phase border by reversible inhibition of CDK1. Cell Cycle. 5:2555–2556.
116. Couzens AL, Knight JD, Kean MJ, Teo G, Weiss A, Dunham WH, Lin ZY, Bagshaw RD, Sicheri F, Pawson T, Wrana JL, Choi H, Gingras AC. 2013. Protein interaction network of the mammalian Hippo pathway reveals mechanisms of kinase-phosphatase interactions. Sci Signal. 6(302):rs15.
117. DeLuca JG, Moree B, Hickey JM, Kilmartin J V, Salmon ED. 2002. hNuf2 inhibition blocks stable kinetochore-microtubule attachment and induces mitotic cell death in HeLa cells. J. Cell Biol. 159:549–555.
118. Vagnarelli P, Ribeiro S, Sennels L, Sanchez-Pulido L, de Lima Alves F, Verheyen T, Kelly DA, Ponting CP, Rappsilber J, Earnshaw WC. 2011. Repo-Man Coordinates Chromosomal Reorganization with Nuclear Envelope Reassembly during Mitotic Exit. Dev. Cell 21:328–342.
119. Ayad NG, Rankin S, Murakami M, Jebanathirajah J, Gygi S, Kirschner MW. 2003. Tome-1, a trigger of mitotic entry, is degraded during G1 via the APC. Cell. 113:101–113.
120. Rankin S, Ayad NG, Kirschner MW. 2005. Sororin, a substrate of the anaphase-promoting complex, is required for sister chromatid cohesion in vertebrates. Mol. Cell. 18:185–200.
121. Gassmann R, Carvalho A, Henzing AJ, Ruchaud S, Hudson DF, Honda R, Nigg EA, Gerloff DL, Earnshaw WC. 2004. Borealin: A novel chromosomal passenger required for stability of the bipolar mitotic spindle. J. Cell Biol. 166:179–191.
122. Qian J, Lesage B, Beullens M, Van Eynde A, Bollen M. 2011. PP1/repo-man dephosphorylates mitotic histone H3 at T3 and regulates chromosomal aurora B targeting. Curr. Biol. 21:766–773.
123. Ying WC, Fava LL, Uldschmid A, Schmitz MHA, Gerlich DW, Nigg EA, Santamaria A. 2009. Mitotic control of kinetochore-associated dynein and spindle orientation by human Spindly. J. Cell Biol. 185:859–874.

124. Papini D, Langemeyer L, Abad MA, Kerr A, Samejima I, Eyers PA, Jeyaprakash AA, Higgins JM, Barr FA2, Earnshaw WC. 2015. TD-60 links RalA GTPase function to the CPC in mitosis. Nat. Commun. 6:7678.
125. Iyer J, Tsai MY. 2012. A novel role for TPX2 as a scaffold and co-activator protein of the Chromosomal Passenger Complex. Cell Signal. 24(8):1677-1689.
126. Adams RR, Carmena M, Earnshaw WC. 2001. Chromosomal passengers and the (aurora) ABCs of mitosis. Trends Cell Biol. 11(2):49-54.
127. Brunet S, Dumont J, Lee KW, Kinoshita K, Hikal P, Gruss OJ, Maro B, Verlhac MH. 2008. Meiotic regulation of TPX2 protein levels governs cell cycle progression in mouse oocytes. PLoS One. 3(10):e3338.
128. Ritchey L, Chakrabarti R. 2014. Aurora A kinase modulates actin cytoskeleton through phosphorylation of Cofilin: Implication in the mitotic process. Biochim. Biophys. Acta - Mol. Cell Res. 1843:2719–2729.
129. Tsou AP, Yang CW, Huang CY, Yu RC, Lee YC, Chang CW, Chen BR, Chung YF, Fann MJ, Chi CW, et al. 2003. Identification of a novel cell cycle regulated gene, HURP, overexpressed in human hepatocellular carcinoma. Oncogene. 22(2):298-307.
130. Silljé HHW, Nagel S, Körner R, Nigg EA. 2006. HURP Is a Ran-Importin β-Regulated Protein that Stabilizes Kinetochore Microtubules in the Vicinity of Chromosomes. Curr. Biol. 16:731–742.
131. Yu CTR, Hsu JM, Lee YCG, Tsou AP, Chou CK, Huang CYF. 2005. Phosphorylation and stabilization of HURP by Aurora-A: implication of HURP as a transforming target of Aurora-A. Mol. Cell. Biol. 25:5789–5800.
132. Wong J, Lerrigo R, Jang CY, Fang G. 2008. Aurora A regulates the activity of HURP by controlling the accessibility of its microtubule-binding domain. Mol. Cell. Biol. 19(5):2083-2091.
133. Wakefield JG, Stephens DJ, Tavaré JM. 2003. A role for glycogen synthase kinase-3 in mitotic spindle dynamics and chromosome alignment. J. Cell Sci. 116:637–646.
134. Den Hollander J, Rimpi S, Doherty JR, Rudelius M, Buck A, Hoellein A, Kremer M, Graf N, Scheerer M, Hall MA, et al. 2010. Aurora kinases A and B are up-regulated by Myc and are essential for maintenance of the malignant state. Blood. 116:1498–1505.
135. Takahashi Y, Sheridan P, Niida A, Sawada G, Uchi R, Mizuno H, Kurashige J, Sugimachi K, Sasaki S, Shimada Y, et al. 2015. The AURKA/TPX2 axis drives colon tumorigenesis cooperatively with MYC. Ann Oncol. 26(5):935-942.
136. Uhlen M, Zhang C, Lee S, Sjöstedt E, Fagerberg L, Bidkhori G, Benfeitas R, Arif M, Liu Z, Edfors F, et al. 2017. A pathology atlas of the human cancer transcriptome. Science. 357(6352): eaan2507.
137. Lu L, Han H, Tian Y, Li W, Zhang J, Feng M, Li Y. 2015. Aurora kinase A mediates c-Myc's oncogenic effects in hepatocellular carcinoma. Mol Carcinog. 54(11):1467-1479.

138. González V, Hurley LH. 2010. The c-MYC NHE III(1): function and regulation. Annu Rev Pharmacol Toxicol. 50:111-129.
139. Huang Y, Guo W, Kan H. 2014. TPX2 is a prognostic marker and contributes to growth and metastasis of human hepatocellular carcinoma. Int. J. Mol. Sci. 15:18148–18161.

Appendices

Appendix A: Generation of BirA* Constructs

Abridged Version

Three BirA* constructs of particular interest were generated for BioID. These constructs are WT FLAG CDCA7-BirA*, T163A FLAG CDCA7-BirA* and c-Myc-BirA*.

Methods

Polymerase Chain Reaction (PCR): The genes encoding WT FLAG CDCA7 and T163A FLAG CDCA7 in the pCMV-3X-FLAG vector and c-Myc in the pcDNA 3.0 vector were subjected to the Q5 PCR protocol, as detailed in Chapter 2. The forward and reverse primers for WT FLAG CDCA7 and T163A FLAG CDCA7 were identical and introduced AgeI and BspEI restriction enzyme cut sites at the 5' and 3' ends of the PCR products, respectively. The forward and reverse primers for c-Myc introduced the restriction enzyme cut site AgeI at the 5' end and BamHI at the 3' end of its PCR product.

Restriction Enzyme Digests: Restriction enzyme digestion followed the general protocol outlined in Chapter 2. The blunt end PCR products of WT FLAG CDCA7 and T163A FLAG CDCA7, as well pcDNA 3.1 MCS-BirA(R118G)-HA (BirA* backbone vector) were subjected to partial restriction digests with AgeI (NEB Catalog# R0552) in NEBuffer™ 1.1 (NEB Catalog# B7201) for 30 minutes at 37°C, followed by restriction digest with BspEI (NEB Catalog# R0540) in NEBuffer™ 3.1 (NEB Catalog# B7203) for 30 minutes at 37°C. The blunt end PCR product of c-Myc and the BirA* backbone vector were subjected to double restriction digests

with AgeI (NEB Catalog# R0552) and BamHI (NEB Catalog# R0136) in Cut Smart® Buffer (NEB Catalog# B7204) for 1 hour at 37°C. To verify positive ligations, miniprepped DNA from colonies of WT FLAG CDCA7-BirA* and T163A FLAG CDCA7-BirA* ligations were double digested with NheI (NEB Catalog# R0131) and XhoI (NEB Catalog# R0146) in Cut Smart® Buffer at 37°C for 1 hour. For c-Myc BirA*, miniprepped DNA from ligation reaction colonies were double digested with NheI and ClaI (NEB Catalog# R0147) in Cut Smart® Buffer at 37°C for 1 hour. The T163A mutation in CDCA7 was engineered to incorporate a BssHII cut site not present in the WT CDCA7 gene. Verification of the T163A deletion was done via restriction digest of BssHII (NEB Catalog# R0199) in Cut Smart® Buffer at 37°C for 1 hour.

Results

In order to generate the plasmids containing WT FLAG CDCA7-BirA*, T163A FLAG CDCA7-BirA* and c-Myc-BirA*, the PCR products of WT FLAG CDCA7, T163A FLAG CDCA7 and c-Myc were generated with primers that included restriction enzyme sites at their 5' and 3' ends (Figure A.1a). The PCR products were then purified from agarose gels, subjected to restriction digests along with the BirA* backbone vector and once again purified from agarose gels (Figure A.1b). The restriction digested desired insert and BirA* backbone vectors were ligated with one another and transformed into DH5α *E. coli* cells. Colonies were selected, miniprepped and subjected to restriction digests in order to verify inserts (Figure A.2, A.3). T163A mutation of the CDCA7 gene was also confirmed with restriction enzyme digestion (Figure A.4). Positive colonies were then midiprepped and sequence verified.

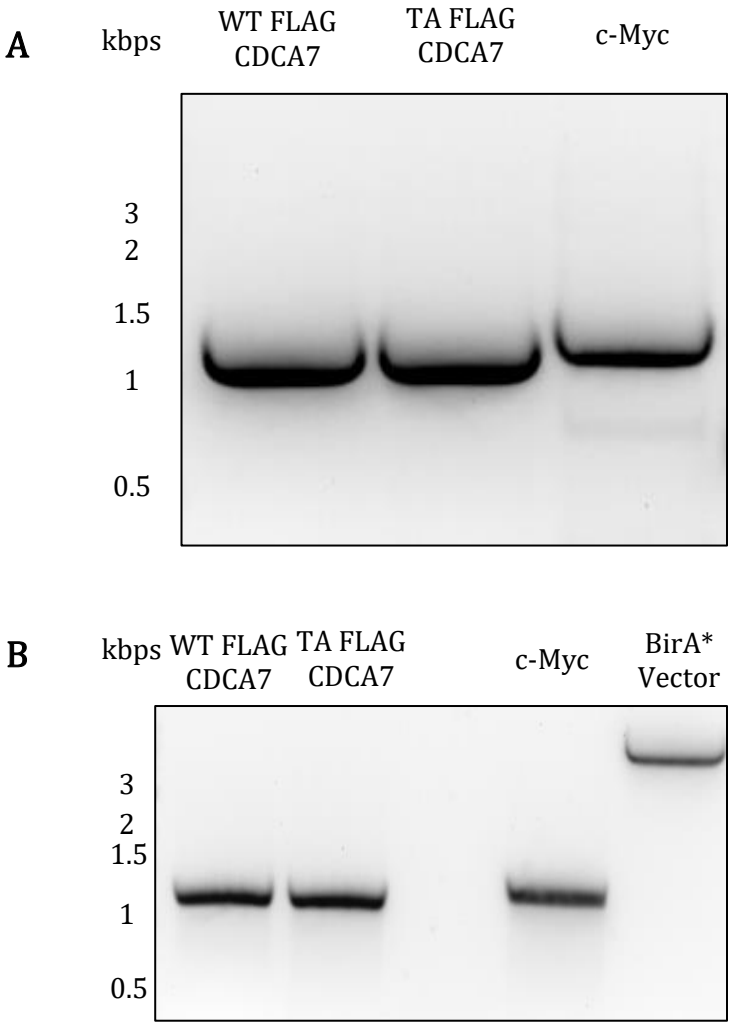

Figure A.1: Polymerase Chain Reaction (PCR) and Restriction Enzyme Digestions of BirA* construct gene insertions. PCR of desired gene inserts. The abbreviation kbps stands for kilo base pairs. A) WT CDCA7 and T163A CDCA7 which resided in the pCMV-3X-FLAG vector and c-Myc which resided in the pcDNA 3.0 vector were subjected to PCR. The primers used for PCR engineered unique restriction enzyme (RE) sites AGE1 and BSPE1 into the 5' and 3' ends of WT/T163A FLAG-CDCA7 (1116 bps). The PCR primers for c-Myc (1365 bps) introduced unique 5' AGE1 and 3' BAMH1 RE sites to c-Myc. All PCR products were purified with a gel extraction kit. B) The WT FLAG-CDCA7 and T163A FLAG-CDCA7 PCR products were sequentially digested with RE AgeI and BspEI. The c-Myc PCR product and BirA* vector backbone (6382 bps) were co-digested with AgeI and BamHI. The BirA* backbone was also sequentially digested with AgeI and BspEI on another gel (not shown). All digested products were purified with a gel extraction kit.

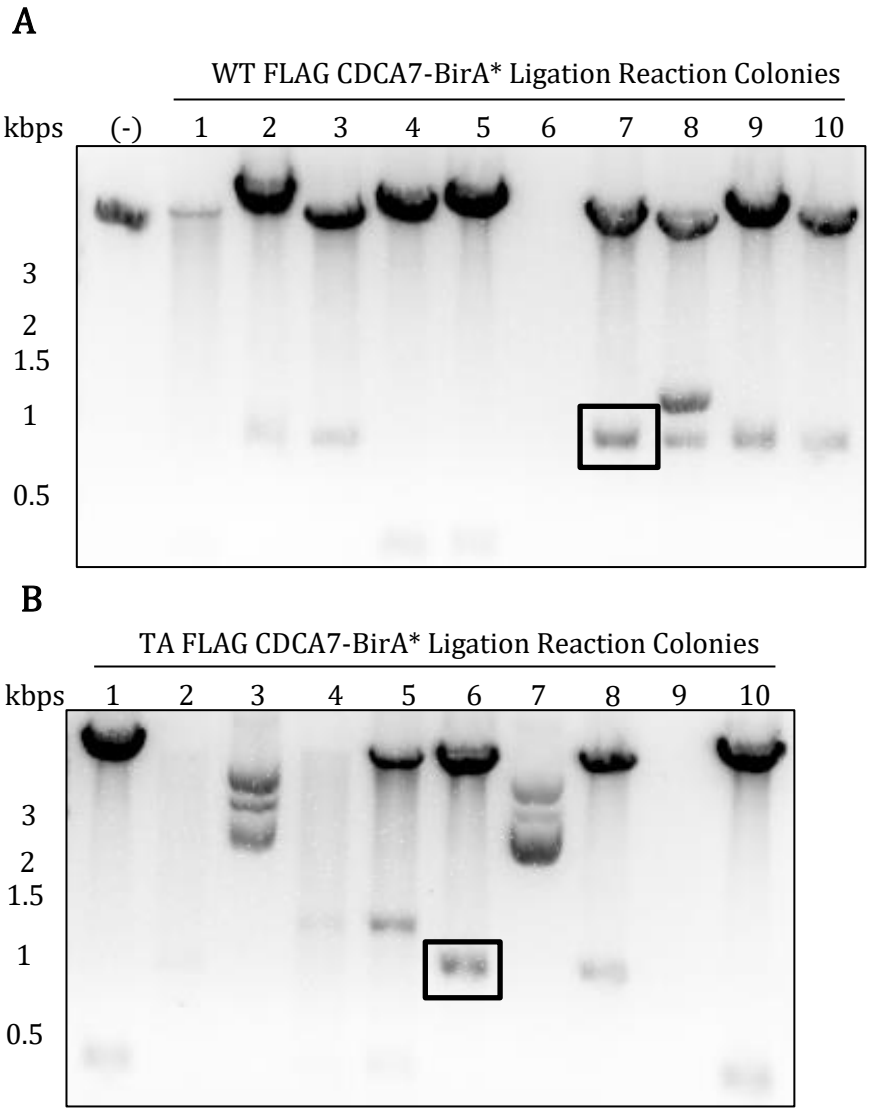

Figure A.2: Screen for positive ligation reactions of WT/T163A CDCA7-BirA*. Following ligation, Numbered columns indicate the order in which colonies were chosen. The abbreviation kbps stands for kilo base pairs. DNA was transformed and ten colonies from each transformation were selected, miniprepped and subjected to restriction enzyme (RE) double digests. The digests were designed to cut once in the inserted gene and once in the BirA* vector backbone. A) and B) WT FLAG CDCA7-BirA* and T163A FLAG CDCA7-BirA* were digested with NheI and XhoI. Positive colonies consisted of two fragments, with sizes 6692 bps and 792 bps. Colony 7 (black box) was selected for WT FLAG-CDCA7-BirA* and colony 6 (black box) was selected for T163A FLAG-CDCA7-BirA* and were verified with sequencing. The negative control in A) consisted of the BirA* backbone alone.

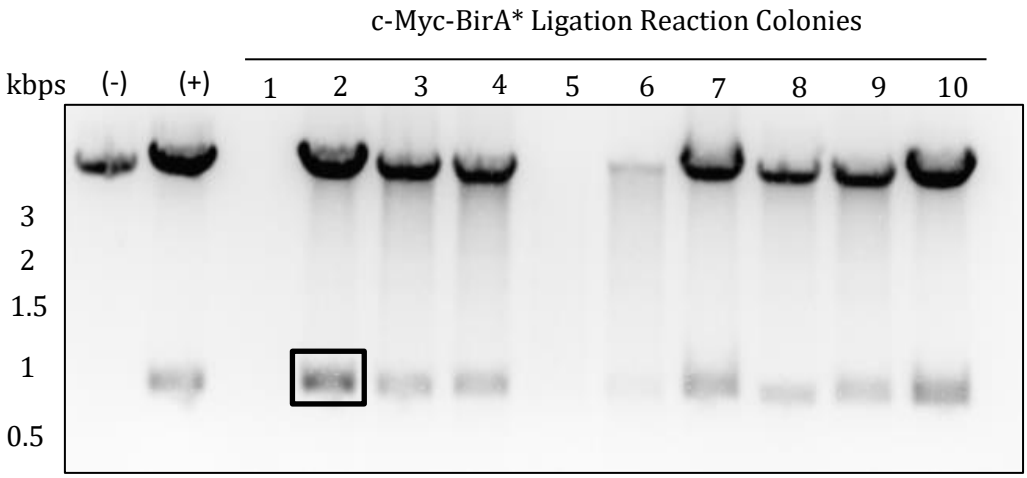

Figure A.3: Screen for positive ligation reactions of c-Myc-BirA*. Following ligation, Numbered columns indicate the order in which colonies were chosen. The abbreviation kbps stands for kilo base pairs. DNA was transformed and ten colonies from each transformation were selected, miniprepped and subjected to restriction enzyme (RE) double digests. The digests were designed to cut once in the inserted gene and once in the BirA* vector backbone. NheI and ClaI were used to digest c-Myc-BirA*. Positive colonies consisted of two fragments, with sizes 6881 bps and 852 bps. Colony 2 (black box) was selected and verified with sequencing. The negative control consisted of the BirA* backbone alone. The positive control consisted of a Myc-BirA* construct that was previously cloned by another lab member.

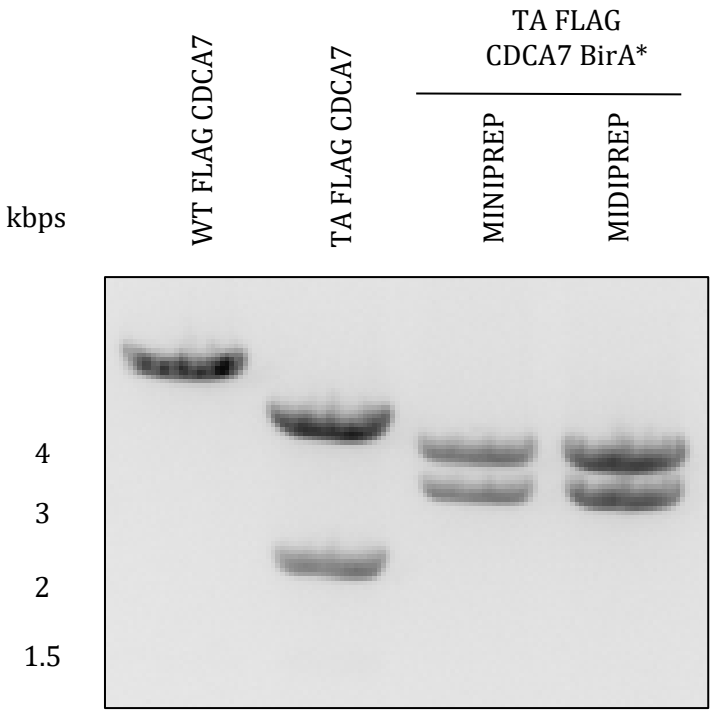

Figure A.4: Confirmation of T163A mutagenesis of the CDCA7 gene. The abbreviation kbps stands for kilo base pairs. To confirm that T163A CDCA7-BirA* contained the T163A mutation, restriction digest was performed with BssHII. The T163A mutation was designed with a uniquely engineered restriction enzyme site for BssHII, which would distinguish it from WT FLAG CDCA7. BssHII is a unique restriction enzyme site in the pCMV-3X-FLAG vector and BirA* backbone vector. WT FLAG CDCA7 in the pCMV-3X-FLAG vector (7489 bps) was used as negative control as it lacks the BssHII cut site in the CDCA7 gene. T163A (TA) FLAG CDCA7 was used as a positive control and generates two fragments (2201 bps and 5288 bps). Miniprep and midiprep DNA of T163A CDCA7-BirA* tested positive of BssHII digestions, generating two fragments at 3313 bps and 4171 bps.

Appendix B: Generation of TPX2 Construct

Abridged Version

For ectopic expression of wild-type TPX2 under the regulation of a CMV promoter, wild-type TPX2 was excised from a mCherry plasmid containing TPX2 and inserted into the plasmid pcDNA3.1/Hygro(+).

Methods

Restriction Enzyme Digests: Restriction enzyme digestion followed the general protocol outlined in Chapter 2. The plasmid DNA from pmCherry-TPX2 and pcDNA3.1/Hygro(+) were both subjected to double restriction enzyme digests. Both plasmids were cut with HindIII (NEB Catalog# R0104) and BamHI (NEB Catalog# R0136) in NEBuffer™ 2.1 (NEB Catalog# B7202) for 1 hour at 37°C. Verification of wild-type TPX2 insertion into pcDNA3.1/Hygro(+) following ligation was also done with the same combination of restriction enzymes.

Results

To produce a plasmid that solely expressed the wild-type TPX2 gene, the plasmids pmCherry-TPX2 which contained the TPX2 wild-type gene and pcDNA 3.1/Hygro(+) which contained the CMV promoter were subjected to double restriction enzyme digestion (Figure B.1a), purified from agarose gels and subjected to ligation reactions. Ligated DNA was transformed, colonies were picked, miniprepped and screened with restriction enzyme digestion (Figure B.1b). A positive colony was picked, midiprepped and sent for sequencing where insertion was verified.

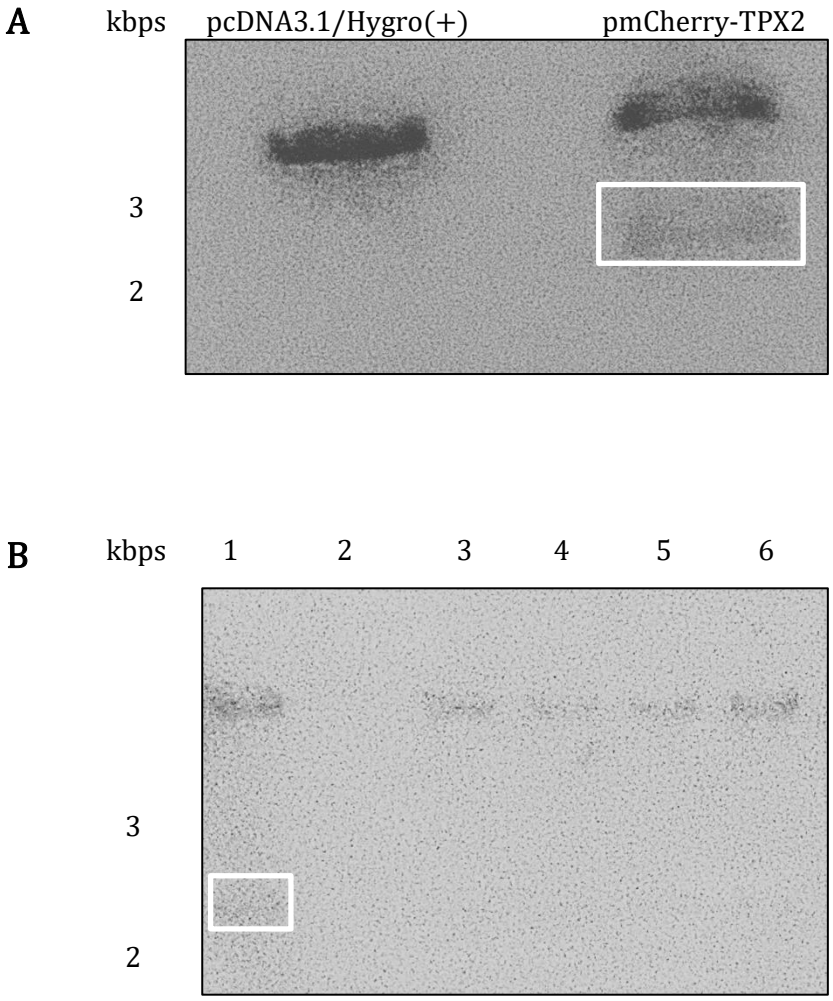

Figure B.1: Construction of wild-type TPX2 plasmid. Plasmid generation entailed two steps: excision of wild-type TPX2 from the pmCherry-TPX2 plasmid and insertion of wild-type TPX2 into the pcDNA3.1/Hygro(+) plasmid. A) Both pmCherry-TPX2 and pcDNA3.1/Hygro(+) were restriction enzyme digested with HindIII and BamHI. A band between 3-2 kilo base pairs (kbps) matches the size of wild-type TPX2 (2.3 kbps) and is indicated in the white box. Both wild-type TPX2 (white box) and pcDNA3.1/Hygro(+) were purified following restriction digests for the upcoming cloning stages. B) Wild-type TPX2 and pcDNA3.1/Hygro(+) were ligated and transformed. A sample of transformed colonies were miniprepped and subject to restriction digest with HindIII and BamHI. Insertion of TPX2 was confirmed by the presence of a 2.3 kbps fragment. A positive colony (white box) was transformed and midiprepped. Wild-type TPX2 insertion was verified through sequencing. Numbered columns indicate the order in which colonies were picked.